UNIVERSITI TEKNOLOGI MARA

THE EFFECTS OF OVEROXIDATION ON THE MORPHOLOGICAL AND ELECTRICAL PROPERTIES OF POLYANILINE (PANI) – BASED SOLID POLYMER ELECTROLYTE (SPE)

NUR NAJIHA BINTI MALIAMAN

Msc

May 2026

UNIVERSITI TEKNOLOGI MARA

THE EFFECTS OF OVEROXIDATION ON THE MORPHOLOGICAL AND ELECTRICAL PROPERTIES OF POLYANILINE (PANI) – BASED SOLID POLYMER ELECTROLYTE (SPE)

NUR NAJIHA BINTI MALIAMAN

Thesis submitted in fulfilment
of the requirements for the degree of
Master of Science
(Material Science and Technology)

Faculty of Applied Science

May 2026

CONFIRMATION BY PANEL OF EXAMINERS

I certify that a Panel of Examiners has met on 4 December 2025 to conduct the final examination of Nur Najiha binti Maliaman on her Masters of Science thesis entitled "The Effects of Overoxidation on the Morphological and Electrical Properties of Polyaniline (PANI) – Based Solid Polymer Electrolyte (SPE)" by Universiti Teknologi MARA Act 1976 (Akta 173). The Panel of Examiners recommends that the student be awarded the relevant degree. The Panel of Examiners was as follows:

Norazila Ibrahim, PhD
Associate Professor
Faculty of Applied Sciences
Universiti Teknologi MARA
(Chairman)

Rosmamuhamadani Ramli, PhD
Associate Professor
Faculty of Applied Sciences
Universiti Teknologi MARA
(Internal Examiner)

Mohamad Wafiuddin Ismail, PhD
Associate Professor
Kuliyyah of Sciences
International Islamic University
Malaysia
(External Examiner)

PROFESSOR DR HJH ZURAEDA IBRAHIM
Dean
Institute of Postgraduates Studies
Universiti Teknologi MARA
Date: 13 May 2026

AUTHOR'S DECLARATION

I declare that the work in this thesis was carried out in accordance with the regulations of Universiti Teknologi MARA. It is original and is the result of my own work, unless otherwise indicated or acknowledged as referenced work. This thesis has not been submitted to any other academic institution or non-academic institution for any degree or qualification.

I hereby acknowledge that I have been supplied with the Academic Rules and Regulations for Post Graduate, Universiti Teknologi MARA, regulating the conduct of my study and research.

Name of Student	:	Nur Najiha binti Maliaman
Student ID. No.	:	2023342239
Programme	:	Master of Science (Material Science and Technology) – AS762
Faculty	:	Applied Sciences
Thesis Title	:	The Effects of Overoxidation on the Morphological and Electrical Properties of Polyaniline (PANI) – Based Solid Polymer Electrolyte (SPE)
Signature of Student	:	……..
Date	:	May 2026

ABSTRACT

This study investigates the impact of overoxidation on polyaniline (PANI)-based solid polymer electrolytes (SPEs) by examining changes in their structural, electrical, and morphological properties. SPEs have recently gained significant attention for solid-state lithium-ion batteries (LIBs) due to their flexibility, safety, and compatibility with electrodes. Unlike conventional liquid electrolytes, SPEs eliminate issues such as leakage and flammability, but they remain vulnerable to degradation under excessive oxidative conditions. Addressing this gap, this work presents the first investigation into the overoxidation behaviour of PANI:PEO:PVDF:LiTFSI composites, thereby contributing new insights into the stability of conducting-polymer-based electrolytes. Composite SPE films were fabricated via solvent casting with varying PANI loadings (1 wt. %, 3 wt. %, and 5 wt. %) alongside polyethylene oxide (PEO), polyvinylidene fluoride (PVDF), and lithium bis(trifluoromethanesulfonyl)imide (LiTFSI). Overoxidation was induced using cyclic voltammetry (CV), while structural and electrochemical changes were analysed via Fourier-transform infrared spectroscopy (FTIR), field emission scanning electron microscopy (FESEM), X-ray diffraction (XRD), and electrochemical impedance spectroscopy (EIS). The 1 wt.% PANI composite exhibited the highest initial ionic conductivity of 1.76×10^{-5} S/cm, which decreased to 1.79×10^{-6} S/cm after overoxidation. In contrast, the 3 wt.% and 5 wt.% samples displayed lower conductivities (1.41×10^{-6} S/cm and 1.25×10^{-6} S/cm, respectively), which further declined to 4.17×10^{-7} S/cm and 1.79×10^{-7} S/cm post-treatment. FTIR confirmed the generation of carbonyl and hydroxyl groups, while FESEM revealed disrupted interpenetrating polymer networks (IPN), both correlating with conductivity loss and material degradation. The findings demonstrate that overoxidation significantly compromises the electrochemical and morphological stability of PANI-based SPEs, limiting their long-term efficiency in LIB applications. The novelty of this study lies in introducing the first PANI:PEO:PVDF:LiTFSI composition and providing the first systematic analysis of its overoxidation effects. These insights are crucial for designing more stable polymer electrolytes and developing mitigation strategies such as protective coatings or electrolyte modifications. Ultimately, this research advances the understanding of polymer degradation mechanisms, contributing toward safer and longer-lasting solid-state batteries for applications in electric vehicles, portable electronics, and renewable energy storage.

ACKNOWLEDGEMENT

First and foremost, I am deeply grateful to Allah for granting me the strength and opportunity to pursue and complete my Master's degree journey, which has been both demanding and rewarding. I would like to express my heartfelt appreciation to my main supervisor, Assoc. Prof. Dr. Mohd Muzamir Mahat, my co-supervisor, Ts. Dr. Nur Aimi Jani, and Asst. Prof. Dr. Saiful Arifin Shafiee, for their invaluable guidance, continuous support, and constructive feedback throughout the course of this research.

I would also like to extend my sincere gratitude to the members of The Muzamir Research Group and the Ceramic Laboratories, who are Dr. Faiz, Dr. Dania, Dr. Zharfan, Awatif, Adlan, Hidayah, Ain, Syifaa', and Fatin, for their support, encouragement, and contributions throughout this study. I am especially thankful to those who have helped, and encouragement has been instrumental in the completion of this project.

Lastly, I dedicate this thesis to my father (Maliaman) and my mother ([redacted]) whose unwavering belief in the power of education and whose sacrifices made this achievement possible. This accomplishment is for both of you. Alhamdulillah. I would also like to express my deepest gratitude to my entire family for their endless prayers, patience, and encouragement throughout this journey. A special mention goes to my siblings, my beloved nieces, and nephews. You have all been my constant source of strength, motivation, and joy throughout this journey.

TABLE OF CONTENTS

LIST OF TABLES

LIST OF FIGURES

LIST OF SYMBOLS

Symbols

A	Absorbance
A	Area (cm^2)
I	Current (A)
R	Resistance (Ω)
R_b	Bulk resistance (Ω)
t	thickness
V	Voltage (V)
v	Scan rate (V/s)
σ	Electronic conductivity (S/cm)

LIST OF ABBREVIATIONS

Abbreviations

CPs	Conducting Polymers
CV	Cyclic voltammetry
EIS	Electrochemical Impedance Spectroscopy
ETD	Everhart-Thornley detector
EV	Electric Vehicle
FESEM	Field Emission Scanning Electron Microscopy
IPN	Interpenetrating Network
LIBs	Lithium-ion batteries
$LiFePO_4$	Lithium iron phosphate
LiTFSI	Lithium bis(trifluoromethanesulfonyl)imide
PAN	Polyacrylonitrile
PANI	Polyaniline
PEDOT	Poly(3,4-ethylenedioxythiophene)
PEGDA	Poly(ethylene glycol) diacrylate
PEGDE	Poly(ethylene glycol) diglycidyl ether
PEO	Polyethylene oxide
PMMA	Poly(methyl methacrylate)
PVC	Polyvinyl chloride

PVDF	Polyvinylidene fluoride
PVDF-HFP	PVDF-co-hexafluoropropylene
PPO	Polypropylene oxide
PPy	Polypyrrole
SDGs	Sustainable Development Goals
SPE	Solid Polymer Electrolyte
XRD	X-Ray Diffractometry

CHAPTER 1
INTRODUCTION

1.1 Research Background

With the rise of portable electronics and electric vehicles (EVs), the demand for long-lasting, high-performance, and environmentally friendly batteries has become critical. Lithium-ion batteries (LIBs), developed by Nobel Prize laureates John B. Goodenough, M. Stanley Whittingham and Akira Yoshino have transformed modern energy storage. LIB's market has since expanded to roughly 40 billion USD (Bae & Kim, 2021). LIBs are widely used in consumer electronics and electric vehicles (EVs) such as the Tesla Model S, which requires around 12 kg of lithium (Campbell, 2022). One of the key components in manufacturing LIB is its electrolyte. In LIBs, electrolytes serve as ionic conductors, enabling the transport of Li-ions between the positive and negative electrodes during charge and discharge cycles (Ue, 2009). In batteries, traditional electrolytes are composed of chemicals such as potassium hydroxide (KOH) and lithium hexafluorophosphate ($LiPF_6$), an inorganic salt combined with dielectric solvents, including water and ethylene carbonate. However, these liquid electrolytes pose safety risks, making solid polymer electrolytes (SPEs) a more suitable alternative due to their enhanced safety features (Hallinan & Balsara, 2013).

SPEs eliminate issues like internal short-circuiting, electrolyte leakage, and the formation of combustible reaction products at the electrode surface, which are common in liquid electrolytes (Stephan, 2006). SPE is a membrane capable of conducting ions with an ionic conductivity of approximately 10^{-4} S/cm at room temperature. The discovery of an ion-conducting polymer, polyethylene oxide (PEO), combined with an alkali metal like Li, was first reported in 1973 (Agrawal & Pandey, 2008). SPEs have gained significant interest in LIBs due to their low cost, robust mechanical properties, high safety standards, electrode compatibility, and ease of fabrication. The polymer matrix facilitates Li-ion transport in these systems through segmental motion in the amorphous regions (Chen et al., 2021). SPE functions to transport Li ions between the anode and cathode during charging and discharging, hence why SPE in LIBs needs to have high ionic conductivity as it is closely related to its performance, efficiency, and

practicality. SPEs are typically formed by dissolving ionic salts, such as Li salts, into polar coordinating polymer hosts like PEO or polypropylene oxide (PPO), followed by casting the membrane through solution casting or hot-pressing methods. However, the high crystallinity of polyether-lithium salt complexes results in low ionic conductivity (10^{-8} to 10^{-7} S/cm) at room temperature, as crystallinity hinders ion transport. Since ion mobility occurs mainly in the amorphous phase, enhancing the amorphous content of the polymer matrix is critical (Leš & Jordan, 2020). Reducing polymer crystallinity and promoting amorphous behaviour are essential to improve ionic conductivity. In addition to crystallinity reduction, the electrochemical stability window of SPEs plays a crucial role in determining their suitability for high-energy-density LIB applications. As LIB operating voltages continue to increase to meet performance demands, SPEs must remain chemically and electrochemically stable over extended voltage ranges. Inadequate electrochemical stability can lead to interfacial degradation, electrode passivation, and electrolyte decomposition, ultimately compromising battery efficiency and safety. Therefore, the development of SPEs requires a balanced optimisation of ionic conductivity, mechanical integrity, and electrochemical stability. Achieving this balance remains a major challenge in polymer electrolyte research, particularly when functional additives or conductive components are introduced into the polymer matrix. This can be achieved by introducing interpenetrating polymer networks (IPNs) into SPEs (Murata et al., 2000). IPNs are molecularly interlaced networks of two or more polymers, which enhance the ionic conductivity and mechanical properties of SPEs, like increased flexibility and improved toughness, by lowering crystallinity (Tan et al., 2018). These features make IPNs suitable for LIBs, extending their application to supercapacitors and solar cells. The incorporation of conducting polymers into SPEs further enhances the multifunctionality of these materials by introducing mixed ionic–electronic conduction pathways. This dual conduction behaviour is particularly beneficial for electrochemical devices, as it improves charge-transfer kinetics and interfacial compatibility between the electrolyte and electrode materials. However, the introduction of conducting polymers also introduces new challenges related to chemical stability and long-term durability. While conducting polymers can improve electrochemical performance under moderate conditions, their behaviour under prolonged electrochemical stress remains insufficiently understood. As a result,

understanding the stability and degradation behaviour of conducting polymer-based SPEs is essential for their reliable application in advanced energy storage systems. For instance, creating semi-IPNs (sIPNs) with poly(3,4-ethylene dioxythiophene) (PEDOT), a conducting polymer (CP) embedded in an ionically conducting PEO matrix, demonstrated superior capacitance compared to bare PEDOT (Fong et al., 2017). The PEO matrix reduced ion diffusion distances and improved charge storage, establishing the potential of IPNs in developing advanced materials for energy storage (Leš & Jordan, 2020).

Thus, compositing SPE with CP can improve its ionic conductivity due to the existence of IPN. CP, like polyaniline (PANI), has attracted significant research interest for its electrical conductivity, environmental stability, and versatile applications. PANI stands out among other ICPs due to its superior thermal stability, processability, and conductivity. Moreover, PANI's economic advantage stems from the lower cost of its monomer, aniline, compared to other ICP monomers. The synthesis of PANI is straightforward, allowing for easy tuning of its properties and opening a wide range of potential applications (Bhadra et al., 2009). Overall, PANI's superior properties and ease of use make it a compelling choice over other ICPs. CPs consist of π-conjugated backbones with alternating single and double bonds, including compounds like pyrrole, aniline, and thiophene (Namsheer & Rout, 2021). Figure 1.1 shows the chemical structure of PANI.

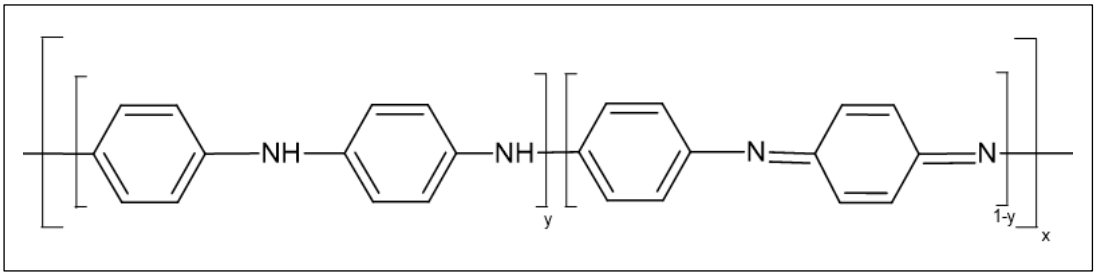

Figure 1.1 Chemical structure of polyaniline

Adapted from Bhandari (2017)

PANI is a promising CP since it is easy to synthesise, has a low-cost monomer, and is stable (Bhadra et al., 2009). PANI shows superior thermal stability, good processability,

and conductivity. PANI was mixed with PEO and polyvinylidene fluoride (PVDF) through this research. PEO is an ionically conductive polymer, thus allowing Li-ion to move across the polymer matrix. PVDF was used as it can enhance the mechanical properties of the film. The best formulation of this polymer mixture that gives optimum conductivity was studied.

Despite the promising advantages of incorporating conducting polymers into SPE systems, their long-term electrochemical stability remains a critical concern. During repeated charge-discharge cycling or exposure to high anodic potentials, conducting polymers may undergo irreversible chemical transformations that alter their intrinsic properties. These degradation processes are particularly problematic in solid-state systems, where material failure cannot be mitigated through electrolyte replacement or self-healing mechanisms. Therefore, understanding degradation phenomena in conducting polymer–based SPEs is not only scientifically important but also essential for ensuring device reliability, safety, and operational longevity. Among the various degradation pathways, electrochemical overoxidation has emerged as one of the most detrimental mechanisms affecting conducting polymer performance. However, CPs are prone to overoxidation during synthesis or under high voltages, which alters their molecular structure and diminishes electrical conductivity (Holze, 2022). Overoxidation disrupts the π-conjugation, causing defects that impair device performance. Managing oxidation levels is crucial to preserving material properties, particularly in SPEs, as excessive oxidation compromises LIB performance and disables redox exchange (Refaey et al., 1999). At high anodic potentials, PANI undergoes electrochemical overoxidation, forming quinone-like compounds that degrade its properties (Gao et al., 2011). Overoxidation can be studied through cyclic voltammetry (CV), which evaluates electrochemical behaviour using a working electrode (WE), reference electrode (RE), and counter electrode (CE) in an electrolyte medium (Elgrishi et al., 2018). This study focuses on PANI-based SPE films prepared using a solvent-cast method, incorporating PANI, PVDF, lithium bis(trifluoromethanesulfonyl) imide (LiTFSI), and PEO. Unlike prior research, this work investigates the effects of overoxidation on the morphological, structural, and electrochemical characteristics of SPE composites. Films with varying PANI concentrations (1 wt.%, 3 wt.%, and 5 wt.%) are analysed using CV to induce

overoxidation. By examining degradation mechanisms and stability, the study aims to enhance the design of PANI-SPEs for applications in batteries and supercapacitors. The findings may reveal strategies to minimize overoxidation and improve the performance and longevity of SPE materials.

Most existing studies on PANI-based SPEs primarily focus on enhancing ionic conductivity, mechanical stability, and electrochemical performance under normal operating conditions, with limited consideration of degradation mechanisms at high anodic potentials. In contrast, this study specifically focuses on the overoxidation of PANI, a phenomenon that differs from conventional PANI investigations as it involves irreversible chemical and structural changes that disrupt π-conjugation and impair charge transport. Overoxidation has not been extensively explored in the context of PANI-incorporated SPE systems. This gap is significant for SPE development because overoxidation directly affects the long-term stability, electrochemical reliability, and practical applicability of SPEs in LIBs and related energy storage devices. By addressing this gap, this study improves the understanding of how overoxidation affects the stability and performance of PANI-based SPEs.

1.2 Problem Statements

SPEs are increasingly investigated as alternatives to liquid electrolytes in LIBs due to their enhanced safety, mechanical stability, and leakage-free operation. However, their practical application remains limited by low ionic conductivity and restricted electrochemical stability, particularly under high-voltage operating conditions. To address these limitations, CPs, especially PANI, have been incorporated into SPE systems because of their tunable electrical conductivity, redox activity, and chemical versatility. PANI-based SPEs have attracted significant attention for energy storage applications, as PANI can facilitate charge transport and improve interfacial properties within polymer electrolyte matrices. Nevertheless, a critical issue associated with the use of PANI is its susceptibility to overoxidation, which can occur during synthesis or electrochemical operation. Oxidizing agents such as ammonium persulfate (APS), commonly employed in the polymerization of PANI and polypyrrole (PPy), can induce overoxidation when exposed to oxygen-containing environments such as air (Holze,

2022). More critically for battery applications, PANI can undergo rapid electrochemical overoxidation under high anodic potentials or strongly oxidizing conditions, which are relevant to LIB operating voltages (Holze, 2022).

Overoxidation leads to the disruption of the conjugated π-electron system that is essential for charge transport in PANI. This process results in irreversible chemical and structural changes, including the formation of quinone-type species such as hydroquinone and benzoquinone (HQ/BQ), which attach to or interact with the PANI backbone (Gao et al., 2011). The generation of hydroxyl and carbonyl functional groups during overoxidation further degrades electrical conductivity and introduces structural defects (Rodríguez et al., 2000). Therefore, the redox activity, electrical conductivity, and morphological integrity of PANI are significantly compromised. In the context of SPE-based LIBs, these degradation processes directly limit electrochemical stability, charge-transfer efficiency, and long-term cycling performance. Excessive overoxidation suppresses the redox exchange capability of PANI-containing SPE films, leading to increased internal resistance, reduced ionic-electronic synergy, and accelerated performance decay during battery operation (Refaey et al., 1999). Although PANI is extensively employed in electrochemical systems, the mechanisms and degree of its overoxidation and the effects on SPE performance and long-term stability remain poorly understood, particularly under conditions relevant to LIB operation.

This lack of understanding represents a critical knowledge gap that hinders the reliable design and optimization of PANI-based SPEs for practical energy storage applications. Therefore, a systematic investigation into how overoxidation affects the morphological, structural, and electrochemical properties of PANI-containing SPEs is essential. In this study, PANI-based SPE films are fabricated via a solvent-casting technique using PANI, poly(vinylidene fluoride) (PVDF), lithium bis(trifluoromethanesulfonyl)imide (LiTFSI), and polyethylene oxide (PEO). SPE films with varying PANI loadings (1 wt.%, 3 wt.%, and 5 wt.%) are subjected to cyclic voltammetry (CV) to intentionally induce overoxidation. Unlike previous studies that primarily emphasize conductivity enhancement under normal conditions, this work focuses on elucidating the degradation behaviour of PANI within SPE composites under over oxidative stress. By correlating overoxidation-induced changes with electrochemical stability and material integrity, this research aims to provide insights

into mitigating PANI degradation and improving the performance and lifetime of SPEs for LIB and supercapacitor applications.

1.3 Research Questions

a) How do the chemical structure, morphology, crystallinity, and conductivity of PANI-based solid polymer electrolytes (SPEs) vary with different PANI concentrations?

b) How does the concentration of PANI influence the electrochemical behaviour of SPE membranes during the overoxidation process, as observed through CV?

c) What are the effects of overoxidation on the chemical structure, morphology, crystallinity, and conductivity of PANI-based SPE membranes?

1.4 Research Objectives

i) To examine the influence of PANI concentration on the chemical, structural, morphological, and electrical properties of PANI-based solid polymer electrolytes (SPEs).

ii) To investigate the electrochemical behaviour of PANI-based SPE under overoxidation conditions.

iii) To evaluate the effects of overoxidation on the chemical, structural, morphological, and electrical properties of PANI-based SPE.

1.5 Research Hypothesis

i) Varying the PANI concentration in SPEs will influence their chemical structure, morphology, crystallinity, and conductivity, with an optimal

concentration yielding the highest conductivity and most favourable structural properties.

ii) SPE films with lower PANI concentrations will exhibit reduced redox activity and electrochemical reversibility during overoxidation compared to those with higher PANI content.

iii) The overoxidation process will induce structural and morphological changes such as decreased crystallinity, altered functional group composition, and increased porosity, which collectively enhance the ionic conductivity of the PANI-based SPE up to an optimal PANI concentration.

1.6 Significance of the Study

The study on the effects of overoxidation on the morphological and electrical properties of PANI-based SPEs holds great significance in both scientific research and technological advancements. CPs such as PANI have garnered widespread attention due to their tunable electrical properties, ease of synthesis, and potential applications in various electrochemical devices. However, overoxidation remains a major challenge that can degrade the structural integrity and electrical performance of these materials. Understanding the extent and nature of these changes is crucial for optimising their applications, particularly in energy storage devices like lithium-ion batteries (LIBs). One of the key contributions of this research is its potential to enhance the performance and stability of PANI-based SPEs. By investigating the morphological and electrical alterations caused by overoxidation, this study provides valuable insights into how these materials can be engineered to exhibit improved durability and efficiency. This knowledge is particularly relevant for energy storage devices such as batteries and supercapacitors, where the stability of SPEs directly affects the overall lifespan and functionality of the system.

Furthermore, this research focused on the detrimental effects of overoxidation on the performance of LIBs, which can lead to irreversible structural damage and a reduction in electrical conductivity. By analysing these effects in detail, the study contributes to a deeper theoretical understanding of how oxidation influences polymer electrolytes, thereby guiding future research in the development of more stable SPEs.

From an industrial perspective, this research supports the advancement of next-generation energy storage technologies, providing insight that may improve the commercial viability of polymer-based batteries in sectors such as electric vehicles, portable electronics, and renewable energy storage systems. Governmental and policy-level relevance lies in how this work can inform materials selection and safety standards for energy storage systems, aligning with national and international strategies for energy resilience and clean technology adoption. Environmentally, enhancing the stability and efficiency of SPEs contributes to the development of safer, non-volatile, and recyclable battery components, thereby minimising environmental harm and supporting low-carbon technology transitions. Socially, the outcomes of this research could enable more accessible and safer battery technologies for daily use, contributing to energy equity and improved quality of life, particularly in remote or underserved regions.

Hence, this study is highly relevant in sustainable energy applications. SPEs play a crucial role in emerging technologies such as fuel cells and flexible electronic devices. The ability to enhance the stability of PANI-based SPEs by minimising the adverse effects of overoxidation can lead to more reliable and environmentally friendly energy solutions. This research supports the objective of creating sustainable and high-performance electrochemical systems, aligning with the Sustainable Development Goals (SDGs), particularly SDG 7 (Affordable and Clean Energy), SDG 9 (Industry, Innovation, and Infrastructure), SDG 12 (Responsible Consumption and Production), and SDG 13 (Climate Action). By improving the efficiency and stability of polymer electrolytes, this study contributes to the advancement of clean energy technologies, innovation in sustainable industries, promotes responsible material usage, and supports global efforts to combat climate change.

Eventually, this study contributes to both theoretical knowledge and practical advancements in the field of CPs and electrochemical devices. The insights gained will benefit researchers, engineers, and manufacturers who are working on polymer-based energy storage and conversion systems. This study strengthens the potential of polymer electrolytes for use in advanced energy technologies by tackling the problems related to overoxidation and opening the door for the creation of more robust and effective polymer electrolytes. In addition, it is possible to determine which PANI formulation with PEO and PVDF will yield the highest level of optimal conductivity from this study.

The conductivity study is significant in this research, as improved conductivity will lead to enhanced performance of LIBs. This project will contribute to the development of new knowledge on the effects of overoxidation on CP-based SPE in LIBs and related systems under realistic operating and electrochemical conditions. Additionally, the outcomes of this study may serve as a reference framework for future material optimisation and performance evaluation of polymer electrolytes.

1.7 Scopes of study

This study is confined to investigating the effects of PANI concentration and overoxidation on the physicochemical and electrochemical properties of PANI-based SPEs. The scope is limited to identifying an optimal PANI concentration that balances electrochemical performance and material stability within a defined polymer electrolyte system. All SPE films are prepared using a solvent-casting technique and are formulated exclusively as composite membranes consisting of PEO and PVDF. The PANI content is restricted to three concentrations, namely 1 wt.%, 3 wt.%, and 5 wt.%, to allow a controlled and systematic evaluation of concentration-dependent effects. PANI loadings outside this range are not investigated; therefore, the findings may not reflect the behaviour of SPEs with significantly lower or higher PANI concentrations. The study focuses on evaluating the influence of PANI loading on chemical structure, morphology, crystallinity, electrical conductivity, and electrochemical behaviour of the SPEs before and after exposure to overoxidation.

Overoxidation is induced under controlled electrochemical conditions to simulate oxidative degradation that may occur during LIB operation. However, these conditions represent a simplified model and do not fully capture the combined effects of prolonged cycling, thermal stress, or mechanical deformation encountered in practical battery systems. Consequently, the analysis is limited to material-level degradation behaviour rather than real-world battery performance. This research does not include full LIB fabrication, long-term cycling stability tests, thermal ageing analysis, rate capability studies, or mechanical durability assessment under operational stress. Furthermore, only a single polymer matrix system (PEO/PVDF) and a fixed lithium salt composition are considered, while variations in polymer ratios, alternative

host polymers, and different lithium salts are beyond the scope of this work. As such, the outcomes of this study are intended to provide fundamental and comparative insights into the effects of PANI concentration and overoxidation within a specific SPE formulation, rather than broad generalisation across diverse SPE systems or LIB configurations.

CHAPTER 2
LITERATURE REVIEW

2.1 Lithium-Ion Batteries (LIBs)

Lithium, with the symbol Li, has been known for 200 years, with its first discovery by Johann August Arfvedson in the year 1817 (Matlin et al., 2019). It appears silver in colour by nature, and this colour fades when exposed to air as it undergoes oxidation. It is also known as the lightest and least dense element that exists as a solid at room temperature and is combustible. Positioning itself as one of the Group 1 elements of the Periodic Table, lithium is known for its high reactivity. Figure 2.1 shows the Periodic Table of chemical elements.

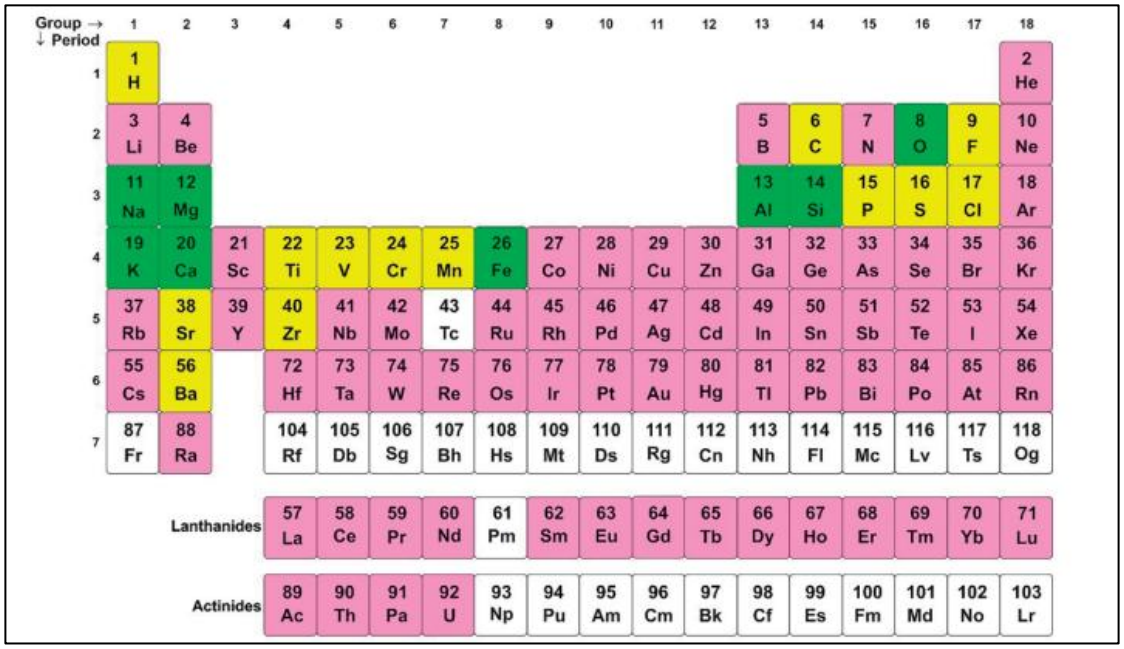

Figure 2.1 Periodic Table of chemical elements

(Matlin et al., 2019)

Handling and storage of Li should be done carefully; for instance, Li in its elemental form should always be kept in mineral oil to prevent it from reacting with air. The physical, chemical, and electrochemical properties of Li make it a useful

component for the industry. It is used in the manufacturing of batteries, glasses, ceramics, greases, chemical reagents, pharmaceuticals, and nuclear fuels (Wu et al., 2022). One of its most notable applications is in batteries, specifically lithium-ion batteries (LIBs). LIBs are remarkable as they offer a great number of advantages, among them, because of their high energy density (Mossali et al., 2020; Shin et al., 2015; Wanger, 2011; Yang et al., 2020). A high-energy-density battery can store a large amount of energy per unit mass, typically measured in MJ/kg. Hence, most LIBs are smaller and have a lower weight than lead acid batteries, which are relatively bigger and heavier. Battery energy storage systems with high energy density are popular because they can counter issues like environmental pollution and energy shortage (Shen et al., 2018). Besides, the market of LIBs is also blooming because of their other advantage, which is the reduced memory effect (Mossali et al., 2020; Wanger, 2011). Having a low memory effect can increase the battery service time (Sasaki et al., 2013). Furthermore, LIB is a promising battery as it proposes a longer life cycle and a lower self-discharge rate in comparison with other rechargeable battery systems (Mossali et al., 2020; Makwarimba et al., 2022; Yang et al., 2020). Able to withstand temperature variation, it is also called a tough battery (Wanger, 2011). Not to mention, LIB is also a great choice because of its easy handling properties.

Because of their great practicality, LIBs contribute a lot to the better development of electronic devices, mainly portable electronic devices like smartphones, power banks, and laptops. Since the properties of batteries are essential in manufacturing electronic devices, developers must find batteries that have great advantages over the devices without devastating environmental effects. LIB is also in demand in the electric vehicles (EVs) market, which is growing exponentially. According to the International Energy Agency (IEA), EV stocks may reach 245 million units globally by 2030. EV market blooms as its uses reduce fossil fuel consumption and greenhouse gas emissions (Dunn et al., 2015). EVs are environmentally good as they produce less carbon dioxide (CO_2); consequently, the production and use of LIBs will continuously increase.

LIB was first marketed in Japan by Sony Corp. in 1990 and first developed by Asahi Chemicals in the early 1980s (Yoshio et al., 2009). LIB's early generation consists of graphite as the anode and $LiCoO_2$ (LCO) as the cathode material. But cobalt

in batteries has some disadvantages; cobalt is expensive and has a high tendency for thermal runaway to happen (Wang & Friedrich, 2015). Thermal runaway can occur when the exothermic reaction is uncontrollable. It happens when the temperature increases, causing the exothermic reaction rate to increase. This leads to further temperature increases and further increases in reaction rate, which will lead to an explosion. Thermal runaway in Li-ion batteries can occur due to the exothermic reaction between the electrolyte, cathode, and anode. One of LIB's promising cathode materials is lithium iron phosphate, $LiFePO_4$, as it has high power capability, is low in cost, is non-toxic, and has thermal safety (Shin et al., 2005; Xu et al., 2008). LIBs production has skyrocketed over the past few decades; their sale in 2009 were approximately 10 billion U.S. dollars (Bae et al., 2016). The search for large-scale energy storage devices has increased, which makes LIB come into the scene.

The key to developing LIBs lies in designing a system that securely contains all components, such as cathode and anode active materials, electrolytes, separators, and current collectors within a compact and enclosed space while ensuring maximum energy output is achieved without compromising safety (Yoshio et al., 2009). The LIBs compartment comprises aluminium, cathode, separator, anode, copper, Li ions, electrolytes, and graphite. During the discharging process or the use of LIB, Li^+ ions move from the anode to the cathode, while during charging, Li^+ ions move from the cathode to the anode. This movement of Li^+ ions allows the battery to power electronic devices. Figure 2.2 shows the structure of a cylindrical LIB (left) and the mechanism of how a LIB works (right).

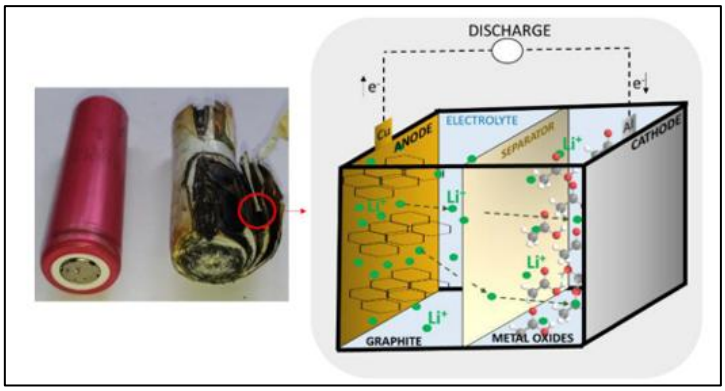

Figure 2.2 Inner structure of a cylindrical LIB (left) and electrochemical operating mechanism of a LIB cell (right)

(Mossali et al., 2020)

This figure shows that during LIB operation, Li^+ produced via reversible reactions at the negative electrode migrates toward the cathode, where it reacts to form metal oxides. The electrolytes in LIBs function as ionic conductors, facilitating the movement of Li ions between the positive and negative electrodes during the charging and discharging processes (Ue, 2009). The electrolyte is the primary drive behind advancements in LIBs, such as improvements in their energy density, safety, and cycle life (Yoshitake, 2009). A good electrolyte for LIBs needs to possess the properties of being flexible and having a high ionic conductivity.

2.2 Polymer Electrolytes

In conventional batteries, liquid electrolytes (LEs) are generally formulated by dissolving salts such as potassium hydroxide (KOH) or lithium hexafluorophosphate ($LiPF_6$) in dielectric solvents, including water or ethylene carbonate. LEs exhibit high ionic conductivity (10^{-3} to 10^{-2} S/cm) and establish effective interfacial contact with electrode active materials, thereby providing efficient pathways for Li ions transport during charge-discharge cycles (Chae et al., 2023). During the fabrication of LIBs, LEs can be readily injected and are able to penetrate both electrodes and separators. However, this type of electrolyte is unsafe; hence, polymer electrolytes are a good replacement, as they are safer (Hallinan & Balsara, 2013; Nourisabet et al., 2022). To overcome these issues, solid-state electrolytes have been explored as alternatives.

Oxide-based electrolytes provide good stability but face challenges with processability and high interfacial resistance. In contrast, sulphide-based electrolytes exhibit high ionic conductivity but are chemically unstable and highly sensitive to moisture, producing toxic hydrogen sulphide (H_2S). In contrast, polymer-based electrolytes (PEs) are more flexible, processable, and safer, with improved electrode contact, though their thermal and mechanical stability is relatively lower. PEs can be divided into several categories: solid polymer electrolytes (SPEs), which are solvent-free and stable but have low ionic conductivity at room temperature; gel polymer electrolytes (GPEs), which combine good ionic conductivity with safety but lack strong mechanical strength; composite polymer electrolytes (CPEs), which incorporate fillers to enhance conductivity and stability; and polymeric ionic liquid electrolytes (PILEs), which combine polymers with ionic liquids and show great promise, although their ion transport mechanisms remain unclear (Chae et al., 2023).

This is because there is no internal short-circuiting, electrolyte leakage, or combustible reaction products at the electrode surface, which often occur in liquid electrolytes (Stephan, 2006). The benefits of this technology include the lack of volatile and potentially hazardous components, the simplicity of fabrication, and the lower cost of polymers compared to liquid electrolytes (Bicy et al., 2022). Besides, PEs are lighter and more flexible compared to liquid electrolytes (Nourisabet et al., 2022). PE is a type of electrolyte, used in electrochemical devices, that utilizes a polymer matrix to conduct ions. PE can conduct ions at an ionic conductivity of around 10^{-4} S/cm at room temperature. In 1973, an ion-conducting polymer, PEO, combined with an alkali metal, was discovered (Agrawal & Pandey, 2008).

PEs are used in various applications, including LIBs, fuel cells, and water desalination. PEs are a crucial part of LIBs as they serve as a medium for ion transport in LIBs and as a separator to separate both electrodes in LIBs. One example of this type of electrolyte is a blend of LiTFSI, a lithium salt with a cross-linked PEO (Hallinan & Balsara, 2013). For it to serve as a good electrolyte for LIB, PE should possess characteristics of having a high ionic conductivity to transport Li ions in the LIBs under both room temperature and cold conditions, strong mechanical resilience, a notable transference number, thermal and electrochemical stability, and compatibility with

electrodes (Stephan, 2006). Only GPEs and SPEs will be reviewed in this thesis because they are the topic of interest, as they can form film layers, while LPEs cannot.

2.2.1 Gel Polymer Electrolytes (GPEs)

Gel polymer electrolytes (GPEs) represent a unique electrolyte variety that blends the characteristics of both liquid and solid polymer electrolytes. They possess solid properties of being cohesive and liquid properties of being dispersive. These properties give GPEs an advantage, as they can function as both electrolytes and separators. They involve a polymer framework saturated with a liquid electrolyte, usually an organic solvent containing dissolved salts. This fusion offers better safety and flexibility compared to conventional liquid electrolytes. In GPEs, a polymeric structure serves as the foundational material, ensuring robust mechanical strength. For GPEs, numerous polymer hosts have been created and assessed, encompassing materials such as PEO, PVDF, PVDF-co-hexafluoropropylene (PVDF-HFP), PPO, polyacrylonitrile (PAN), poly(methyl methacrylate) (PMMA), and polyvinyl chloride (PVC) (Stephan, 2006).

In GPEs, Li-ion transport occurs primarily within the liquid phase, while the polymer matrix serves as a scaffold to maintain a gel-like state (Chen et al., 2021). Although GPEs generally offer higher ionic conductivity and better temperature adaptability compared to SPEs, they suffer from several limitations. Most notably, GPEs possess weaker mechanical integrity than SPEs (Srivastava & Tiwari, 2009). This mechanical weakness may weaken the structural stability of the electrolyte layer during prolonged cycling, especially under high-pressure conditions in LIBs. Additionally, because GPEs contain liquid components, they may still present safety risks such as leakage, flammability, and instability at elevated temperatures, issues that SPEs are designed to mitigate. Strong mechanical properties in polymer electrolytes are crucial for preventing the growth of lithium dendrites, which can penetrate the separator layer and lead to internal short circuits. Tensile testing is often conducted to evaluate these mechanical properties, where a higher tensile modulus has been shown to delay or prevent dendrite propagation (Sun et al., 2019). Moreover, enhancing the mechanical robustness of polymer electrolytes also ensures their long-term functionality as effective

electrode separators, which is particularly crucial in high-performance and next-generation battery systems (Snyder et al., 2007).

GPEs can be fabricated by two main approaches: the ex-situ method, where the polymer matrix is prepared outside the battery and later inserted, often resulting in poor electrode-electrolyte contact and higher resistance; and in situ polymerization, where liquid precursors are injected directly into the electrodes and then polymerized by thermal or UV curing. In situ polymerization offers improved interfacial contact, reduced resistance, and better electrochemical performance. This process typically involves monomers such as trimethylolpropane ethoxylate triacrylate (ETPTA), poly(ethylene glycol) diacrylate (PEGDA), and trimethylolpropane propoxylate triacrylate (TPPTA), along with lithium salts, solvents, and initiators. Thermal curing is reliable but slow, requiring 20-30 minutes and posing a risk of damaging cell components, whereas UV curing is much faster, completed in seconds, but must occur before cell sealing, limiting manufacturing flexibility. Despite these challenges, in situ GPEs have demonstrated high ionic conductivity (~10^{-3}-10^{-2} S/cm), excellent flexibility, wide electrochemical stability up to 5 V, and strong suppression of lithium dendrites. The advantages include superior interfacial adhesion, reduced resistance, enhanced cycle stability, high coulombic efficiency, and improved safety, making them highly suitable for flexible and next-generation batteries. However, some limitations remain, such as the long curing time for thermal methods, the fabrication restrictions of UV curing, and the need to further improve the mechanical strength of gels for large-scale applications. In short, GPEs, particularly those prepared via in situ polymerization, are highly promising for developing safer, high-performance LIBs, as they successfully merge the conductivity of liquids with the stability of solids, though further optimization is necessary for commercial adoption.

Figure 2.3 illustrates the working principle of LIBs using LEs compared to GPEs. While LEs rely on free ion transport through a separator, GPEs incorporate a polymer matrix that enhances interfacial contact with electrodes, improves ion transport pathways, and provides better mechanical and electrochemical stability.

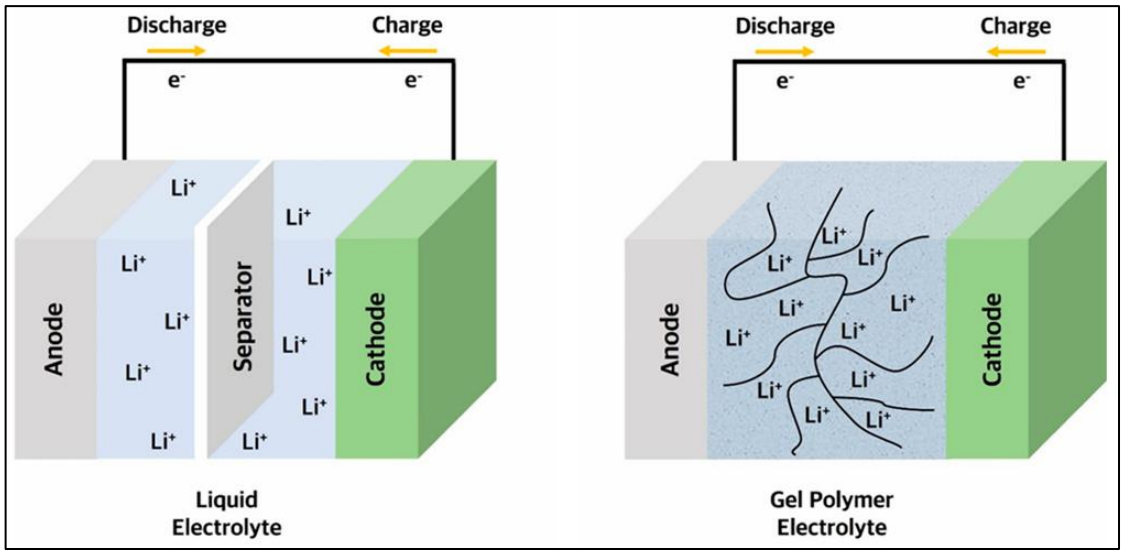

Figure 2.3 Schematic illustration of LIBs employing (a) LE and (b) GPE

(Chae et al., 2023)

The figure compares the operation of lithium-ion batteries when using a LE (left) versus a GPE (right). On the left side (LE system), the battery consists of an anode, a cathode, and a separator soaked with an LE. Lithium ions (Li^+) migrate freely through the liquid medium during charging and discharging. During discharge, Li^+ ions move from the anode to the cathode through the liquid electrolyte, while electrons (e^-) travel externally through the circuit to generate current. During charging, the process is reversed, with Li^+ ions returning to the anode. Although liquid electrolytes provide high ionic conductivity, the figure highlights that ion transport is largely confined to the separator region, which may result in poor interfacial contact and potential safety risks such as leakage or dendrite formation. On the right side (GPE system), the separator is replaced by a gel polymer matrix, which not only holds the LE but also provides structural support. The polymer chains entrap the electrolyte, creating continuous ion-conduction pathways that allow Li^+ ions to move more uniformly between the anode and cathode. This design improves interfacial adhesion between the electrolyte and electrodes, reduces interfacial resistance, and enhances mechanical stability. The schematic also implies that the polymer framework helps suppress lithium dendrite growth, leading to safer and more reliable cycling compared to conventional LE systems. Overall, the comparison visually demonstrates how incorporating a GPE transforms the electrolyte

region from a simple liquid-filled separator to a polymer-supported network, thereby improving both safety and performance of LIBs.

2.2.2 Solid Polymer Electrolytes (SPEs)

In 1975, Wright discovered a PEO-alkaline metal ion complex that exhibits ionic conductivity of 1×10^{-7} S/cm at room temperature. Since then, the research and development of SPEs have focused on improving their ionic conductivity at ambient temperatures (Murata et al., 2000). An SPE is an electrolyte commonly used in electrochemical systems such as batteries and fuel cells, where a solid polymer matrix replaces the liquid medium to enable ion conduction. SPEs consist of lithium or sodium salts incorporated into a polymer matrix, most commonly PEO. To prepare SPE membranes, the salt-polymer mixture is dissolved in a solvent such as acetonitrile or methanol, then cast into a film, followed by solvent evaporation (Bekaert et al., 2017). SPEs have garnered significant attention in the realm of LIBs due to their low cost, adequate mechanical properties, exceptional safety features, compatibility with electrodes, and ease of processing. In 2011, a company named Bollore introduced a fully electric vehicle 2011 called Bulecar, powered by solid polymer lithium batteries. These batteries utilised PEO as SPE with lithium metal as the anode and $LiFePO_4$ as the cathode. They achieved an energy output of around 180 Wh/kg, which is comparable to the performance of liquid-electrolyte-based automotive batteries (Zhou et al., 2019). Figure 2.4 presents the schematic structure of an LIB employing SPE, highlighting its key components, including the anode, cathode, electrolyte, and current collector, showing a magnified view of the Li|SPE|$LiFePO_4$ cell configuration with carbon black for enhanced conductivity.

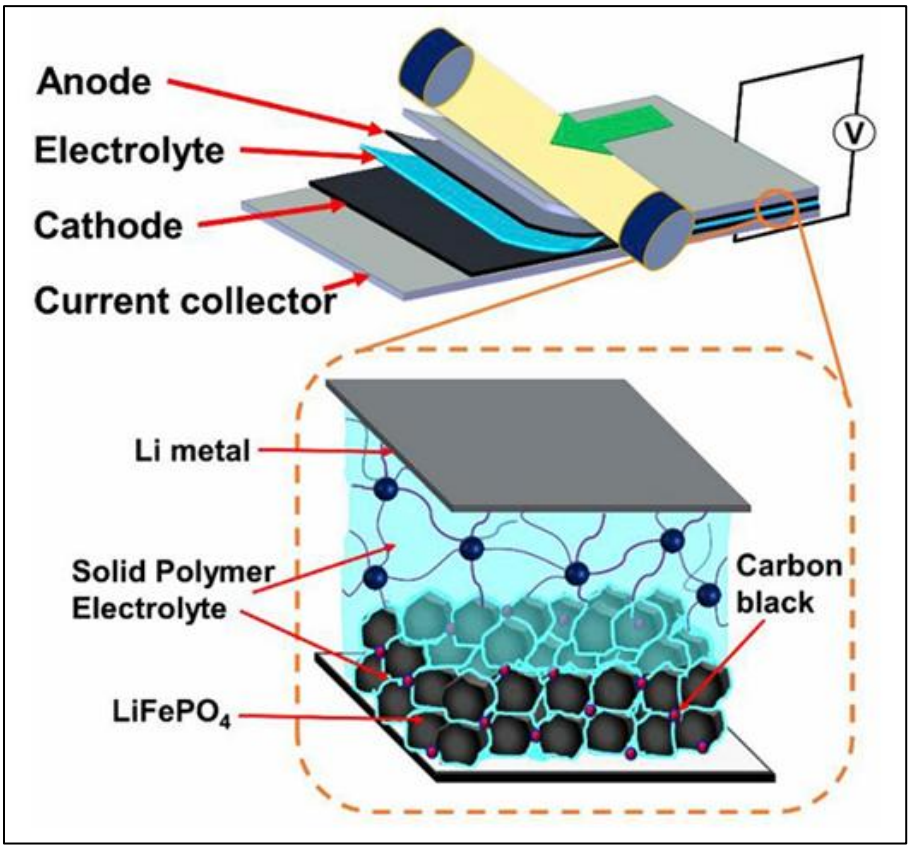

Figure 2.4 Schematic representation of an LIB incorporating an SPE. The top illustration shows the layered configuration consisting of the anode, cathode, electrolyte, and current collector, while the enlarged view highlights the Li metal anode, SPE, and $LiFePO_4$ cathode with carbon black as a conductive additive

(Hsu et al., 2020)

This figure shows that in this battery configuration, the outer region of the free-standing film was effectively integrated with the cathode layer through the SPE embedded within it, while the central region of the film preserved its mechanical strength and reliably separated the cathode from the anode. The strong compatibility between the SPE within the cathode and the free-standing film facilitated rapid Li^+ transport across the electrolyte-cathode interface. Figure 2.4 illustrates that this design demonstrates the practicality of roll-to-roll fabrication for Li|SPE|$LiFePO_4$ batteries using the proposed free-standing SPE.

All-solid-state LIBs have attracted considerable interest owing to the dependable nature of their solid electrolyte components. Flexible solid electrolytes based on PEO are extensively studied; however, their low Li ion conductivity, typically

in the range of 10^{-8} to 10^{-6} S/cm at room temperature, remains a significant challenge. The use of SPEs aligns with the research objective of developing PANI-based SPE membranes with improved electrochemical performance, particularly in terms of conductivity, morphology, and chemical structure. This approach directly addresses the research questions related to the effects of formulation, PANI concentration, and overoxidation on the overall properties of the SPEs.

Hsu et al. (2020) studied the development of a networked SPE designed to address the safety and performance limitations of conventional liquid and gel electrolytes in LIBs. Unlike traditional polymer electrolytes that often rely on solvents, ionic liquids, or semisolid additives, the proposed SPE is a solvent-free system that integrates LiTFSI within a polymer framework reinforced by polyhedral oligomeric silsesquioxane (POSS) hubs. These POSS units act as cross-linking centres, connecting poly(ethylene oxide-co-propylene oxide) (P(EO-co-PO)) chains into a robust three-dimensional network. This architecture minimizes chain entanglement, enhances salt dissociation, and promotes selective Li^+ transport. The SPE exhibits high ionic conductivity at room temperature, a low activation energy for ion movement, and a high lithium transference number, making it highly efficient for Li^+ conduction. To demonstrate its practical application, the researchers assembled a Li|SPE|$LiFePO_4$ cell using a free-standing SPE membrane. The battery delivered high discharge capacity, stable cycling performance, and strong mechanical integrity, while the electrolyte firmly partitioned the anode and cathode and enabled fast Li^+ transfer across the interface. Importantly, the free-standing nature of the SPE membrane supports roll-to-roll processing, highlighting its scalability for industrial LIB manufacturing.

2.2.2.1 Ion Transport Mechanism in SPE

In SPEs, ion transport is a complicated mechanism that occurs through the polymer matrix and typically involves a combination of ion hopping between coordination sites and the segmental motion of the polymer chains. The polymer host in SPEs facilitates the delivery of Li ions through the motion of segments within the amorphous sections (Chen et al., 2021). SPEs are made by dissolving ionic salts like Li ion salts into coordinating polar polymer hosts, such as PEO and PPO. The film or

membrane is then cast using either the traditional solution-cast method or a recently developed hot-press technique. PEO and PPO are polyether, a type of polymer comprising monomers connected by ether linkages, which are two carbon atoms bound to one oxygen atom (Umoren et al., 2022). Depending on the mobility of the chain segment, polymers that have electron-donating groups like carbonyl or ether groups can coordinate with Li ions and subsequently transfer Li ions. PEO is a polymer that exhibits both crystalline and amorphous phases, in which Li ions can normally only be conducted via the amorphous phase. Li ions can follow the motion of flexible chain segments by coordinating with ether oxygen atoms on the backbone, as shown in Figure 2.2 (Chen et al., 2021). Furthermore, Li ions can hop between two major chains at high temperatures, facilitating ion transport.

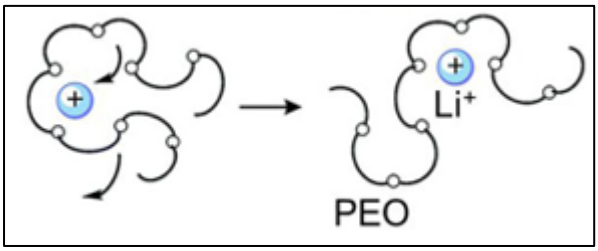

Figure 2.5 Ion transport mechanism in the amorphous section of PEO

(Chen et al., 2021)

This figure illustrates the mechanism of Li ion transport in PEO; a polymer commonly used as a solid electrolyte in LIBs. The black curved lines represent the PEO polymer backbone, and the small circles along the chain represent ether oxygen atoms that can coordinate with lithium ions (Li^+). The Li ion, shown as a blue circle with a positive charge, becomes solvated by these oxygen atoms, forming coordination complexes. As the polymer segments move, the Li^+ ion can hop from one coordination site to another, enabling its migration through the polymer matrix. This hopping process is the basis of ionic conductivity in PEO-based electrolytes and allows Li ions to move effectively in solid-state battery systems.

PEO and PPO are favourable polymer hosts for SPEs as they create stable dry compounds that demonstrate a relatively greater ionic conductivity than other solvating polymers due to the arrangement of oxyethylene groups ($-CH_2-CH_2-O-$) and polar

groups (-O-, -H-, -C-H-) within the polymer chains. These groups can dissolve the ionic salts (Agrawal & Pandey, 2008). Figure 2.6 shows the chemical structure of PEO and PPO.

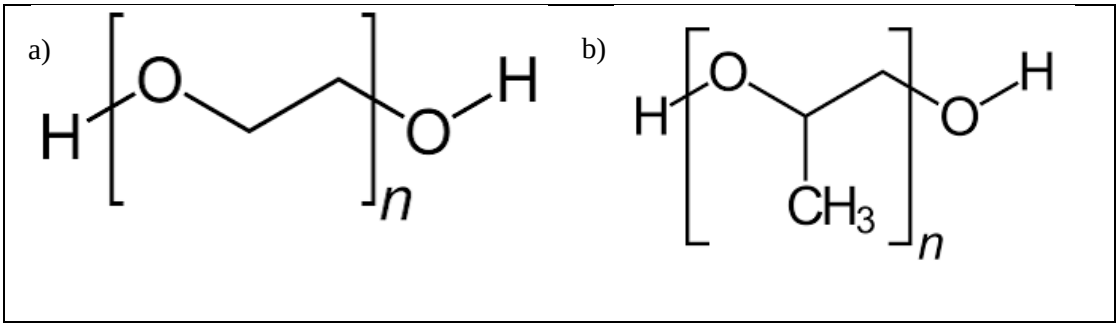

Figure 2.6 Chemical structure of (a) PEO and (b) PPO

Adapted from Al-Akhras et al. (2023); Alsabagh et al. (2016)

This figure shows the chemical structures of two polymers: (a) PEO and (b) PPO. In part (a), PEO consists of repeating units of $-CH_2-CH_2-O-$, with ether oxygen atoms along the polymer backbone. These oxygen atoms are important because they can coordinate with lithium ions, making PEO a widely studied polymer electrolyte material. In part (b), PPO has a similar repeating structure but with an additional methyl group ($-CH_3$) attached to the carbon adjacent to the oxygen atom, giving the repeating unit $-CH(CH_3)-CH_2-O-$. This structural difference makes PPO more hydrophobic and less crystalline compared to PEO, which influences its mechanical and transport properties. Overall, the figure highlights the structural similarity between PEO and PPO, while also emphasizing the key difference that the presence of the methyl group in PPO alters its physical and chemical behaviour.

PEO is a non-ionic polymer with a high molecular weight, featuring a hydrophilic, linear, and non-cross-linked structure, and it dissolves readily in both aqueous and organic solvents (Gelardi et al., 2016). Figure 2.6. a) shows the chemical structure of the ethylene oxide repeating unit, which consists of a hydrophobic ethylene group and a hydrophilic oxygen atom that also serves as a hydrogen-bonding site. PEOs are produced through the polymerization of ethylene oxide in the presence of a metallic catalyst. They are available across a broad molecular weight range, from 200 to 7.0 ×

10^6 g/mol, with the low-molecular-weight variants referred to as PEGs. These polymers are fully soluble in both cold and warm water (Gelardi et al., 2016). Unlike PEO, PPO is insoluble in water at room temperature, as the additional methyl group in each repeating unit provides steric hindrance that shields the polymer backbone (Umoren et al., 2022). Figure 2.6. b) shows that PPO consists of a repeating unit of $-(CH_2CH(-CH_3)O)_n-$ with the presence of a methyl group in each unit.

The complexes of polyether to lithium salt have ionic conductivity in the order of 10^{-8} to 10^{-7} at ambient temperature due to their high crystallinity. A high crystallinity can hinder the ionic transport of SPE, as the movement of ions through SPEs typically occurs in an amorphous state. Ions' movement in SPEs is facilitated by the segmental motion of the polymer chains (Leš & Jordan, 2020). Thus, modification needs to be done to enhance the amorphous region of the SPE, as ionic conduction primarily occurs through the amorphous phase, where polymer chain mobility is higher. Increasing the amorphous content can facilitate the segmental motion of polymer chains, which in turn improves the transport of lithium ions. This can be achieved through polymer blending, plasticization, or by incorporating conductive fillers. In this study, the blending of PEO with PVDF is used as a strategy to disrupt the crystalline regions of PEO and promote amorphous phase formation, thereby enhancing ionic conductivity. This modification supports the research objective of improving the electrochemical properties of PANI-based SPEs and directly contributes to addressing the research questions on conductivity and structural changes due to formulation and overoxidation.

2.3 Composite Materials for Conducting Polymers (CPs)-based Solid Polymer Electrolytes (SPEs)

2.3.1 Conducting Polymers (CPs)

CPs are organic polymers with a π-conjugated structure. This structure includes aliphatic monomer chains like polyacetylene and aromatic monomer compounds such as phenylene, thiophene, pyrrole, and aniline. CPs have garnered significant research interest due to their remarkable properties, including enhanced environmental stability compared to conventional inorganic materials and electrical conductivity that spans

from semiconducting to metallic behaviour (Namsheer & Rout, 2021). They exhibit electronic conductivity due to mobile charge carriers that can travel along conjugated segments of the polymer and hop between them (Holze, 2022). They enable the conduction of electricity through a sequence of alternating single and double bonds along the polymer backbone. Moreover, the electrical conductivity of CPs can be adjusted through doping within the polymer matrix.

Compositing SPEs with CPs results in an IPN, which enhances ion transport pathways and mechanical stability. The basis of this IPN creates a prospect for developing interpenetrating materials-CPs. Hence, research on using CPs as materials for electrodes and separators in LIBs is being done (Leš & Jordan, 2020). IPN structure improves the SPE's overall ionic conductivity and structural integrity, making it highly beneficial for LIB applications by facilitating efficient ion movement and reducing the risk of electrolyte degradation. CPs are a unique class of organic materials that combine the flexibility and processability of polymers with the electrical conductivity of metals or semiconductors, making them highly valuable for applications in electronics, energy storage, and sensors. Figure 2.7 presents examples of CPs, including polyacetylene, PT, PEDOT, PPy, PPO, and PANI, which highlight the structural diversity and functionality of this class of materials. These polymers possess unsaturated backbones that host delocalized π-electrons, which can move freely to create conductive pathways for mobile charge carriers.

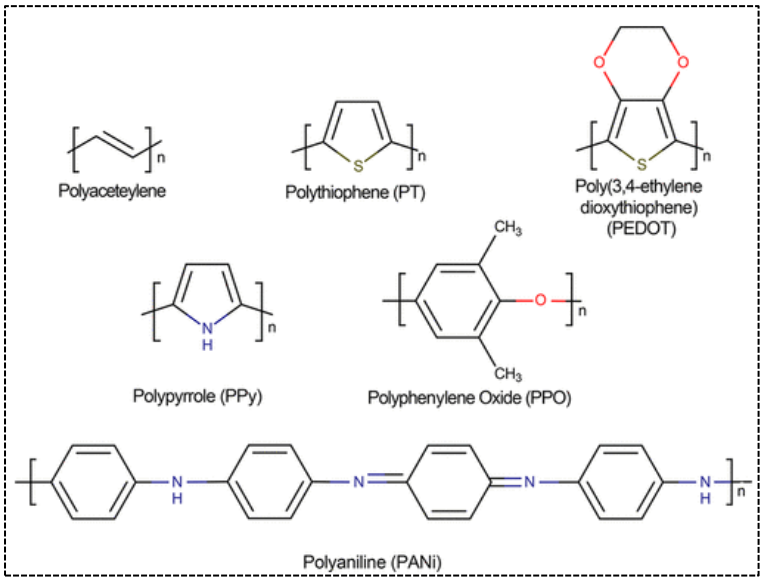

Figure 2.7 Chemical structures of representative CPs, including polyacetylene, PT, PEDOT, PPy, PPO, and PANI

(Nezakati et al., 2018)

This figure presents the chemical structures of several well-known CPs. At the top left is polyacetylene, one of the earliest discovered CPs, consisting of alternating single and double bonds along its backbone. Next to it is PT, a sulphur-containing heterocyclic polymer widely studied for electronic applications. PEDOT, shown to the right, is a derivative of polythiophene with additional oxygen-containing groups that enhance stability and conductivity. Below, PPy contains nitrogen in its five-membered heterocyclic ring, while PPO has aromatic rings with oxygen substituents, making it a useful engineering thermoplastic. At the bottom, PANI is displayed, featuring alternating benzene rings connected by nitrogen atoms, which can be doped to achieve tunable conductivity. Together, these structures highlight the diversity of conducting polymers, each with unique chemical features that contribute to their electrical, mechanical, and chemical properties.

2.3.2 Interpenetrating Polymer Network (IPN) of CP-SPE Composites

The ionic conductivity of an SPE can be improved by suppressing the crystallization of its host polymer chains, such as PEO, as ionic transport primarily occurs in the amorphous regions, where the increased flexibility and segmental motion of the polymer chains facilitate ion movement. This can be achieved by introducing an IPN into the SPE to disrupt crystallinity and promote amorphous structure formation (Murata et al., 2000). While CPs and SPEs are polymeric materials, their roles differ; CPs mainly contribute to electronic conductivity, whereas SPEs are responsible for ionic conductivity. Therefore, it is crucial to target the crystallinity of the polymer matrix responsible for ionic conduction (e.g., PEO) while also considering the structural impact of incorporating CPs like PANI, which may influence the overall morphology and conductivity balance of the system.

IPN is a type of polymer in which two or more polymer networks are interlaced on a molecular scale. The networks are not covalently bonded to each other, but they are physically entangled so that they cannot be separated without breaking chemical bonds (Purkait et al., 2018). It has been proven that IPN can increase the ionic conductivity and mechanical properties of SPEs by reducing their crystallinity (Tan et al., 2018). This good property leads IPN to be exploited in LIB applications. Besides, IPN is also used in supercapacitors and solar cells. For instance, Fong et al. (2017) invented a supercapacitor electrode made up of poly (3,4-ethylene dioxythiophene) (PEDOT), which is an electronically conductive polymer (CP), within an ionically conducting polymer matrix. This research focused on developing PEDOT's sIPNs with PEO, an ionically conducting polymer, and comparing them to the bare PEDOT. This study found that this sIPN electrode exhibits a greater specific capacitance value than bare PEDOT, due to the morphology of the sIPN, shown in Figure 2.8.

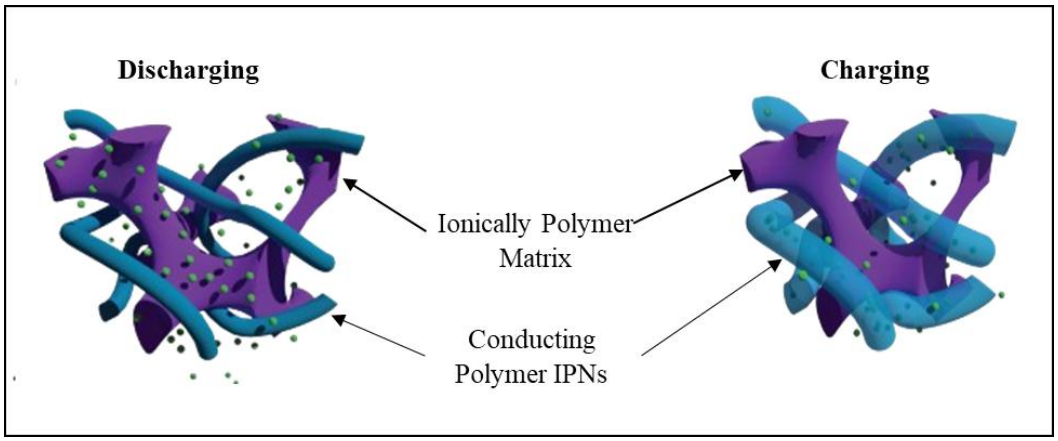

Figure 2.8 Schematic illustration of the morphology of the sIPN.

Adapted from Fong et al. (2017)

This figure shows that an ionically conductive polymer, PEO, stores ions in its matrix surrounding PEDOT, an electrically conducting polymer. Thus, the distance over which ions diffuse through the electrode decreases, enabling PEDOT to store charges. Siddhanta & Gangopadhyay (2005) synthesized a new sIPN gel that combines PANI and poly (2-acrylamido-2-methyl propanesulphonicacid) (PAMPS). The pure PAMPS gel's conductivity was $\leq 10^{-5}$ S/cm, an order of magnitude lower than that of the PANI-PAMPS composite. The resulting gel has a good electrical conductivity, swellability, and mechanical strength.

2.3.3 Polyaniline (PANI) as a Composite Material for CP-SPE Composites

PPy and PEDOT are among the most widely studied CPs due to their excellent electrical conductivity and stability. However, despite these advantages, their inherent limitations make them less suitable for this research. In the case of PPy, it is not easy to obtain a homogeneous material with a uniform structure, and it often forms very thick films that are challenging to control in terms of thickness. Furthermore, synthesizing rigid, insoluble polymer structures remains a significant challenge (Pang et al., 2021). In the case of PEDOT, maintaining the film thickness can be challenging, and issues with poor adhesion to the substrate are commonly encountered, which may affect the

overall performance and stability of the material in practical applications (Fenoy et al., 2021). PANI is a promising material to be incorporated into the CP-SPE system, as it is easy to synthesize, has a low-cost monomer, and is stable (Bhadra et al., 2009). PANI is a CP created through the oxidative polymerization of aniline. This material boasts a variety of characteristics, encompassing electrical conductivity, optical features, and redox behaviour (Holze, 2022; Patil et al., 1988; Plieth et al., 2006). Due to its diverse properties, it has been extensively researched for its potential applications in batteries, sensors, solar cells, and actuators. PANI can be formed as a thin film that has magnetic, redox, antioxidant, anticorrosive, electrical, and sensing attributes. PANI, being a highly conductive polymer, has garnered significant interest owing to its exceptional properties, simple synthesis, cost-effectiveness, and environmental resilience across a range of applications such as electronics, pharmaceuticals, and anti-corrosion materials (Beygisangchin et al., 2021).

During aniline polymerization, PANI exists in one of three idealized oxidation states, which are leucoemeraldine (white or clear), emeraldine (salt-green and base-blue), and pernigraniline (violet or blue). When PANI is fully oxidized, it is recognizable as pernigraniline base. Half of the oxidized PANI is reduced to the emeraldine base, while fully reduced PANI is called leucoemeraldine. Among the different forms, emeraldine is the most stable and conductive, exhibiting a conductivity of approximately 10^{-10} S/cm in its base form, while its salt form demonstrates a significantly higher conductivity of around 30 S/cm (Beygisangchin et al., 2021). This is why emeraldine salt of PANI was chosen for this research, as its enhanced conductivity makes it more suitable for electrochemical applications. The emeraldine salt form is produced by doping the emeraldine base with acids, preferably non-oxidizing ones such as hydrochloric acid (HCl), sulphuric acid (H_2SO_4), or various organic acids, through a process known as oxidative doping. Figure 2.9 shows the chemical structure of PANI in its respective oxidation states.

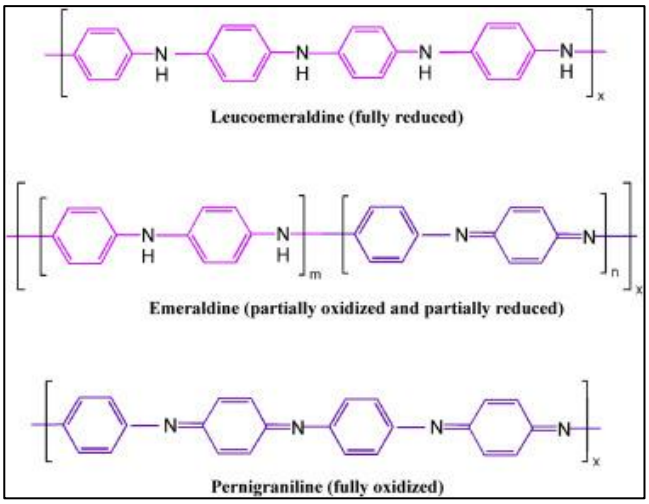

Figure 2.9 Chemical structure of PANI in different oxidation states

(Bhandari, 2017)

As shown in Figure 2.9, PANI can exist in multiple oxidation states. In its fully reduced leucoemeraldine form, the polymer consists of benzenoid (B) units where hydrogen atoms are bonded to the nitrogen atoms. In contrast, the fully oxidized pernigraniline form contains quinonoid (Q) units with no hydrogen atoms attached to the nitrogen atoms. The redox state of PANI depends on the ratio of *m* to *n* within its polymer chains. This benzenoid-to-quinonoid ratio (*m:n*, Fig. 2.9) is ideally 1:0 for fully reduced leucoemeraldine, 0:1 for fully oxidized pernigraniline, and 1:1 for the partially oxidized emeraldine state. The ratio can be adjusted through synthesis conditions and the degree of doping. While leucoemeraldine (light yellow) and pernigraniline (violet) are non-conductive, the partially doped emeraldine salt exhibits electrical conductivity (Bhandari, 2017).

PANI stands out among other CPs due to its superior thermal stability, processability, and conductivity. Moreover, PANI's economic advantage stems from the lower cost of its monomer, aniline, compared to other CP monomers. The synthesis of PANI is straightforward, allowing for easy tuning of its properties and opening a wide range of potential applications (Bhadra et al., 2009). PANI was synthesized by polymerizing aniline with ammonium persulfate in an acidic medium at room temperature. The reaction was carried out for various durations ranging from 1 to 6 hours. After completion, the resulting PANI was filtered and dried under vacuum to a

constant weight (Armes & Miller, 1988). PANI's superior properties and ease of use make it a compelling choice as SPE over other CPs. PANI as a CP has been combined with PEO in SPE fabrication to improve PEO's ionic conductivity, which is relatively low at ambient temperature (Dissanayake et al., 2020). Although PEO has low Li ion conductivity, its combination with a CP can lead to the formation of an IPN, enhancing overall performance. For instance, Fong et al. (2017) developed a supercapacitor electrode by incorporating PEDOT, an electronically conductive polymer, into an ionically conducting PEO matrix. This study focused on synthesizing sIPNs of PEDOT with PEO and comparing their performance to bare PEDOT. The results showed that the sIPN electrode exhibited a higher specific capacitance than the pure PEDOT.

CPs have attracted significant attention in recent years for a wide range of applications due to their electrical conductivity, which spans from semiconducting to metallic behaviour. PANI exhibits electronic conductivity due to mobile charge carriers that can travel along conjugated segments of the polymer and hop between them (Holze, 2022). They enable the conduction of electricity through a sequence of alternating single and double bonds along the polymer backbone. Moreover, the electrical conductivity of conducting polymers can be adjusted through doping within the polymer matrix.

2.3.4 Polyethylene Oxide (PEO) and Polyvinylidene Fluoride (PVDF) as Composite Materials for CP-SPE Composites

PEO and PVDF have been utilized individually as primary materials for SPEs and combined to develop composite SPEs. PEO is a highly regarded member of the conventional polymer class, known for its low glass transition temperature, exceptional flexibility, and, most importantly, its ability to easily form complexes with various polymers and different salts, an attribute that other polymer hosts cannot readily achieve (Bilal et al., 2019). The discovery of PEO as an SPE material originated from Wright and colleagues' proposal regarding fast ionic conduction in high-molecular-weight PEO doped with sodium salts (Fenton et al., 1964). A few years later, its potential for application in solid-state electrochemical devices was recognized due to its promising technological advantages (Quartarone et al., 1998). Meanwhile, PVDF is a thermoplastic polymer known for its exceptional chemical resistance and thermal

stability, along with distinctive mechanical characteristics, electronic activity, and outstanding aging resistance compared to other thermoplastics. Its distinctive mechanical performance arises from its semicrystalline structure (Bhandari, 2017). Figure 2.10 shows the chemical structure of PVDF with the formula of -(CH_2-CF_2) n-.

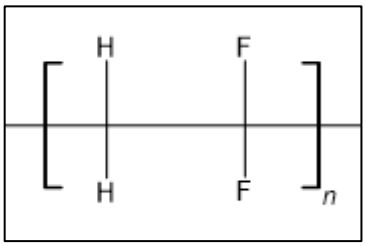

Figure 2.10 Chemical structure of PVDF

Adapted from Damdinov et al. (2021)

PVDF contains backbone fluorine atoms that act as strong electron-withdrawing groups, conferring excellent electrochemical stability and a high dielectric constant, thereby making it a preferred material for membrane preparation. PVDF also possesses a relatively high melting point, outstanding mechanical strength even at elevated temperatures, strong resistance to chemicals, hydrolysis, ultraviolet, wear, ignition, and radiation, as well as physiological inertness and very low thermal conductivity (Dallaev et al., 2022). PVDF and its copolymers are widely utilized as separators in LIBs due to their excellent properties, including high mechanical strength, thermal stability, chemical inertness, and ease of processing (K et al., 2022). Due to their outstanding flexibility and ease of processing, PVDF-based electrolytes hold a potential for use in high-energy-density flexible batteries (Wu et al., 2022). PVDF also offers chemical, thermal, and electrical stability and distinctive piezoelectric and pyroelectric characteristics (Sedlak et al., 2021).

In developing SPEs, combining PEO and PVDF as composite materials has gained significant attention due to their complementary properties and potential to enhance ionic conductivity and mechanical stability. They are favoured over other polymers like PMMA and PAN because of their excellent chemical stability and high dielectric constant (Miao et al., 2008). PEO and PVDF have crystalline structures that restrict the mobility of Li ions. Therefore, polymer blending is a widely used approach

to enhance the performance of polymer electrolytes by reducing the crystalline phase concentration, which in turn improves ionic conductivity and mechanical strength (Nourisabet et al., 2022). Table 2.1 shows various studies on the PEO and PVDF composites as SPEs.

Table2.1
The studies that utilise PEO and PVDF as composite materials for SPEs

Material	**References**
PEO/PVDF/LiTFSI	Li et al. (2022)
PEO/PVDF-HFP/LiTFSI	Manjunatha et al. (2022)
PVDF/PEO/Lithium perchlorate ($LiClO_4$)	Sengwa & Dhatarwal (2020)

Li et al. (2022) studied the optimization of optimal composition of PEO/PVDF-based electrolytes to improve ionic conductivity and found that at a weight ratio of 1:5 for LiTFSI to PEO/PVDF, the electrolyte achieves maximum ionic conductivities of 2.98×10^{-5} S/cm at 30 °C and 5.56×10^{-4} S/cm at 60 °C. Manjunatha et al. (2022) investigated a PEO/PVDF-HFP SPE blend prepared with different concentrations of LiTFSI salt, finding that the blend with 20 wt.% salt achieved the highest ionic conductivity. Sengwa & Dhatarwal (2020) investigated SPE films composed of PVDF/PEO (75/25 wt.%) doped with $LiClO_4$ in the range of 5-30 wt.% to examine how salt concentration affects structure and conductivity. Variations in salt content were found to modify crystallinity and phase composition, thereby impacting ion transport. The maximum conductivity (2.01×10^{-5} S/cm at 27 °C) was achieved at 30 wt %. The study highlights that fine-tuning salt concentration is crucial for enhancing SPE performance in solid-state LIBs. The study presented in this thesis introduces a novel approach by incorporating PANI as a CP into the PEO/PVDF system for SPE enhancement. To date, no research has reported the simultaneous integration of PANI, PVDF, and PEO in a single SPE system. This work fills that gap by investigating the synergistic interactions of these three components, aiming to simultaneously boost ionic conductivity and mechanical stability. Overcoming potential compatibility and

processing challenges, this study opens new pathways for the development of advanced, high-performance materials in energy storage applications.

2.4 Overoxidation of CPs

Overoxidation in CPs occurs when excessive oxidation leads to the degradation of their electrochemical stability, resulting in structural damage and a decline in their conductivity. Overoxidation of CPs can occur during synthesis when oxidizing agents like ammonium persulfate (APS), which facilitate the polymerization of PPy and PANI, encounter gaseous environments such as air (Holze, 2022). Overoxidation in CPs can also occur due to the application of excessively high positive electrode potentials or exposure to aggressive oxidizing conditions. This can lead to substantial changes in their molecular structure and material properties (Holze, 2022). However, overoxidation caused by high voltage typically occurs more rapidly than oxidation from air. High voltage accelerates electron transfer reactions, resulting in more aggressive and immediate oxidation. In contrast, air oxidation progresses at a slower rate, as it relies on the gradual interaction of oxygen with the material, which is influenced by temperature and environmental conditions. Overoxidation can disrupt the conjugated π-system responsible for charge transfer in CPs, leading to alterations in their chemical and physical properties. This degradation reduces the electrical conductivity and introduces defects that compromise the performance of devices such as sensors and energy storage systems. Therefore, controlling the oxidation levels is crucial during the fabrication and processing of CPs. Preventing overoxidation in SPE is particularly important, as it can negatively affect LIB's performance by impairing redox exchange capabilities due to excessive oxidative degradation (Refaey et al., 1999). Although overoxidation is generally considered detrimental to SPEs due to its potential to impair redox exchange capabilities and reduce LIB performance, this study deliberately applies controlled overoxidation to PANI to simulate and understand its effects on the structural and electrical properties of the resulting SPE. By investigating the extent of degradation caused by overoxidation, this research aims to provide insight into how such changes may influence the overall performance of SPEs in LIB applications.

2.4.1 Method and Mechanism of Overoxidation in CPs

Overoxidation in LIBs can occur when an SPE undergoes excessive oxidation, resulting in the formation of unwanted functional groups, such as carbonyl and hydroxyl. To examine the impact of overoxidation on SPEs, an experiment can be conducted to replicate its occurrence in real-life scenarios. To study the effects of overoxidation on SPEs, an overoxidation experiment can be performed to simulate the overoxidation process occurring inside batteries. Overoxidation of CPs involves charging the polymer beyond a certain limit, which leads to permanent loss of electroactivity (Krische & Zagorska, 1989). In their study, Krische and Zagorska used CV to investigate this phenomenon in polybithiophene. They observed two main oxidation waves: a reversible one at lower potential and a much larger, irreversible overoxidation wave at around 1.8 V vs Ag/AgCl. This overoxidation wave had about seven times the charge of the reversible wave and marked the point where the polymer's electroactivity was destroyed. While synthesis factors such as temperature or film thickness had little effect, the type of solvent and supporting electrolyte used during CV significantly influenced the overoxidation behaviour. Substituted bithiophenes showed slightly different responses, with some showing reduced overoxidation charge, suggesting better stability. Overall, their findings emphasize the importance of carefully controlling electrochemical conditions to prevent degradation of CPs through overoxidation.

Mondal & Sangaranarayanan (2016) recorded that overoxidation of PANI can be done using the CV method. In this study, the authors used CV to monitor the overoxidation of PANI films on glassy carbon electrodes. Initially, the CV showed a strong oxidation peak around 0.6 V, indicating the conversion of emeraldine to pernigraniline. However, as the number of cycles increased, this peak disappeared, suggesting that overoxidation had occurred and caused irreversible changes to the polymer. This overoxidation became more pronounced with thicker PANI films, as thicker films showed a shift to higher peak potentials and stronger current in the first scan, meaning more energy was needed to oxidize them. After overoxidation, the CV no longer displayed any peaks, confirming the loss of redox activity. This irreversible behaviour is a clear indication of the transformation from conductive PANI to an overoxidized, non-conductive form. The study also showed that the type of electrolyte

used can influence the extent of overoxidation, with neutral solutions like KCl being more effective than acidic or basic ones. They used a saturated calomel electrode (SCE) as the RE and a Pt wire as the CE. PANI-coated glassy carbon electrodes are the WE, and 0.1 M KCl solutions were used as electrolytes. The WE are where the primary interest lies in observing the effect of the overoxidation processes. A potentiostat regulates the WE's applied potential in response to the RE potential. In an electrochemical cell, a RE serves as a benchmark for measuring the potential of other electrodes. When a potential is applied to the WE, current begins to flow, allowing the analyte to undergo reduction (or oxidation). The purpose of the CE is to complete the electrical circuit. The current is measured when electrons move from, WE to CE (Elgrishi et al., 2018). Analytes either receive or lose electrons at the electrode-electrolyte interface. Figure 2.11 illustrates the diagrammatic depiction of an electrochemical cell used for CV experiments.

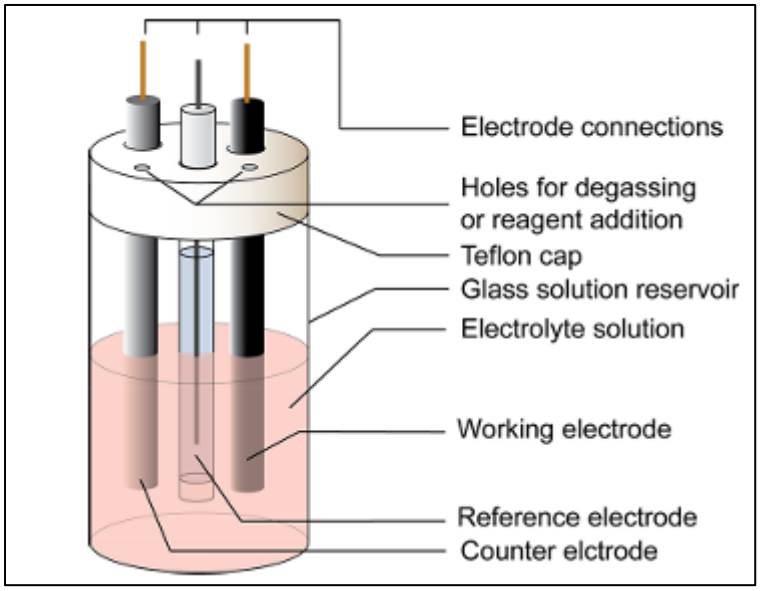

Figure 2.11 A schematic illustration of an electrochemical cell utilized in CV experiments

(Elgrishi et al., 2018)

The figure shows a standard three-electrode electrochemical cell setup used for the CV technique. The main body of the cell consists of a glass solution reservoir containing the electrolyte solution, into which three electrodes are immersed: the WE,

where the electrochemical reaction of interest occurs; the RE, which provides a stable and known potential for accurate measurement; and the CE, which completes the circuit by allowing current to flow between itself and the working electrode. The reservoir is sealed with a Teflon cap equipped with designated holes for electrode insertion, degassing to remove dissolved gases, and the addition of reagents when necessary. Electrode connections are positioned above the cap to enable attachment to a potentiostat or other electrochemical measuring instruments. This configuration helps maintain a controlled and contamination-free environment, ensuring reliable and reproducible measurements of electrochemical behaviour.

Overoxidation disrupts the electrical conductivity of the CP. This process reduces the electroactive capacity of CP as hydroxyl and carbonyl species are formed during the oxidation at positive potentials (Rodríguez et al., 2000). Figure 2.12 shows the mechanism of overoxidation of CP.

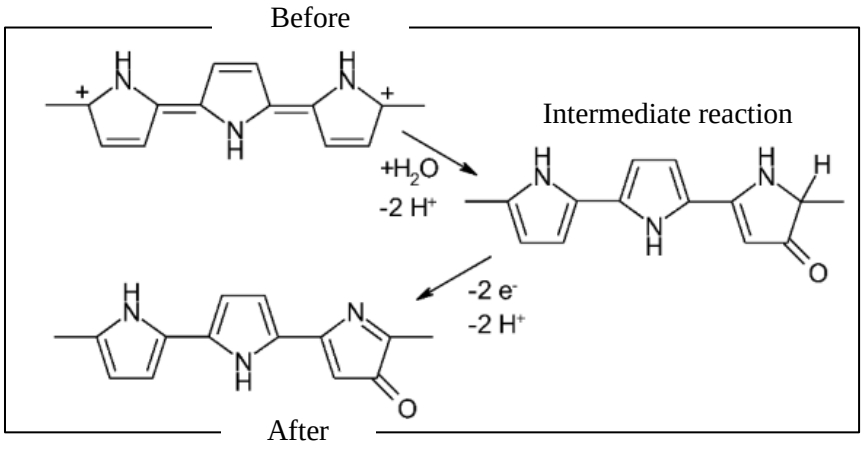

Figure 2.12 The processes of PPy overoxidation, which initiate from the oxidized bipolaronic state (top) and proceed through an intermediate stage. This leads to the formation of PPy-containing pyrrolidone units that disrupt conjugation

(Holze, 2022)

As shown in Figure 2.12, overoxidation adds oxygen and thus alters the PPy structure (Holze, 2022). The top structure represents the oxidized bipolaronic state of PPy, which undergoes a reaction with water, leading to the proton loss ($-2H^+$) and the formation of a partially oxidized intermediate. Further oxidation involves the loss of electrons ($-2e^-$)

and an additional proton removal ($-2H^+$), ultimately resulting in the formation of pyrrolinone units within the PPy backbone. This structural modification interrupts conjugation, which can affect the electrical and electrochemical properties of PPy.

2.4.2 Effects of Overoxidation in CPs

The oxidation of the polymer is generally regarded as a reversible process, whereas overoxidation refers to an irreversible electrochemical reaction that causes excessive oxidation of polymer fragments (Lá et al., 2018). Overoxidation may cause CPs to undergo significant changes in their molecular arrangement and physical characteristics, such as increased brittleness, loss of flexibility, surface roughness, and diminished porosity. These changes, along with the destruction of electroactivity, lead to a reduction in electronic conductivity and charge storage capacity (Holze, 2022). Excessive oxidation also results in the polymer experiencing mass loss (Li & Qian, 2000). Overoxidation in CPs has also been referred to as corrosion due to its degradation effect (Beck et al., 1993). Overoxidation can occur in CP due to the application of excessively high positive electrode potential values or extreme oxidative conditions (Holze, 2022). CP overoxidation takes place when the CP is charged beyond a certain limit (Krische & Zagorska, 1989; Lá et al., 2018).

At high anodic potentials, PANI undergoes electrochemical overoxidation, resulting in substantial degradation and the generation of quinone-like compounds, such as hydroquinone and benzoquinone (HQ/BQ) (Wu & Han, 2005). The quinone derivatives adhere to the PANI chains, potentially interacting with them (Gao et al., 2011). Lá et al. (2018) researched the structural modifications that occur during the overoxidation of PEDOT films electrodeposited from surfactant-free aqueous solutions. When the positive potential limit of the CV extends into the overoxidation region, an oxidation peak appears without a corresponding reduction peak, indicating irreversible changes. Similarly, Ujvári et al. (2011) demonstrated that PEDOT films in modified electrodes undergo structural alterations during overoxidation. These findings align with observations in overoxidized PANI, where irreversible redox behaviour, loss of electroactivity, and structural changes such as reduced conjugation and increased brittleness are also reported. This suggests that, despite differences in polymer type,

overoxidation generally leads to degradation in both PEDOT and PANI through similar electrochemical pathways.

CHAPTER 3
RESEARCH METHODOLOGY

3.1 Introduction

This project was divided into three parts: (i) the fabrication of PANI: PVDF: PEO: LiTFSI SPE, (ii) the overoxidation of the PANI: PVDF: PEO: LiTFSI, using CV, and (iii) the characterisation of PANI: PVDF: PEO: LiTFSI after overoxidation. Phase (iii) aimed to examine the effects of overoxidation on the properties of the SPE through various analytical techniques, including FTIR, XRD, FESEM, and EIS. These phases are closely aligned with the three primary objectives of this research, focusing on the fabrication, modification, and detailed characterisation of the SPE material. All experimental parameters were selected based on prior literature and preliminary considerations to ensure reproducibility and enable systematic evaluation of the effects of PANI content and electrochemical overoxidation on the SPE properties.

3.2 Materials and Chemicals

The materials and chemicals used in this study are listed in Table 3.1:

Table 3.1

Materials and chemicals used in this study

No.	Materials	Brand
1	Polyaniline (PANI)	Sigma-Aldrich
2	Polyethylene oxide (PEO)	Sigma-Aldrich
3	Polyvinylidene fluoride (PVDF)	Sigma-Aldrich
4	N-methylpyrrolidone (NMP, ≥ 99 %)	Sigma-Aldrich

No.	Materials	Brand
5	Lithium bis (trifluoromethanesulfonyl) imide (LiTFSI, ≥ 99 %)	Sigma-Aldrich
6	Potassium chloride (KCl, ≥ 99 %)	Sigma-Aldrich
7	Deionised water	21012 Younglin Water Purifier
8	Silver/silver chloride (Ag/AgCl) reference electrode in a 3 M potassium chloride (KCl) solution	Metrohm
9	1 cm^2 platinum (Pt) sheet as counter electrode	Metrohm

3.3 Methodology and Instrumentation

3.3.1 PANI: PVDF: PEO: LiTFSI Fabrication

Table 3.2 summarizes the formulations of the SPE films fabricated in this study. The blank films consist of PEO (7 wt.%) and PVDF (3 wt.%). Composite films P1, P3, and P5 incorporate PANI at 1 wt.%, 3 wt.%, and 5 wt.% respectively, while maintaining fixed amounts of PEO (7 wt.%), PVDF (3 wt.%), and LiTFSI (2 wt.%).

Table 3.2
Formulations of SPE films fabricated in this study, showing blank films (PEO and PVDF) and composite films (P1, P3, P5) with varying PANI content and fixed PEO, PVDF, and LiTFSI ratios.

Samples	Compositions (%)
PEO	PEO = 7 wt. % (Li et al., 2022)
PVDF	PVDF = 3 wt. % (Li et al., 2022)
P1	PANI: PVDF: PEO: LiTFSI= 1 wt.%: 3 wt.%: 7 wt.%: 2 wt.%
P3	PANI: PVDF: PEO: LiTFSI= 3 wt.%: 3 wt.%: 7 wt.%: 2 wt.%
P5	PANI: PVDF: PEO: LiTFSI= 5 wt.%: 3 wt.%: 7 wt.%: 2 wt.%

The weight percentages of PEO, PVDF, and LiTFSI were selected based on prior optimisation studies of PEO/PVDF-based solid polymer electrolytes, where a PEO: PVDF ratio of 7:3 was reported to provide an optimal balance between ionic conductivity and mechanical stability through the suppression of PEO crystallinity while maintaining sufficient polymer segmental mobility (Li et al., 2022). LiTFSI was incorporated at a fixed proportion relative to the total polymer content to ensure adequate lithium-ion concentration while avoiding ion pairing and salt aggregation, which have been reported to reduce ionic conductivity at higher salt loadings (Li et al., 2022). Fixing the PEO:PVDF:LiTFSI composition ensured a consistent electrolyte matrix across all samples, thereby allowing the effects of PANI content and subsequent electrochemical overoxidation to be systematically isolated and evaluated.

PANI-based SPE films were prepared using the solution-casting method. PANI was first dissolved in NMP solvent at concentrations of 1 wt.% (0.3 g), 3 wt.% (0.9 g), and 5 wt.% (1.5 g) to prepare samples P1, P3, and P5, respectively. Each solution was stirred for 2 hours to ensure complete dispersion of PANI before polymer addition. Subsequently, 7 wt.% (2.2 g) of PEO was added to each solution and stirred for 2 hours, followed by the addition of 3 wt.% (0.9 g) PVDF. The solutions were further stirred for 2 hours to promote homogeneous blending of the polymer matrix. Finally, 2 wt.% (0.6 g) of LiTFSI was introduced, and stirring was continued for an additional 2 hours.

Throughout the preparation process, the temperature was maintained at 60 °C to facilitate polymer dissolution and salt complexation. After the solutions were stirred for 2 hours, the homogeneous solutions were poured into the glass petri dishes (Sigma-Aldrich, soda-lime glass, 150 mm diameter × 25 mm height) and dried in a vacuum oven (Taisite, model VO-24D) at 60 °C for 24 hours. After drying, free-standing films with uniform thickness were formed. The samples were then placed in sealed bags and properly labelled. They were then stored in a vacuum drying chamber set at 40 °C and 25% relative humidity as a precaution to prevent any surface alterations. Figure 3.1 shows the experimental workflow for film fabrication.

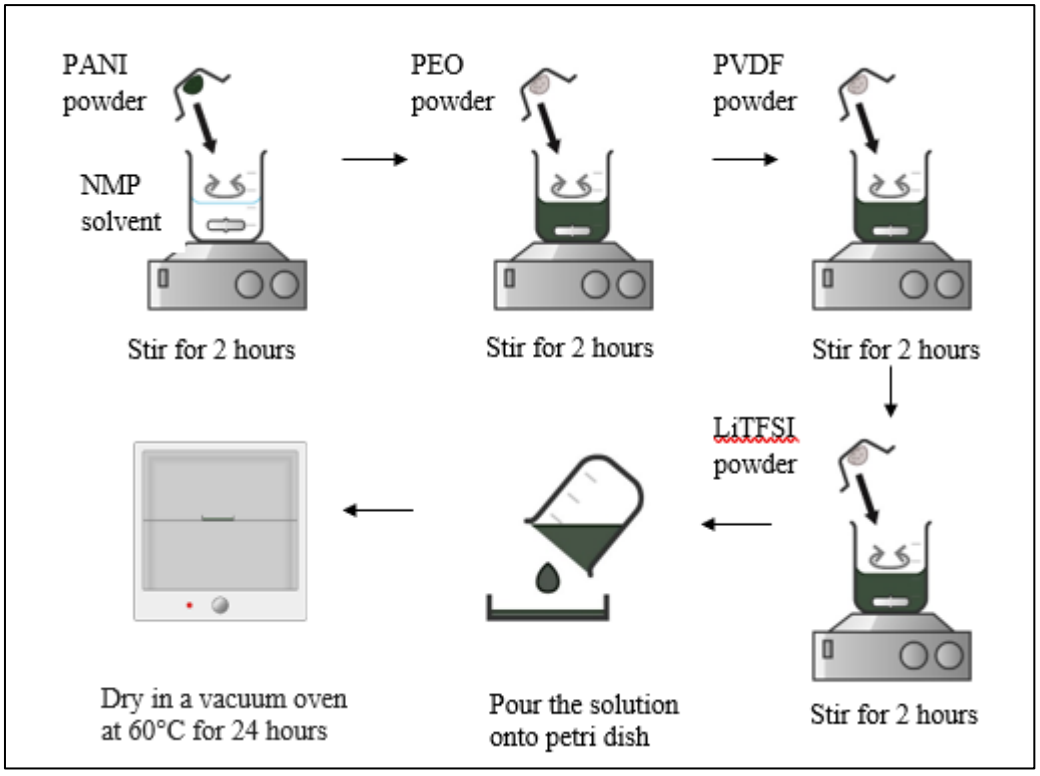

Figure 3.1 Flow for film fabrication by the solvent cast technique

3.3.1 Overoxidation of the PANI: PVDF: PEO: LiTFSI film

Electrochemical overoxidation was carried out by applying a voltage to the film to charge it. Overoxidation increases the ionic conductivity of the film by enhancing the ion-exchange groups and introducing oxygen to the film. The overoxidation of the film was performed using cyclic voltammetry (CV) with a platinum sheet as the counter

electrode (CE), the film as the working electrode (WE), and Ag+/AgCl as the reference electrode (RE). A 0.1 M KCl solution, degassed using dry nitrogen (N_2) gas, was used as the electrolyte. The PANI-SPE film was precisely cut into a square with dimensions of 1 cm × 1 cm, secured using a crocodile clip, and subsequently connected to the WE. The electrochemical reaction occurred at the WE, with the applied potential controlled by a potentiostat (Metrohm AUTOLAB) relative to the RE's potential. The current began to flow when a potential was applied to the WE, allowing for the reduction (or oxidation) of the surface process. The CE completed the electrical circuit, and the current was recorded as electrons flowed between the WE and CE (Elgrishi et al., 2018). The electrolyte acted as a charge carrier to transfer the electrons between the electrode and the species involved in the surface process. The film was subjected to 0-1V at a scan rate of 50 mV/s for 10 cycles to overoxidise it (Mondal & Sangaranarayanan, 2016). The voltage range (0-1 V), scan rate (50 mV s^{-1}), and number of cycles (10 cycles) were selected based on previous studies reporting effective overoxidation of PANI. These parameters were chosen to ensure controlled overoxidation of PANI (Mondal & Sangaranarayanan, 2016). Figure 3.2 illustrates the experimental setup for the overoxidation of SPE films using CV.

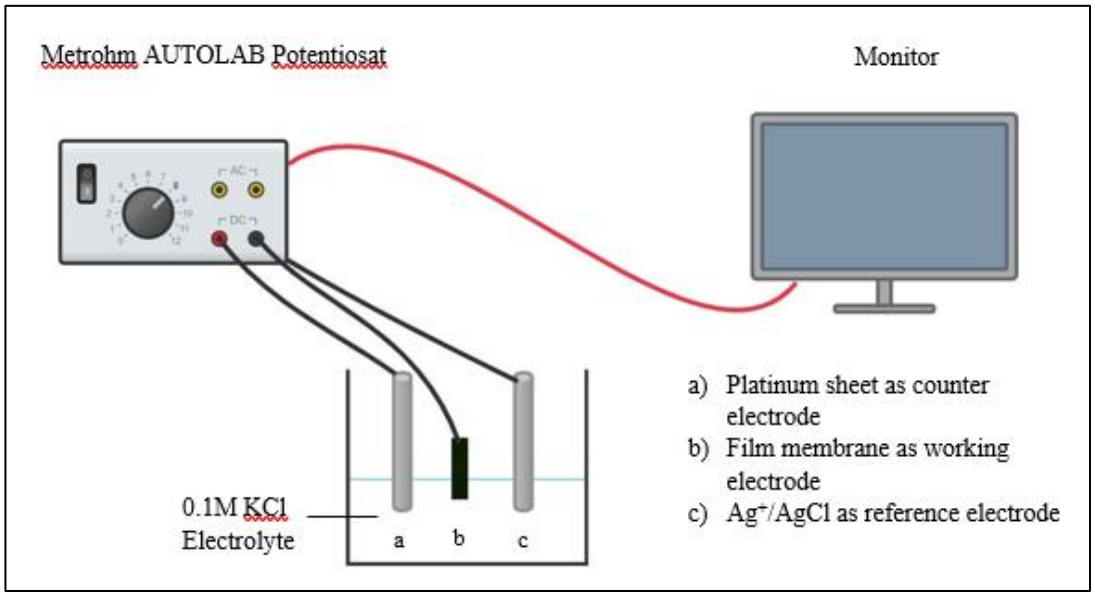

Figure 3.2 The experimental arrangement for the overoxidation of SPE films involved in CV

Figure 3.2 illustrates the schematic representation of the CV setup. The system consists of a Metrohm AUTOLAB potentiostat connected to a three-electrode configuration immersed in 0.1 M KCl electrolyte. The Pt sheet (a) serves as the CE, the film membrane (b) functions as the WE, and the Ag/AgCl electrode (c) acts as the RE. The potentiostat is interfaced with a monitor to record and analyse the electrochemical response. Figure 3.3 presents the actual setup of the CV experiment. The CE, consisting of a Pt sheet, is linked via the black lead, the WE are attached through the red lead, and the RE is connected using the blue lead. All three electrodes are immersed in an aqueous 0.1 M KCl solution that had been degassed by purging with N_2 gas prior to measurement and interfaced with the potentiostat.

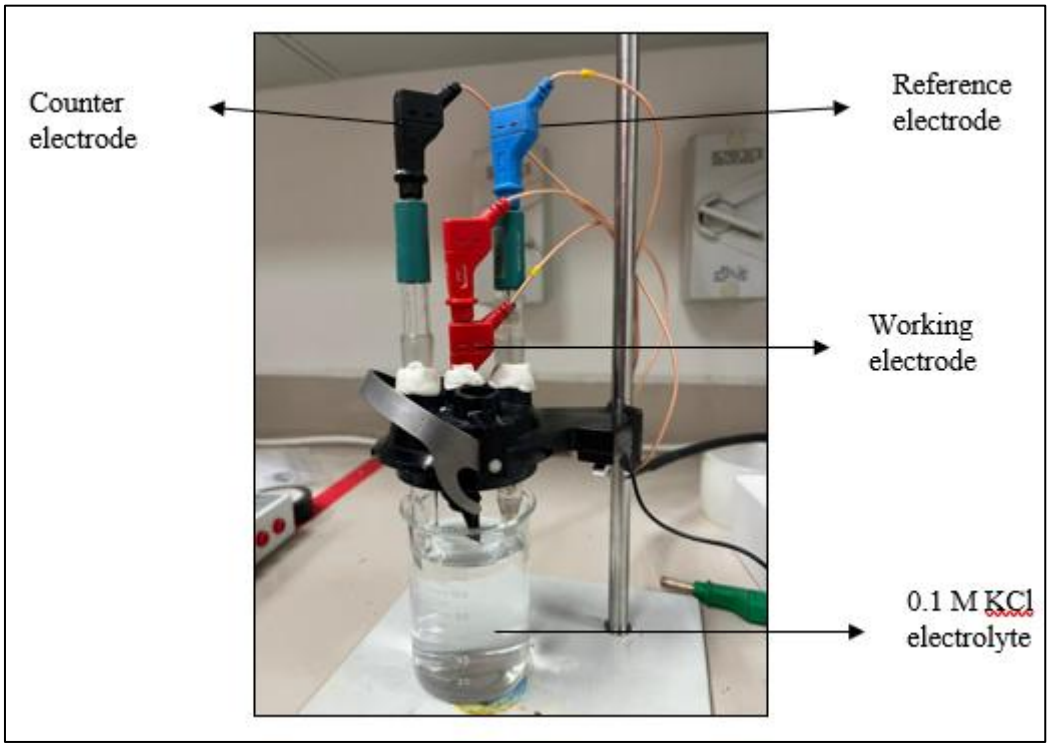

Figure 3.3 Actual setup of the CV experiment using a three-electrode configuration, all electrodes are immersed in an aqueous 0.1 M KCl solution degassed with Nitrogen and connected to the potentiostat

3.4 Characterization of PANI-SPE

3.4.1 Field Emission Scanning Electron Microscopy (FESEM)

FESEM was utilized to observe the surface morphology and microstructural features of the PANI-SPE, providing insight into changes in surface roughness, porosity, and film uniformity after overoxidation. A small portion of the PANI-SPE films was positioned onto an aluminium stub covered with double-sided carbon tape. The samples were sputter-coated with gold to enhance the surface conductivity of the samples, allowing for better imaging under the FESEM. Since PANI and similar polymeric materials are generally non-conductive or semi-conductive, coating them with a thin layer of gold prevents charging effects during electron beam exposure. This results in improved image resolution and contrast, and helps avoid image distortion caused by surface charge accumulation. The stubs were then loaded into a Carl Zeiss Supra 40VP FESEM (Germany) to investigate the surface morphology and microstructure of the samples. The samples were examined under two different magnifications, 1, 000×, and 10, 000× to obtain detailed images of the samples. FESEM images were recorded in high vacuum mode, as gas molecules can interrupt the electron beam and the secondary and backscattered electrons that are emitted and used for imaging (Jaya, 2020). FESEM operated at 10.0 kV electron high tension (EHT).

3.4.2 Fourier-Transform Infrared Spectroscopy (FTIR)

FTIR was used to identify functional groups and confirm chemical interactions among PANI, polymer hosts, and salts, as well as to monitor structural changes associated with overoxidation. The chemical composition of the samples was analysed using the Shimadzu IR Affinity-1 instrument (FTIR). The ASTM E1252 method utilised FTIR to analyse the functional groups in a sample and determine its chemical composition (ASTM International, 2021). The variations in the IR beam induced by these functional groups provided a unique identification signature for the sample. The FTIR instrument was set up to capture 16 scans with a resolution of 4 cm^{-1}, resulting in a series of infrared spectra covering the wavenumber range of 4000 to 500 cm^{-1}. The

increased resolution of 4 cm^{-1} yielded more intricate details regarding the fine structure of the infrared absorption bands, facilitating a more accurate identification of the sample's functional groups. The broader spectral span from 4000 to 500 cm^{-1} included a diverse range of molecular vibrations, encompassing both stretching and bending modes of various chemical bonds. This extensive spectral coverage enabled the detection of a wide array of functional groups, offering a thorough characterization of the chemical composition of the sample.

For FTIR analysis, all film samples were cut into 1 cm^2 squares using a cutter knife. For the PANI and LiTFSI powder, approximately 0.01 g to 0.05 g of sample was used. Prior to scanning, a background spectrum was recorded to eliminate any residual signals originating from the instrument or environment. This was done by ensuring that the ATR crystal surface was completely free of any sample. After the background scan, each sample was placed directly onto the ATR crystal and pressed firmly using a sample presser to ensure good contact for accurate spectral acquisition. All FTIR measurements were performed under identical acquisition conditions to ensure consistency and comparability between pristine and overoxidized samples.

3.4.3 X-Ray Diffraction (XRD)

The phase analysis was carried out using Malvern Panalytical's X'Pert³ diffractometer, which is suitable for both powder and film analysis. The XRD patterns were collected at room temperature with a rotating copper anode, using X-rays of wavelength 1.542 Å. The scanning rate was set to 0.5°/min with a minimum angle step of 0.001°. This analysis was employed to determine the crystalline or amorphous nature of the PANI-SPE films and to evaluate how overoxidation and polymer blending influence crystallinity, which in turn affects ion transport.

3.4.4 Electrochemical Impedance Spectroscopy

The conductivity of the PANI-SPE film was measured using EIS with a HIOKI 3532-50 LCR Hi-TESTER connected to a PGZ100 interface. The measurements were carried out over a frequency range of 42 Hz to 5 MHz at room temperature. The PANI-

SPE film was sandwiched between two cylindrical stainless-steel electrodes, each having an area of 0.1964 cm² and a diameter of 0.5 cm. Prior to measurement, the film thickness was measured at multiple points using a digital micrometre, and the average value was used in conductivity calculations to minimise experimental error. The collected impedance data were plotted as Nyquist plots (imaginary impedance vs. real impedance). The bulk resistance, $R_{b,}$ was obtained from the intercept of the semicircle with the real (Z') axis in the high-frequency region. This value was then used to calculate the conductivity of the film using Equation 3.1:

$$\sigma = \frac{t}{R_b A} \tag{3.1}$$

where σ is the conductivity value, t is the thickness of the film, R_b is the resistance, and A is the area of the film. The instrument setup used for EIS measurements is shown in Figure 3.4. This setup was used to evaluate the conductivity of the PANI-SPE films by analysing impedance over a frequency range of 42 Hz to 5 MHz at room temperature.

Figure 3.4 EIS instrument, HIOKI 3532-50 LCR Hi-TESTER PGZ100

3.5 Flowchart of Methodology

The overall experimental procedures in this study are organised according to the three main research objectives and are summarised in the flowchart shown in Figure 3.5. The first objective focuses on the fabrication of PANI-based SPE films using the solvent casting method. These films were then characterized using FTIR for chemical structure analysis, FESEM for morphological study, XRD for phase identification, and EIS for conductivity measurements. The second objective involves the overoxidation of the PANI-based SPE using a CV approach, where a three-electrode system was employed with 0.1 M KCl as the electrolyte. The scan rate and voltage range were set at 50 mV/s and 0-1 V, respectively. The third objective examines the effects of overoxidation on the PANI-based SPE, with the same characterization techniques applied as in Objective 1 to compare the structural, morphological, and electrical changes. Figure 3.5 presents a clear visual representation of the methodology workflow for each objective.

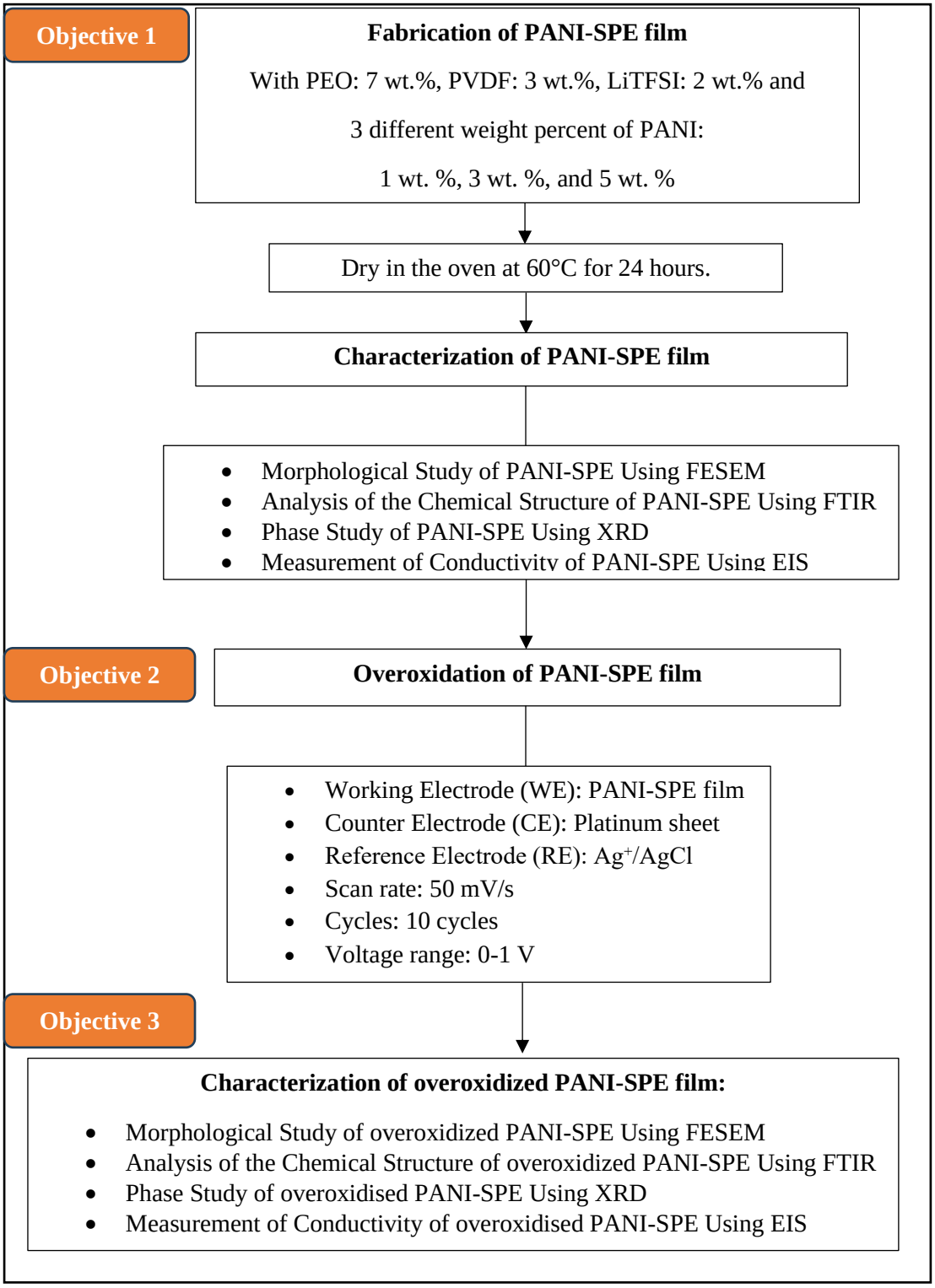

Figure 3.5 Flowchart of the methodology involved in this investigation

CHAPTER 4
RESULTS AND DISCUSSION

4.1 Physical Appearance of PEO, PVDF, and PANI-SPE

Figure 4.1 shows the image of the synthesized polymer electrolyte films, which include pure PEO film, PVDF film, and composites incorporating PANI with PEO, PVDF, and LiTFSI. As shown in Figure 4.1, the films differ in terms of colour, transparency, and surface texture due to their varying compositions. These visual features offer preliminary clues about structural uniformity, flexibility, and compositional effects, which are important aspects that influence their performance in devices such as batteries or sensors.

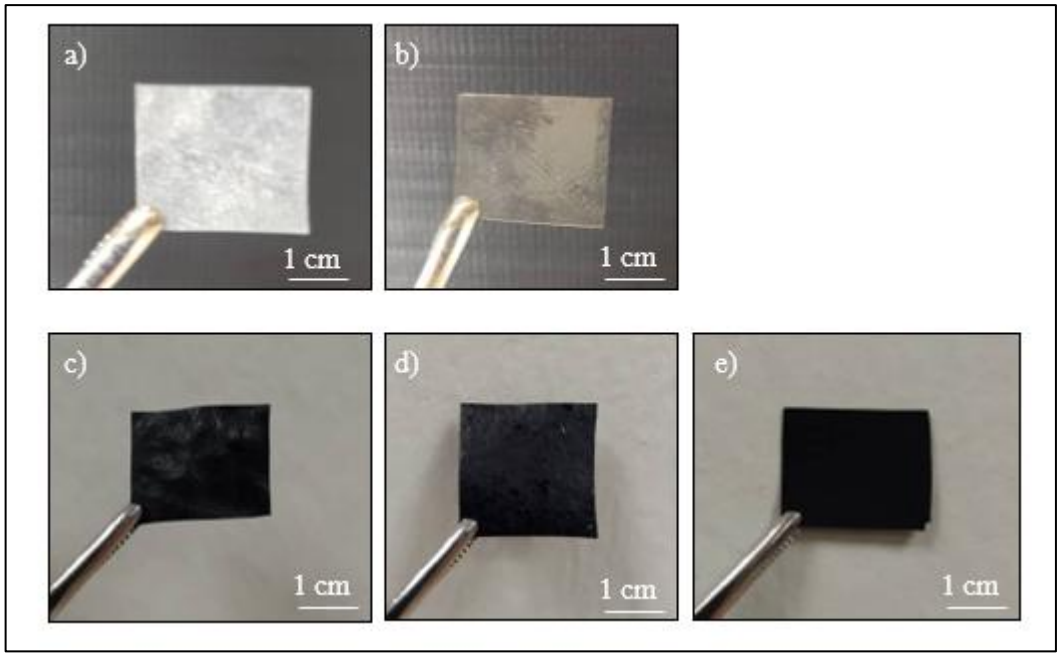

Figure 4.1 The physical appearance of the freshly prepared films: (a) PEO, (b) PVDF, (c) P1, (d) P3, and (e) P5 after being peeled and cut into rectangular shapes with an approximate thickness of 0.02 cm

Figure 4.1 shows the physical appearance of PVDF, PEO, and PANI-SPE films after being dried in an oven at 60 °C for 24 hours and subsequently peeled off. Figure

4.1. a) illustrates the opaque appearance of the PEO film with a smooth and slightly wrinkled surface, reflecting its flexible characteristics (Wang et al., 2024). The FESEM image is shown in Figure 4.2. a), which will be discussed later, further supports this observation. The PVDF film is shown in Figure 4.1. b) appears to be semi-reflective or shiny, typical for casted or spin-coated PVDF films. The PANI-SPE film, consisting of PANI, PVDF, PEO, and LiTFSI in Figure 4.1. c), 4.1. d), and 4.1. e) appeared green in color because of the presence of PANI in its emeraldine salt form, which naturally exhibits a green hue (Fenniche et al., 2022). The uniform colour distribution and absence of visible phase separation in the PANI-SPE films suggest good miscibility among PANI, PEO, PVDF, and LiTFSI. Such visual homogeneity is often associated with favourable interactions between the polymer components and the lithium salt, which are critical for achieving stable ion-conducting pathways in solid polymer electrolytes.

4.2 Properties of PANI-SPE

4.2.1 Morphological Study of PANI-SPE Using FESEM

The surface morphology and microstructural characteristics of the synthesized polymer electrolyte films were analysed using FESEM at a magnification of 10,000×. Figure 4.2 displays micrographs of (a) pure PEO, (b) pure PVDF, and (c–e) PANI-SPE composites (P1, P3, P5), obtained under high vacuum conditions with an Everhart-Thornley detector (ETD). These detailed images highlight key structural features such as surface uniformity, porosity, phase distribution, and interactions between polymer and crystalline domains that play a vital role in determining the films' conductivity and mechanical robustness for electrolyte-based applications.

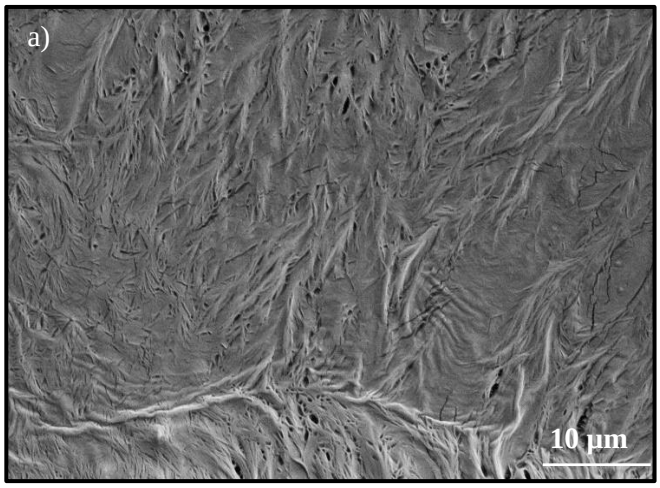
a)
10 µm

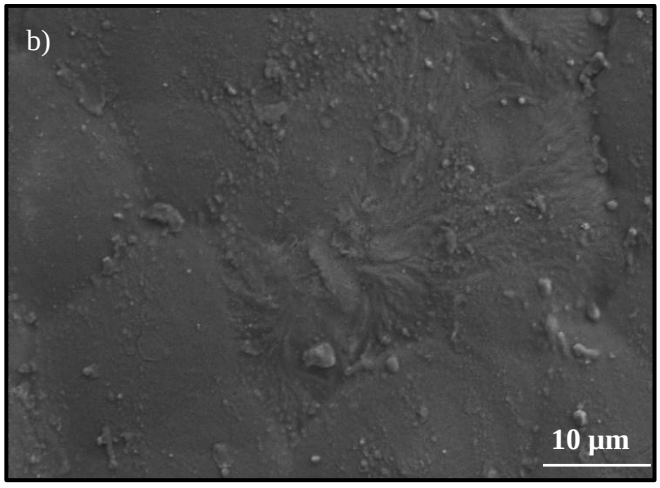
b)
10 µm

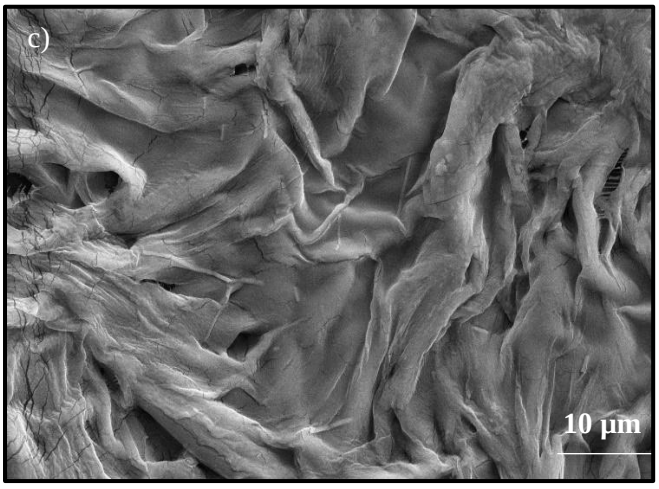
c)
10 µm

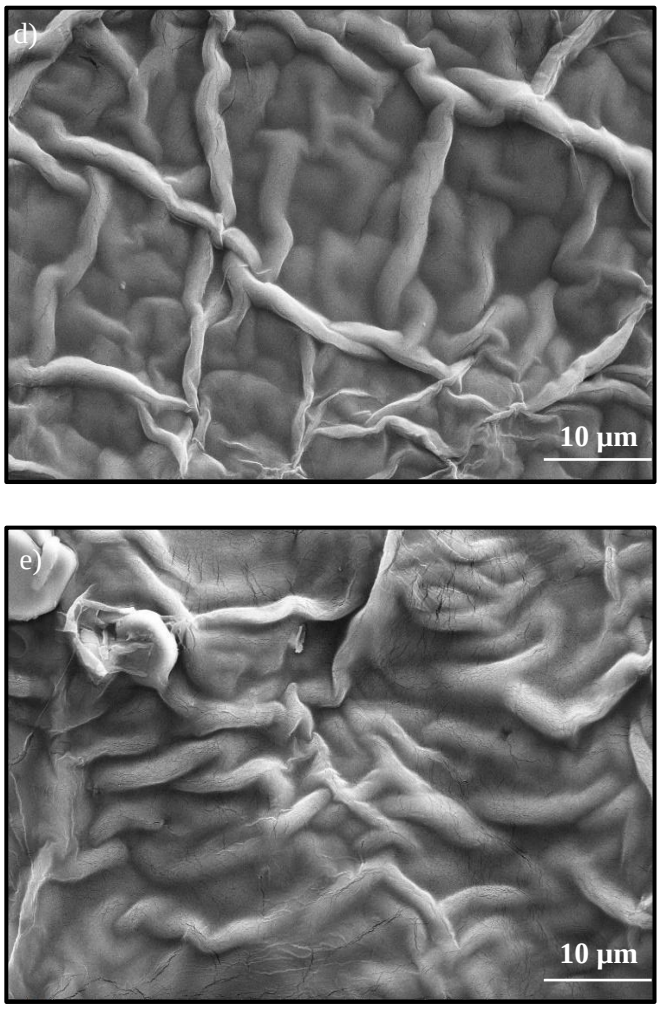

Figure 4.2 FESEM images of (a) PEO film, (b) PVDF film, (c) P1 film, (d) P3 film, and (e) P5 film, taken at a magnification of 10,000× using the ETD in high vacuum mode. The scale bar is shown in every figure.

A detailed analysis of the films' surface morphology was conducted to gain deeper insight into how varying concentrations of PANI influence the composite films. The FESEM images reveal significant differences in the microstructures of the films. Figure 4.2 presents FESEM images of the PEO film, PVDF film, and composite films containing PANI, PEO, PVDF, and LiTFSI with varying PANI concentrations (1, 3, and 5 wt.%). The FESEM image of pure PEO, Fig. 4.2. a), reveals a rough surface morphology with areas of smoother texture, which is attributed to its semi-crystalline

structure (Arya & Sharma, 2019). In Figure 4.2. b), the FESEM image of the PVDF film at 10,000× magnification reveals a smooth, uniform surface free from cracks or tears. The PVDF's FESEM image highlights the presence of numerous spherical structures uniformly distributed across the surface, without any distinct pattern. The surface morphology of PVDF shows the formation of spherulitic structures, consistent with the findings reported by Sarkar et al (2022). The absence of visible pores suggests a compact structure. Due to the low porosity, ion transport in PVDF might be limited.

The presence of PANI appears to enhance lithium salt dispersion, as no crystalline formations were observed in Figure 4.2. c)-e). Introducing PANI into the composite films significantly influences their morphology and structural properties. The composite films consisting of PANI, PEO, PVDF, and LiTFSI demonstrate the formation of an IPN, where multiple polymer chains intertwine at the molecular level without forming covalent bonds, resulting in a physically entangled network (Purkait et al., 2018). Duan et al. (2018) reported an enhancement in both ionic conductivity and mechanical strength of SPEs with the incorporation of IPNs, using polymers such as poly(ethylene glycol) diacrylate (PEGDA) and poly(ethylene glycol) diglycidyl ether (PEGDE). The P1 film (1 wt.% PANI) displayed a porous structure, whereas P3 and P5 films (3 wt.% and 5 wt.% PANI) appeared non-porous. This suggests that increasing the PANI concentration promotes a denser network, facilitating tighter interchain packing within the polymer structure. This densification is attributed to the strong interactions between PANI and the host polymers, PEO, and PVDF. From a molecular perspective, the densification observed at higher PANI content can be attributed to enhanced intermolecular interactions between PANI chains and the host polymers. The nitrogen-containing functional groups in PANI can interact with the ether oxygen atoms of PEO and the polar C-F dipoles of PVDF through hydrogen bonding and dipole-dipole interactions. These interactions restrict polymer chain mobility, suppress pore formation, and promote a more compact IPN. While such structural compactness improves mechanical integrity, it may simultaneously reduce free volume available for ion migration, highlighting the inherent trade-off between mechanical stability and ionic conductivity in SPE systems.

4.2.2 Analysis of The Chemical Structure of PANI-SPE Using FTIR

Figure 4.3 illustrates the chemical structures of PANI, PEO, PVDF, and LiTFSI. The backbone of PANI is composed of alternating benzene and nitrogen units. It features both benzenoid and quinonoid rings, where the benzenoid ring includes a benzene unit, and the quinonoid ring consists of a six-membered carbon ring with two conjugated double bonds (Tang et al., 2009). PEO contains ether oxygen atoms that facilitate the transport of lithium ions along its polymer chains (Chen et al., 2021). PVDF is a semicrystalline polymer made up of repeating vinylidene fluoride units and strong C–F bonds. Vinylidene is a key component in PVDF copolymers, featuring a distinct molecular arrangement of carbon and fluorine atoms that enables the material to exhibit highly ordered crystalline ferroelectric behaviour, particularly in thin film form (Dowben et al., 2009). As a semi-crystalline thermoplastic, PVDF demonstrates stable chemical, thermal, and mechanical properties across a broad temperature range (Dallaev et al., 2022). LiTFSI contains a large and asymmetric anion, $(CF_3SO_2)_2N^-$.

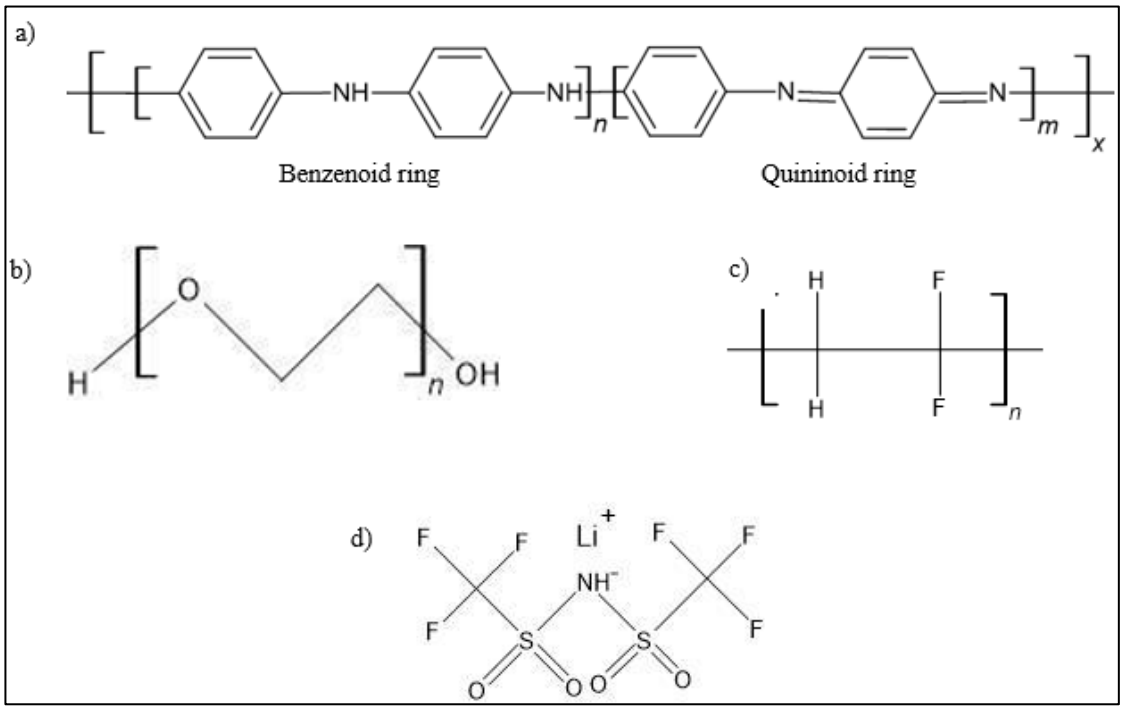

Figure 4.3 Chemical structures of (a) PANI, (b) PEO, (c) PVDF, and (d) LiTFSI

FTIR is an analytical technique based on the principle that molecules absorb distinct frequencies of infrared light that match the vibrational modes of their chemical bonds. This absorption generates a unique spectrum, which can be used to identify functional groups and determine the molecular structure of a sample (Tiquia-Arashiro et al., 2023). Figure 4.4 presents the FTIR spectra of pure PANI, PEO, PVDF, and LiTFSI, which serve as reference benchmarks for comparison. Since PANI and LiTFSI do not easily form self-supporting films, they were examined in powder form, whereas PEO, PVDF, and the composite samples were analysed in film form. The comparison between the powder and film forms is valid, despite morphological differences, as their chemical structures remain unchanged and their spectral profiles are largely similar. The figure also includes FTIR spectra of the composite films with varying PANI content, specifically at 1, 3, and 5 wt. %, to observe the impact of PANI concentration on the chemical structure.

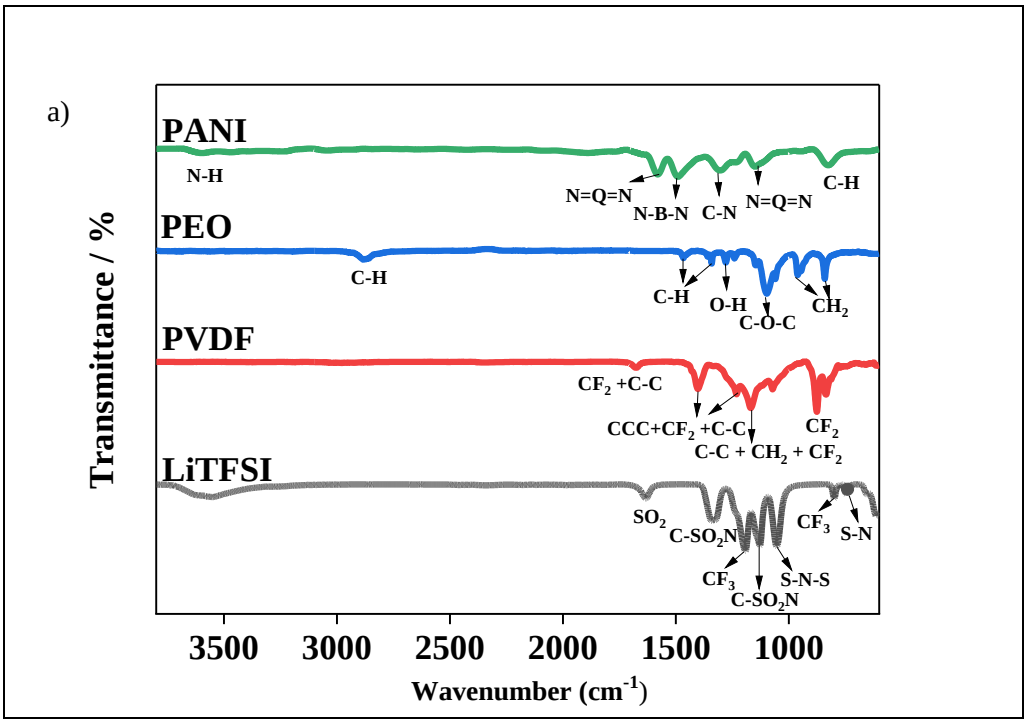

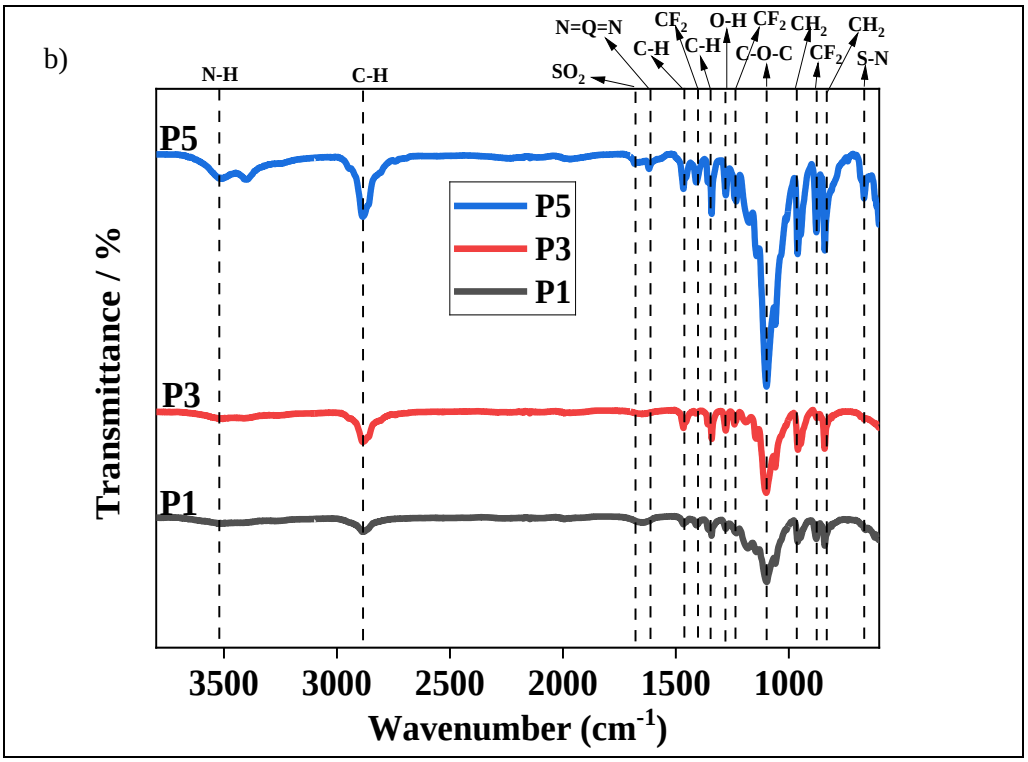

Figure 4.4 FTIR spectra were recorded for (a) individual components: PANI, PEO, PVDF, and LiTFSI; (b) P1, P3, and P5 films. The measurements were performed over a wavenumber range of 4000 cm^{-1} to 500 cm^{-1}, using 16 scans at a resolution of 4 cm^{-1}

The spectrum retrieved from the LiTFSI compound exhibits peaks at 1634, 1330, 1191, 1120, 1048, 799, and 738 cm^{-1}, corresponding to the functional groups of the compound. These peaks are consistent with those reported by Kam et al. (2014), as shown in Figure 4.4. a). Meanwhile, the spectrum obtained from the PVDF thin films shows peaks at 1,401, 1,219, 1,164, and 871 cm^{-1}, which align with those reported by Sousa et al. (2017). The characteristic peaks of PEO appear at 2,879, 1,463, 1,342, 1,269, 1,092, 959, and 832 cm^{-1}, which are consistent with those reported by Em et al. (2016). In contrast, peaks related to PANI are observed at 3,592, 1,579, 1,484, 1,302, 1,136, and 821 cm^{-1}, which match those reported by Sousa et al. (2017). The FTIR spectrum of PANI displays a prominent N-H stretching vibration around 3,592 cm^{-1}, indicating the presence of secondary amine groups (-NH-) that link the aromatic rings, as shown in Figure 3.3. a). Secondary amine groups are when the nitrogen atom is bonded to two alkyl substituents along with a single hydrogen atom (Speight, 2020). In

Figure 4.4. a), the peaks observed at around 1,579 and 1,136 cm^{-1} are attributed to N=Q=N stretching vibrations, where Q corresponds to the quinoid ring structure. Meanwhile, the peak at 1,484 cm^{-1} corresponds to the N-B-N stretching mode, where B represents the benzenoid ring structure. These alternating benzenoid and quinoid moieties, highlighted in Figure 3.3. a), are responsible for the conducting properties of PANI, which is characteristic of the conducting form of PANI. Additionally, the bands at approximately 1,302 and 821 cm^{-1} are associated with C-N stretching and C-H bending vibrations, which reflect the interactions of the amine group and aromatic ring motions (Sousa et al., 2017). Together, these spectral features confirm the existence of a conjugated polymer backbone and the characteristic functional groups of PANI, in agreement with the chemical structure depicted in Figure 3.3. a).

Figure 4.4. b) illustrates the changes in the FTIR spectra with increasing PANI concentration. As the concentration of PANI increases, the spectrum at 3,592 cm^{-1}, linked to N-H bonding in PANI, becomes increasingly pronounced, indicating that N-H bonding in PANI intensifies with more PANI within the composites. The intensity of the C-H stretching peak at 2,879 cm^{-1}, associated with PEO, increases with higher PANI concentrations. Similarly, as the PANI content increases, there is a noticeable enhancement in the spectral intensities corresponding to PEO's O-H stretching (1,286 cm^{-1}), C-O-C stretching (1,098 cm^{-1}), CH_2 rocking (960 cm^{-1}), and CH_2 wagging (838 cm^{-1}) vibrations. The gradual changes in peak intensities and slight shifts observed in the FTIR spectra provide evidence of molecular-level interactions within the composite films. In particular, the enhanced intensity of PEO-related C-O-C and O-H vibrations with increasing PANI content suggests stronger coordination between Li^+ ions and the ether oxygen atoms of PEO, facilitated by the presence of PANI. PANI likely acts as a secondary coordinating matrix, promoting salt dissociation while simultaneously altering the local polymer environment. These interactions facilitate the formation of a coupled ion-polymer network, which is crucial for efficient ion transport in SPE systems.

4.2.3 Phase Study of PANI-SPE Using XRD

Figure 4.5. a) displays the XRD spectra of pure PANI, PEO, PVDF, and LiTFSI, used as reference standards for comparison. As PANI and LiTFSI are not readily capable of forming self-supporting films, they were studied in their powder form, while PEO, PVDF, and the composite samples were analysed as films. In contrast, Figure 4.5. b) shows the XRD patterns of samples P1, P3, and P5, highlighting the evolution of crystallinity and peak intensities within the 2θ range of 5° to 35°.

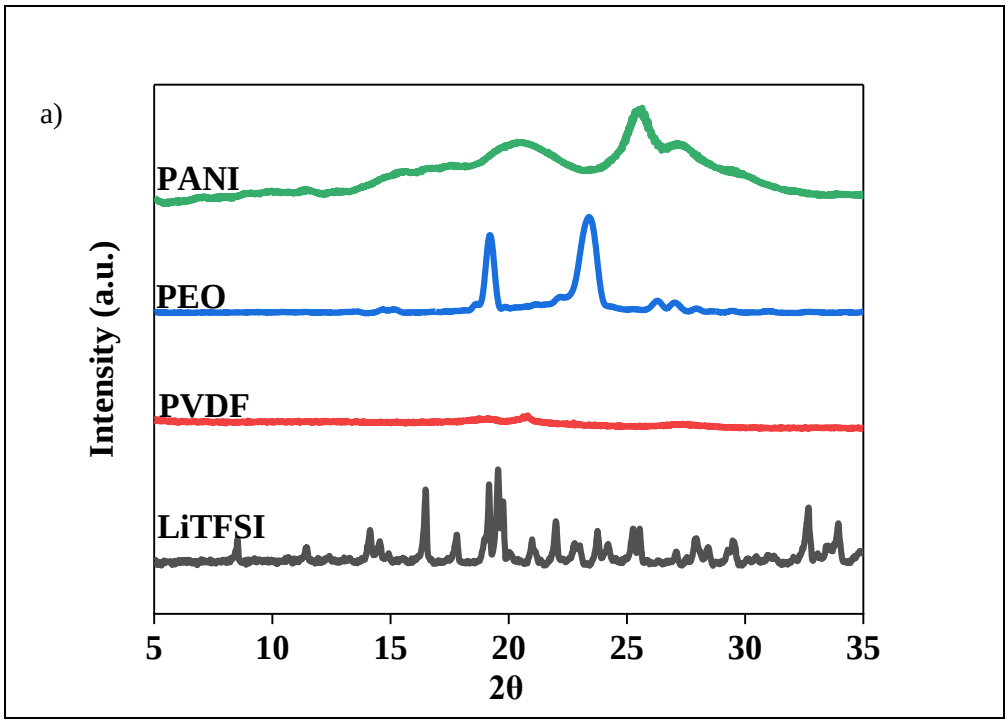

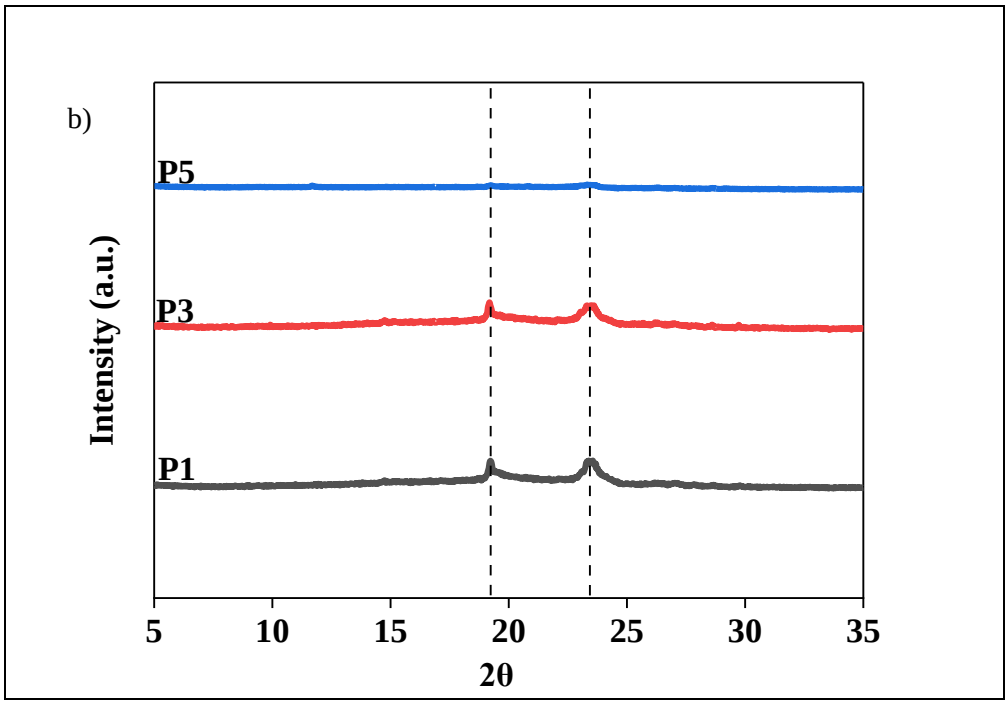

Figure 4.5 XRD patterns of (a) pure components, including PANI, PEO, PVDF, and LiTFSI (b) P1, P3, and P5 films

XRD analysis was conducted on pure LiTFSI, PVDF, PEO, PANI, and SPE films with varying PANI concentrations to investigate how interactions among LiTFSI, PVDF, PEO, and PANI influence film crystallinity. LiTFSI's XRD peaks show numerous sharp, intense peaks observed between 10° and 35°, indicating a highly crystalline and well-ordered structure typical of salts like LiTFSI. Pure LiTFSI exhibits distinct diffraction peaks at 11.4°, 14.1°, 16.4°, 19.6°, 20.9°, 21.9°, 23.7°, 25.4°, 27.9°, 29.4°, 32.7°, and 33.9°, consistent with the LiTFSI peaks reported in the literature (Li et al., 2022). PVDF shows two broad peaks at 18.2° and 19.8°, reflecting its semi-crystalline nature, while PEO presents sharp peaks at 19.3° and 23.4° due to its highly crystalline structure. PANI exhibits two broad diffraction peaks at 20.6° and 25.6°, characterized by its amorphous nature (Ambalagi et al., 2018).

The PANI-SPE composite films, P1 and P3, exhibit broad peaks observed around 19.3° and 23.4°, characteristic of PEO. Compared to pure PEO, these peaks are significantly broadened, indicating that polymer blending reduces the composite film's crystallinity. According to Fan et al. (2002), blending PEO with PVDF improves

mechanical strength and enhances ionic conductivity by suppressing PEO's crystallinity. Meanwhile, as PANI content increased to 5 wt.% (denoted by the P5 peak), the broadening of PEO's characteristic peaks at 19.3° and 23.4° became more pronounced, indicating that PANI further disrupts PEO's crystalline structure, leading to a more amorphous composite. This increase in amorphous character is highly favourable for lithium-ion transport, as ion conduction in polymer electrolytes primarily occurs through segmental motion of polymer chains within amorphous regions (Chen et al., 2021). The disruption of PEO crystallites by both PVDF blending and increasing PANI content enhances chain flexibility and creates transient coordination sites for Li^+ ions. The observed changes in FTIR and XRD spectra provide a molecular-level explanation for the differences in ionic conductivity among the PANI-SPE films. The gradual increase in intensity of PEO-related C-O-C and O-H vibrations with higher PANI content indicates stronger interactions between Li^+ ions and the ether oxygen atoms of PEO, facilitated by PANI. These interactions enhance Li^+ dissociation from LiTFSI, increasing the number of mobile charge carriers. Concurrently, XRD analysis shows that increasing PANI content broadens the characteristic PEO peaks at 19.3° and 23.4°, reflecting reduced crystallinity and the formation of more amorphous regions. Because ion transport primarily occurs in amorphous domains, these structural modifications create more flexible polymer chains and transient coordination sites for Li^+ ions, directly supporting improved conductivity in the SPE films. Therefore, the combination of FTIR and XRD results demonstrates that both chemical interactions and structural disorder work together to facilitate ion mobility. Consequently, the observed XRD peak broadening, together with the molecular interactions revealed by FTIR, directly supports the conductivity trends observed in the PANI-SPE films, particularly at lower PANI loadings where sufficient amorphous content is achieved without excessive network densification.

4.2.4 Measurement of the Conductivity of PANI-SPE Using EIS

The conductivity of PEO, PVDF, and PANI-based SPE films, prepared using the solvent casting method, was analysed using EIS. PANI is a widely studied and readily accessible polymer, with nitrogen sites that facilitate ion-pair dissociation of

salts within the polymer matrix (Tara-Lunga-Mihali et al., 2014). Figure 4.6 presents the conductivity measurements of bare PEO, PVDF, P1, P3, and P5 samples. The error bars represent the standard deviations, highlighting the variability observed in the measurements.

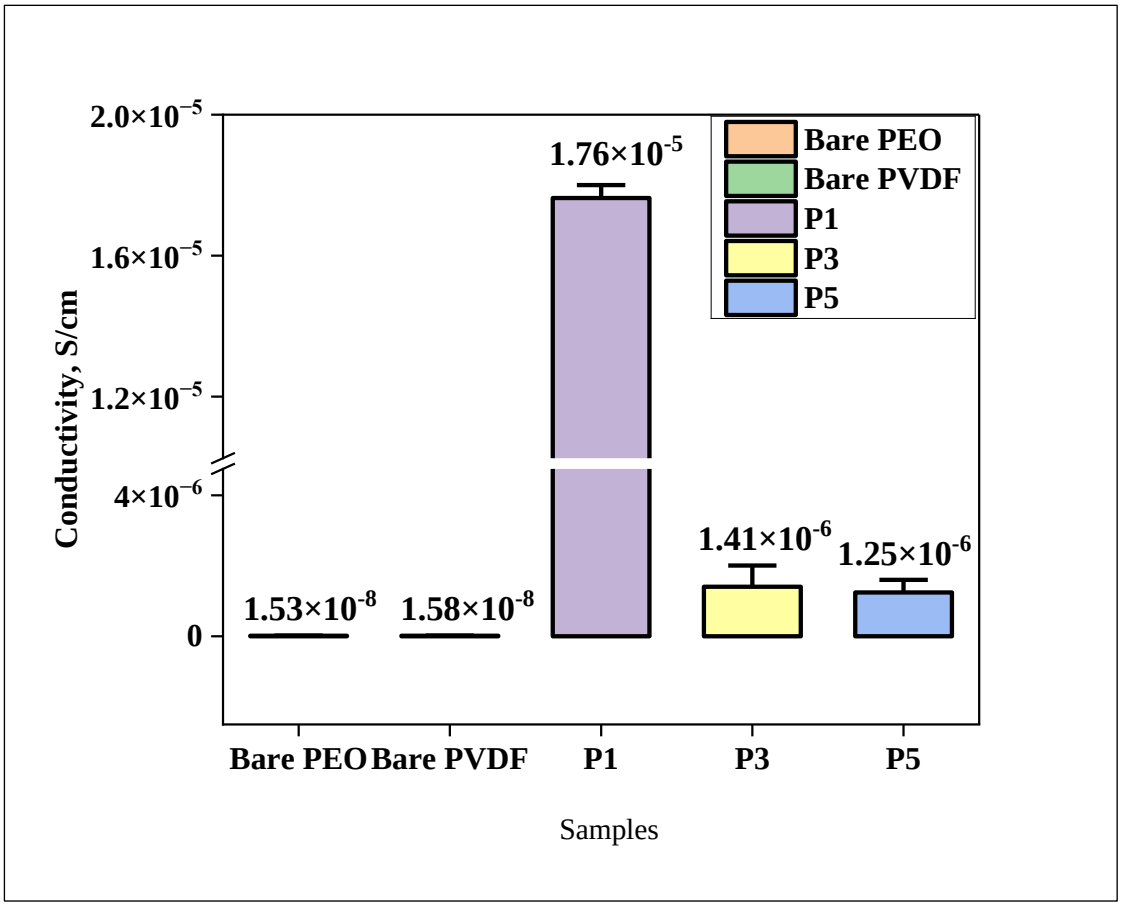

Figure 4.6 The conductivity measurements of Bare PEO, Bare PVDF, and samples P1, P3, and P5, with error bars indicating standard deviations

The conductivity of the bare PEO film was measured at 1.53×10^{-8} S/cm, aligning well with the typical reported value of around 10^{-8} S/cm at room temperature (Gucci et al., 2023). At room temperature, PEO-based electrolytes display very low conductivity in the range of 10^{-8} to 10^{-7} S/cm, primarily because of their high degree of crystallinity (J. Li et al., 2022). In contrast, PVDF exhibited a conductivity of 1.58×10^{-8} S/cm, significantly higher than the commonly cited range of 10^{-11} to 10^{-10} S/cm (Salam et al., 2012). The low conductivity values (in the order of 10^{-8} S/cm) for both materials

highlight a common limitation of bare polymer electrolytes at room temperature; they typically require the addition of salts, plasticizers, or fillers to significantly enhance their ionic conductivity for practical applications in batteries or electrochemical devices. Blending PEO with PVDF can reduce the crystallinity of PEO, thereby enhance ionic conductivity and providing improved mechanical strength (Fan et al., 2002).

Incorporating a secondary polymer into the composite film improves the conductivity compared to pure PEO or PVDF films. Specifically, the P1, P3, and P5 composites exhibited average conductivity values of 1.76×10^{-5}, 1.41×10^{-6}, and 1.25×10^{-6} S/cm, respectively, indicating a decrease in conductivity with increasing PANI content. PANI-based SPE, labelled as P1, P3, and P5, represent composites of PANI:PVDF:PEO:LiTFSI, where the weight percentages of PEO, PVDF, and LiTFSI are kept constant at 7 wt. %, 3 wt.% and 2 wt. % respectively, while the PANI content is varied at 1 wt.%, 3 wt.%, and 5 wt.%, respectively. The highest conductivity, 1.76×10^{-5} S/cm, was achieved with just 1 wt. % PANI, suggesting that even a small addition significantly boosts conductivity. The high conductivity observed in sample P1 can directly correlate with its surface morphology, as the FESEM analysis shows in Figure 4.2. d). Among the three samples, P1 exhibits the highest porosity, which likely contributes to the enhanced ionic transport. In SPEs, porosity can play a significant role in improving ion mobility by increasing the number of pathways available for ion migration. The greater porosity increases the available surface area, thereby promoting more efficient ion transport (Beuse et al., 2021). This structural advantage is less pronounced in P3 and P5, which show relatively denser and more compact morphologies with lower porosity, possibly restricting ion movement and leading to their lower conductivities. Therefore, the superior performance of P1 can be attributed to its favourable morphological features, supporting the idea that increased porosity enhances the overall conductivity of SPEs. Although PANI is intrinsically conductive, excessive PANI content can adversely affect ionic conductivity in SPE systems. At higher loadings (P3 and P5), the dense PANI network restricts polymer chain mobility and reduces free volume, limiting Li^+ ion hopping between coordination sites. Moreover, excessive PANI may introduce electronic conduction pathways that compete with ionic transport, leading to increased interfacial resistance during EIS measurements. This explains why an optimal PANI concentration exists, where

sufficient salt dissociation and amorphous content are achieved without compromising ion mobility. These structural insights from FTIR and XRD help explain the trends observed in the EIS measurements. For instance, P1 exhibited the highest conductivity, which corresponds to the more accessible amorphous domains and stronger Li^+ coordination indicated by the spectroscopic and XRD data. In contrast, higher PANI loadings (P3 and P5) increase network densification, limiting chain mobility and slightly reducing ion transport, consistent with the lower conductivity values measured for these samples.

4.3 Electrochemical Behaviour of PANI-SPE During Overoxidation Using Cyclic Voltammetry

Electrochemical degradation of the films via overoxidation was stimulated using the CV method, with a Pt sheet served as the CE, the PANI-SPE film functioning as the WE, and an Ag/AgCl electrode used as the RE. Figure 4.7 presents the cyclic voltammograms for PANI-SPE films. The scans were performed over a potential range of 0 to 1 V for 10 cycles at a scan rate of 50 mV/s with 0.1 M KCl as the electrolyte.

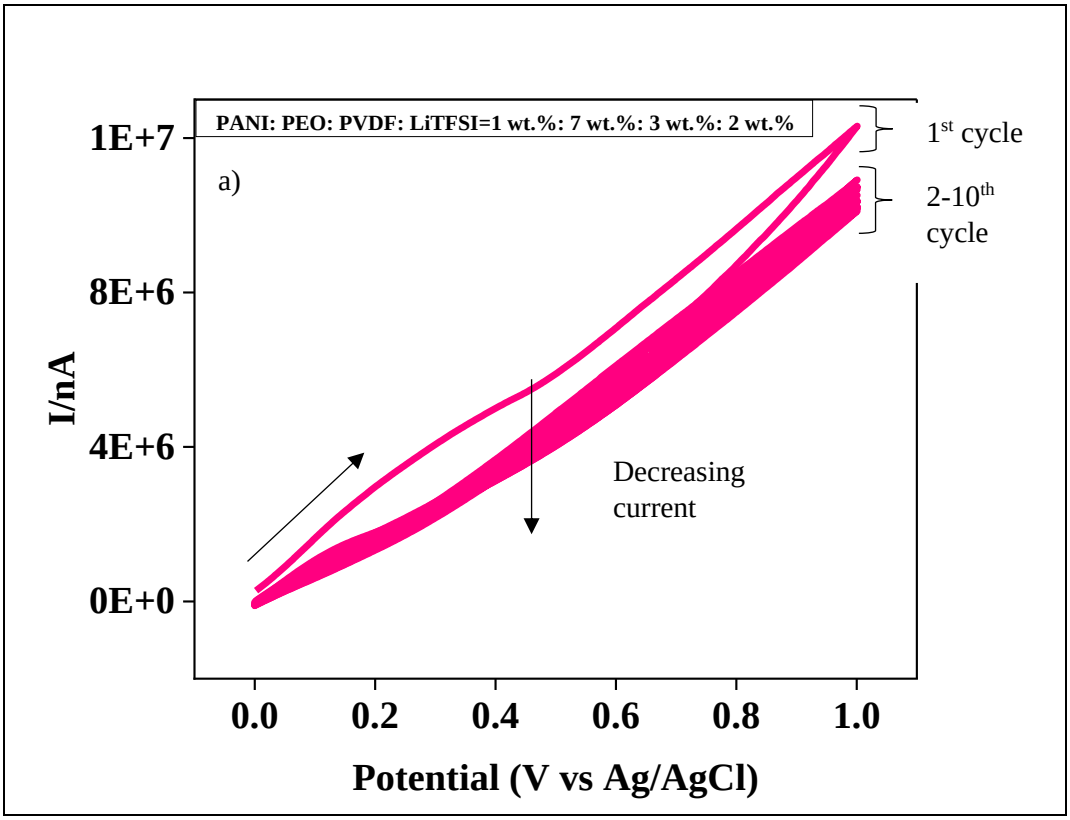

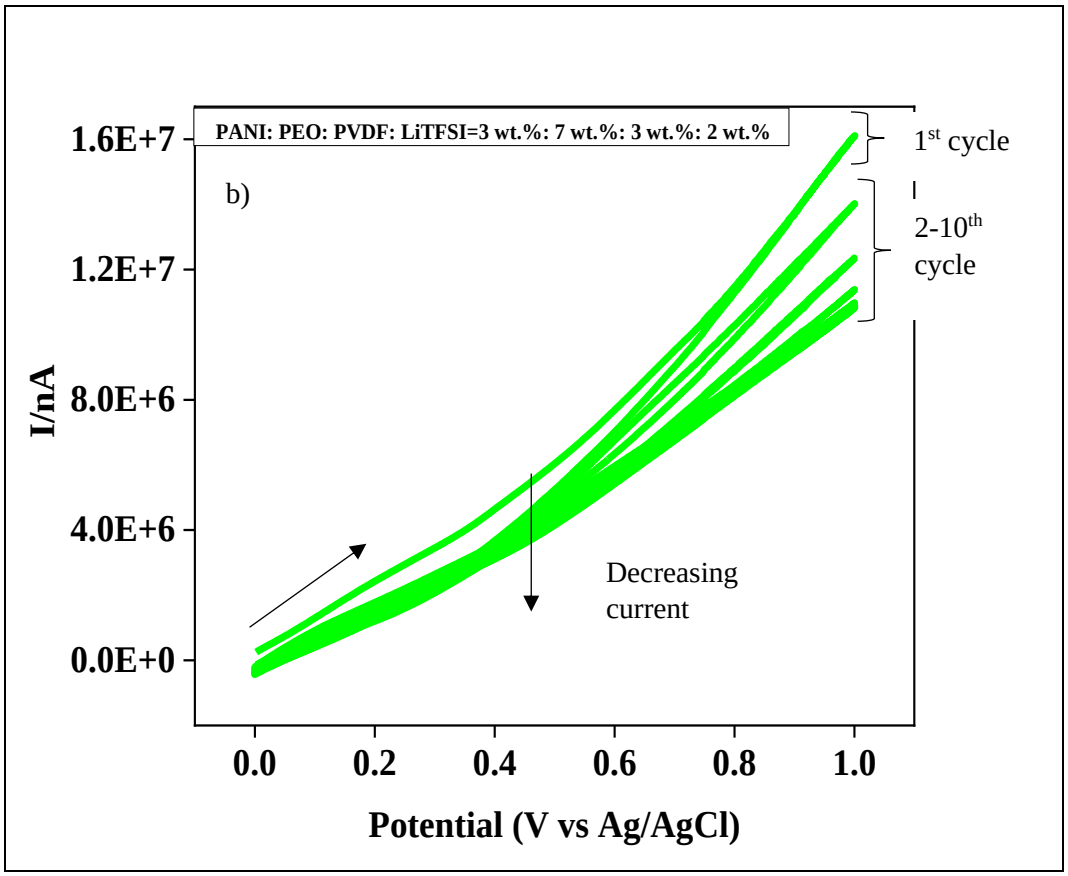
PANI: PEO: PVDF: LiTFSI=3 wt.%: 7 wt.%: 3 wt.%: 2 wt.%
b)
1st cycle
2-10th cycle
Decreasing current
I/nA
1.6E+7
1.2E+7
8.0E+6
4.0E+6
0.0E+0
0.0
0.2
0.4
0.6
0.8
1.0
Potential (V vs Ag/AgCl)

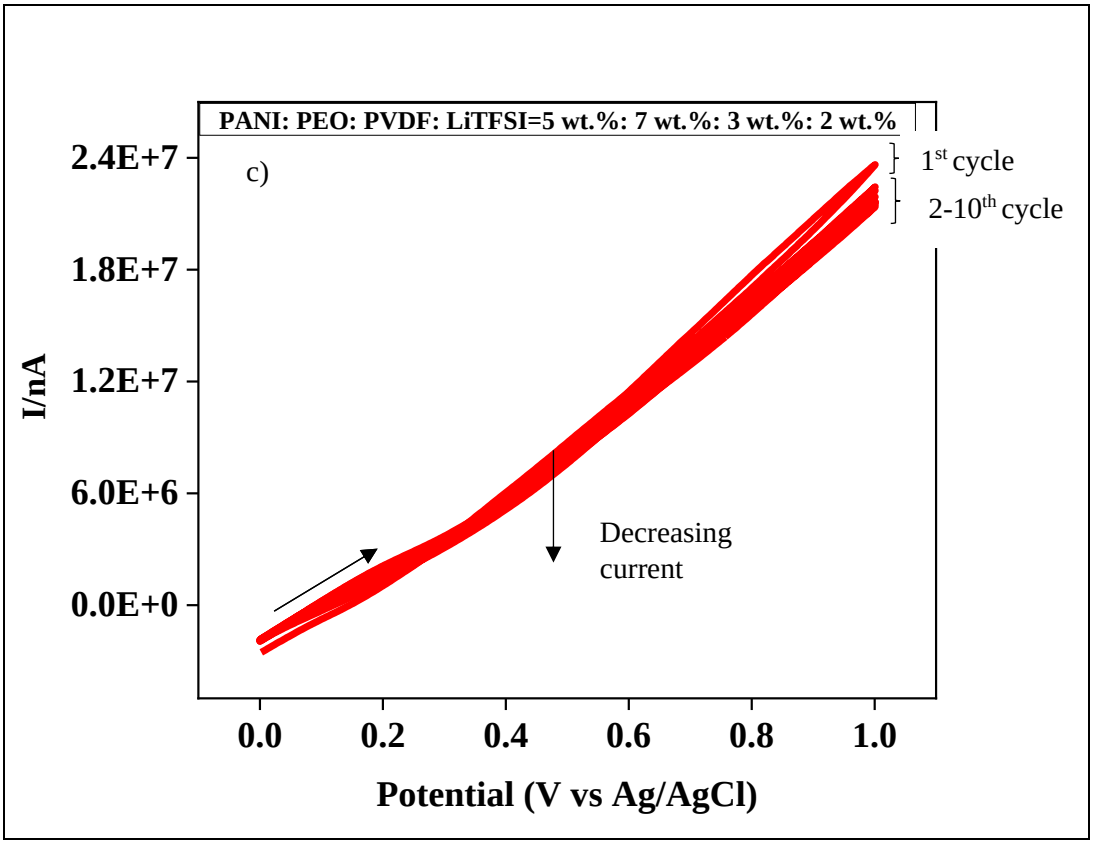
PANI: PEO: PVDF: LiTFSI=5 wt.%: 7 wt.%: 3 wt.%: 2 wt.%
c)
1st cycle
2-10th cycle
Decreasing current
I/nA
2.4E+7
1.8E+7
1.2E+7
6.0E+6
0.0E+0
0.0
0.2
0.4
0.6
0.8
1.0
Potential (V vs Ag/AgCl)

Figure 4.7 Cyclic voltammograms were recorded for the films (a) P1, (b) P3, and (c) P5 using a Pt sheet as the CE, an Ag/AgCl electrode as the RE, and PANI-SPE films as the WE. The measurements were carried out over a potential range of 0 to 1 V for 10 cycles at a scan rate of 50 mV/s with 0.1M KCl as electrolyte

The PANI-SPE films (P1, P3, and P5) were exposed to a voltage range of 0 to 1 V for 10 cycles at a scan rate of 50 mV/s as part of the electrochemical overoxidation process. This process is done to simulate the degradation mechanisms relevant to battery applications. Figure 4.7 presents the CV profiles of the three films, P1, P3, and P5. Before overoxidation, the films exhibited structural and electrochemical properties directly linked to their composition. P1, with the lowest PANI content (1 wt. %), displayed the highest porosity based on FESEM analysis. This porous structure facilitated efficient ion transport pathways, resulting in the highest initial conductivity among the three films. The CV curves of P1 (Figure 4.7. a)) showed a pronounced oxidation peak during the initial cycles, indicative of strong pseudocapacitive behaviour. In contrast, P5, with the highest PANI content (5 wt.%), exhibited a denser morphology, as confirmed by the FESEM image in Figure 4.2. e). This compact structure restricted the ion diffusion, leading to the lowest initial conductivity. The CV curves of P5 (Figure 4.7. c)) featured a smaller oxidation peak compared to P1, reflecting a limited ion accessibility. P3, containing an intermediate PANI concentration (3 wt.%), exhibited moderate levels of porosity and conductivity, displayed a CV profile (Figure 4.7. b)) with a stable redox behaviour and moderate peak current. P1 suffered the most severe electrochemical deterioration. The porous structure that initially enhanced ion transport became a liability, exposing a larger surface area of PANI to oxidative stress. Over repeated cycles, the current decreased, signalling structural collapse of the polymer backbone. Highly porous polymer matrices are prone to accelerated oxidative damage due to increased reactive site exposure. This accelerated degradation can be attributed to enhanced electrolyte penetration into the porous structure, which increases the number of electrochemically active sites exposed to oxidative potentials. As a result, PANI chains in porous matrices undergo more extensive overoxidation, leading to rapid loss of conjugation and mechanical collapse. In contrast, denser structures limit electrolyte access, slowing down oxidative reactions

and preserving the integrity of the polymer backbone. P5, with its dense morphology and high PANI content, demonstrated remarkable stability under overoxidation. Although its initial conductivity was the lowest, the robust PANI network provided mechanical reinforcement and minimized oxidative damage. The CV curves of P5 retained sharp, overlapping peaks over 10 cycles, with minimal changes in peak currents. This stability suggests that the dense structure limited electrolyte infiltration, thereby protecting the PANI matrix from degradation. P3 exhibited an intermediate behaviour.

The CV analysis of PANI-SPE films under overoxidation conditions underscores the necessity of tailoring material composition to application-specific requirements. While P1's porous framework delivers a superior initial conductivity and charge storage, its structural vulnerability under oxidative stress highlights the limitations of low PANI content. P5 has a dense structure due to its high PANI content, making it strong and more resistant to damage. However, this also makes it harder for ions to move through. These findings highlight the need to carefully balance the amount of PANI and ion-conducting additives to create SPEs that perform well and last longer in advanced batteries. For battery applications requiring long cycle life, P5 is optimal due to its exceptional electrochemical stability. However, if high initial power/energy density is critical, P3 offers the best trade-off between performance and durability. P1 is unsuitable for sustained operation due to rapid degradation

4.4 Effects of Overoxidation on PANI-SPE

The overoxidized PANI-SPEs were thoroughly characterized using several techniques, including FESEM to analyse their surface morphology, FTIR to study the chemical structure, and XRD to study the phase composition. Their conductivity was measured using EIS to study the effects of overoxidation on the films.

4.4.1 Morphological Study of Overoxidized PANI-SPE Using FESEM

Figure 4.8 presents the FESEM micrographs of P1, P3, and P5 films alongside their overoxidized counterparts (OP1, OP3, and OP5), allowing direct comparison of

morphological changes induced by overoxidation. The images were taken at 10,000× magnification using the ETD detector under high vacuum conditions. Before imaging, all samples underwent the same preparation steps, which included gold sputter-coating and drying in a vacuum oven to ensure conductivity and surface cleanliness.

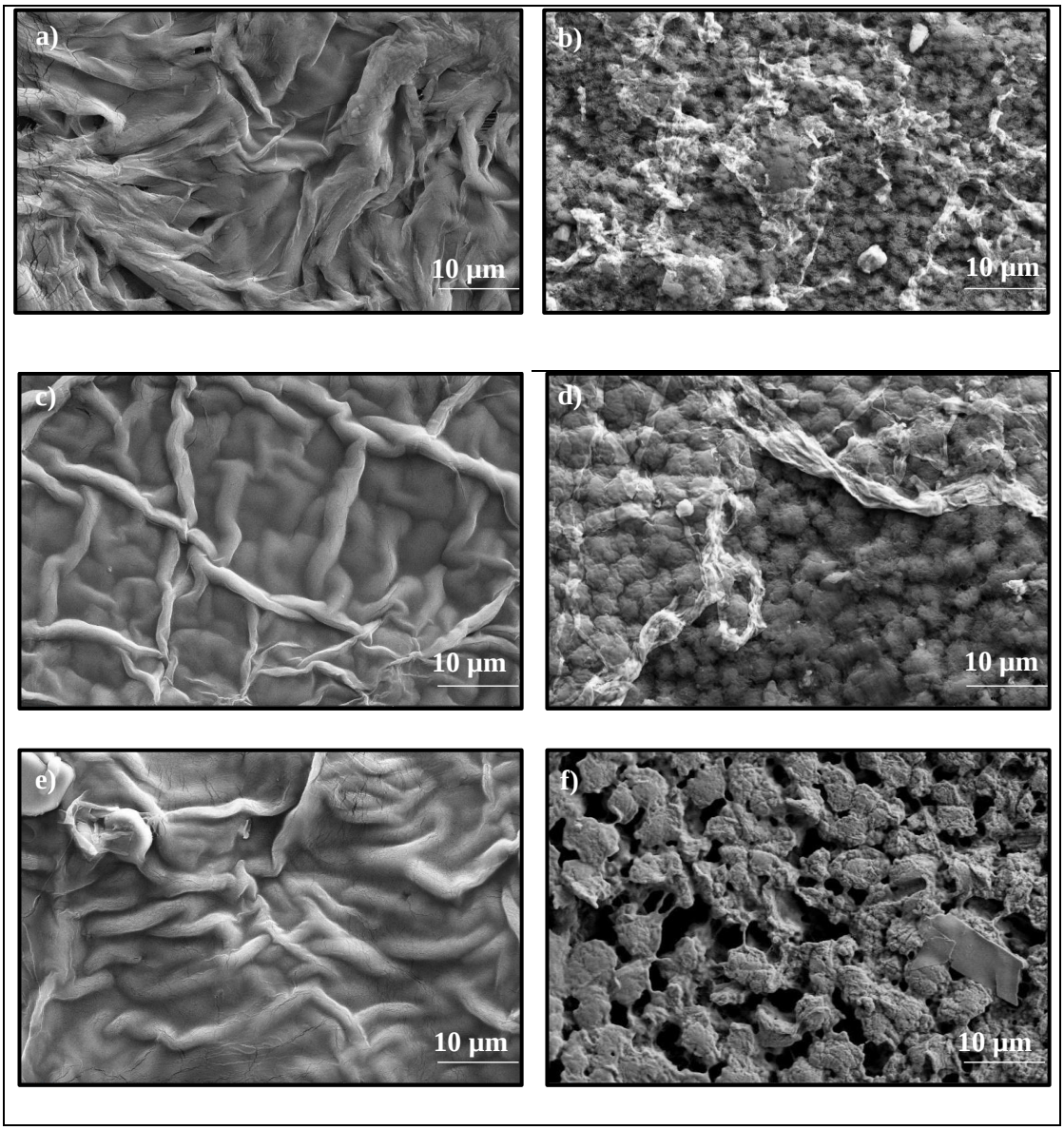

Figure 4.8 FESEM images of (a) P1 film, (b) P3 film, (c) P5 film, (d) OP1 film, (e) OP3 film, and (f) OP5 film, captured at 10,000× magnification using the ETD under high vacuum conditions

FESEM provides detailed insights into the surface morphology of polymer electrolyte films, enabling the visualization of structural features such as smoothness, roughness, porosity, and particle distribution. In this study, FESEM analysis is particularly important for examining the impact of overoxidation on PANI-based membranes, as it allows direct comparison of morphological changes that may influence ionic transport, interfacial stability, and overall electrochemical performance. The morphological evolution of PANI-SPE films under the overoxidation process, as revealed by FESEM analysis in Figure 4.8, provides critical insights into their structural stability and degradation, which are pivotal for battery applications. Excessive oxidation leads to a significant disruption in the IPN structure, characterised by increasing pores. The mechanical integrity of the film is weakened, as indicated by the visible rupture of the polymer matrix. The disruption of molecular chains during overoxidation led to the breakdown of the IPN (Izdebska, 2015). Overoxidation induces profound structural degradation, as seen in Figure 4.8. After overoxidation (OP1, Figure 4.8. b)), the surface becomes slightly rougher and more porous compared to P1, which may be linked to structural degradation and partial disruption of PANI chains during the overoxidation process. Figure 4.8. d) shows the FESEM image of overoxidized P3, showing a rougher surface with more visible irregularities, further supporting the structural changes induced by overoxidation. FESEM image of overoxidized P5, as shown in Figure 4.8. f), the surface becomes considerably more porous and irregular, reflecting the extensive morphological modifications caused by overoxidation. Overoxidation introduces porosity and roughness, which could influence the conductivity of the film.

4.4.2 FTIR Analysis of the Chemical Structure of Overoxidized PANI-SPE

FTIR is a valuable tool for investigating molecular structure, bonding, and compositional changes. It can also detect complex formation in both amorphous and crystalline phases by analysing the infrared spectrum. FTIR analysis can give information on structural changes to the PANI-based SPE due to the overoxidation process. The overoxidation of PANI resulted in a substantial degradation and the generation of quinone-type compounds, such as HQ/BQ (Gao et al., 2011). The

formation of new compounds can be studied through chemical analysis. Figure 4.9 presents the FTIR spectra of the overoxidized PANI-based SPE samples, OP1, OP2, and OP3, corresponding to the overoxidized P1, P3, and P5, respectively. All samples were analysed using the same procedure, where dried films were scanned in the range of 4000-500 cm^{-1} to identify functional group changes after overoxidation.

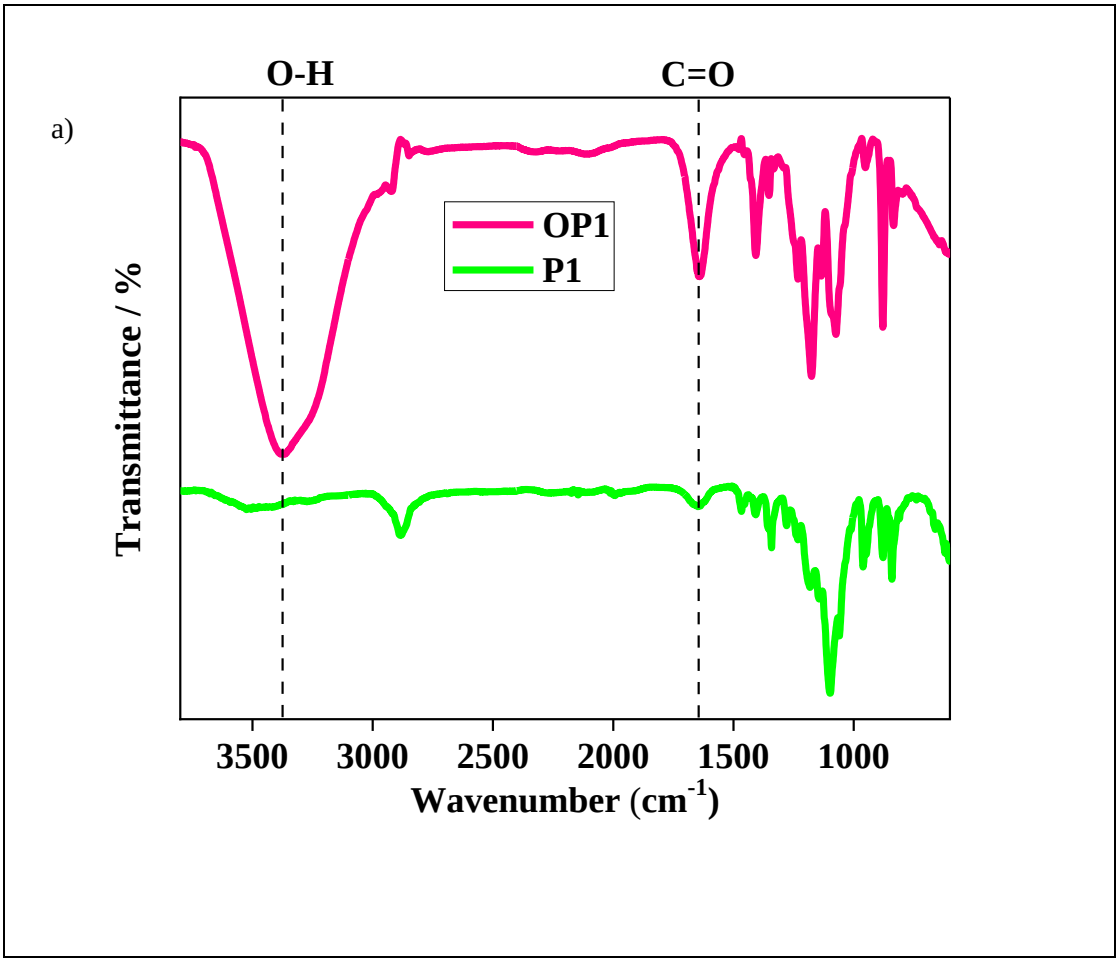

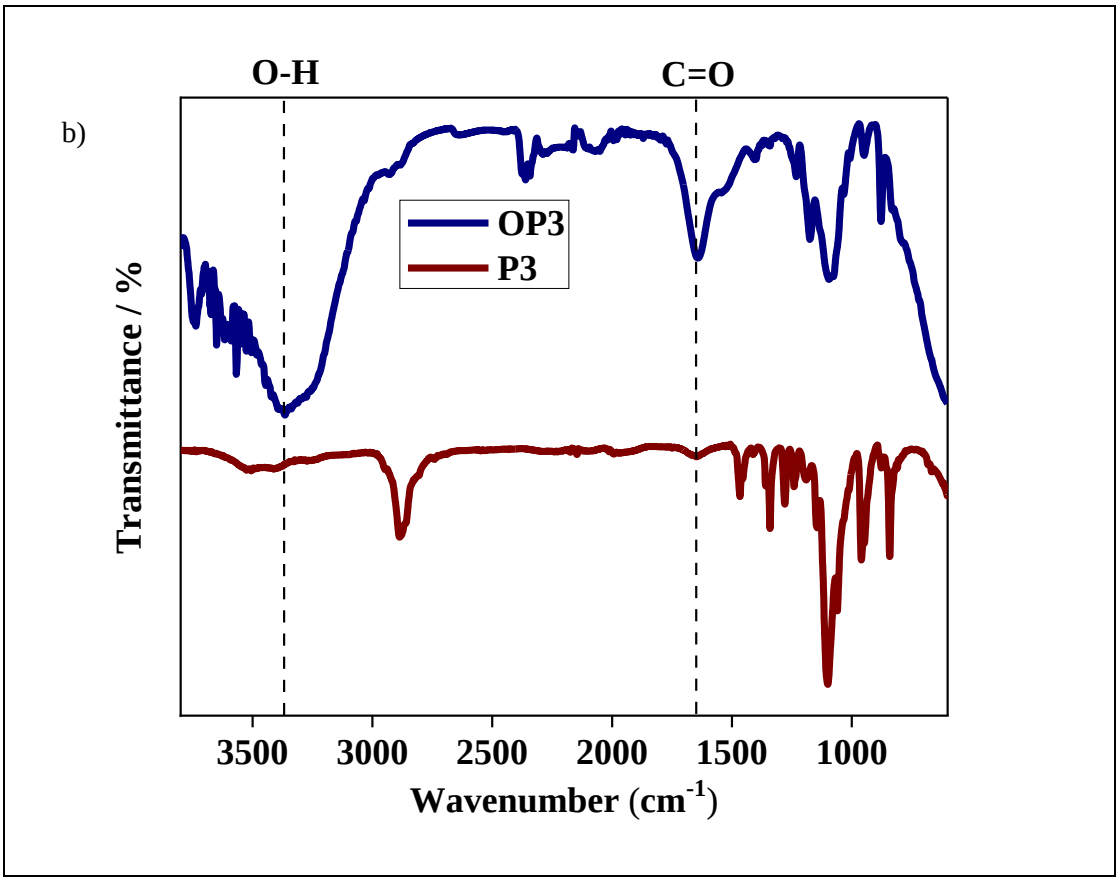
b)
O-H
C=O
OP3
P3
Transmittance / %
3500
3000
2500
2000
1500
1000
Wavenumber (cm-1)

c)

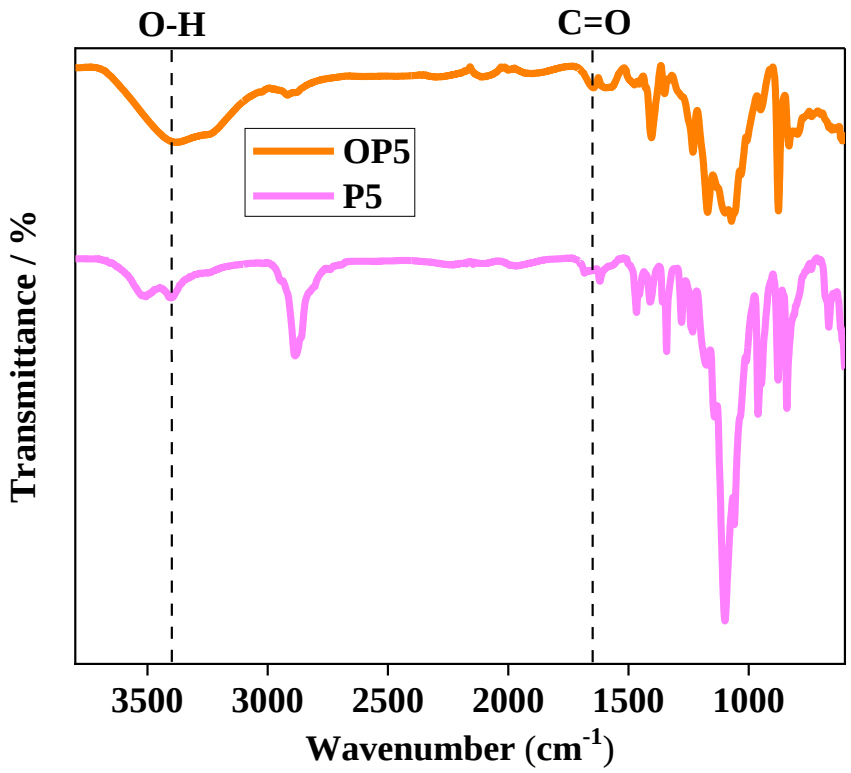
O-H
C=O
OP5
P5
Transmittance / %
3500
3000
2500
2000
1500
1000
Wavenumber (cm-1)

d)

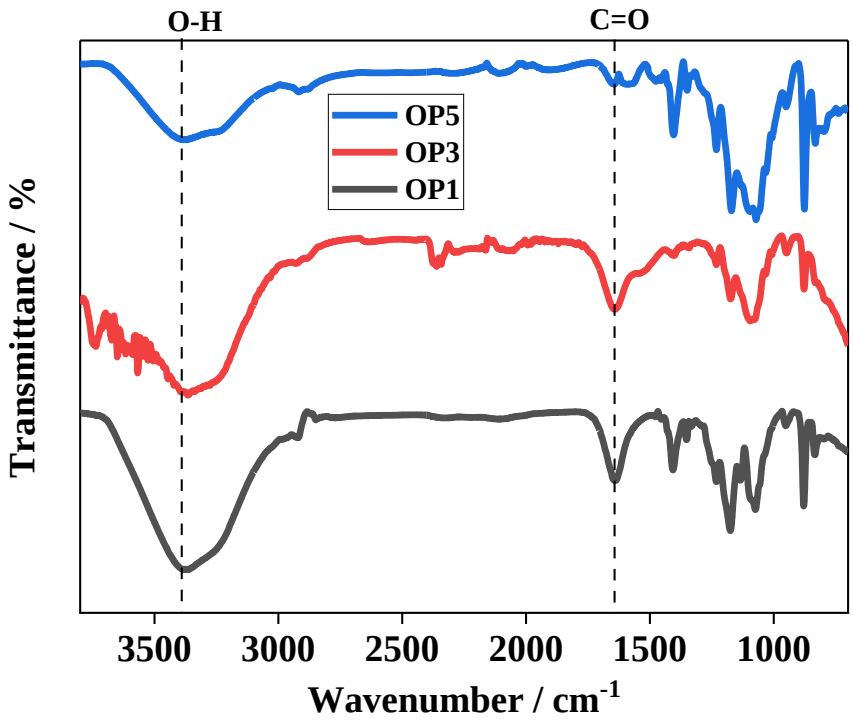
O-H
C=O
OP5
OP3
OP1
Transmittance / %
3500
3000
2500
2000
1500
1000
Wavenumber / cm-1

Figure 4.9 FTIR spectra of (a) P1 and OP1, (b) P3 and OP3, (c) P5 and OP5, and (d) OP1, OP3, and OP5 films

The FTIR spectra in Figure 4.9 offer a comprehensive view of the chemical structural evolution of PANI-SPE films under overoxidation conditions. These spectra, comparing pristine (P1, P3, P5) and overoxidized (OP1, OP3, OP5) films, reveal critical insights into the degradation mechanisms of PANI in battery-relevant environments. The analysis underscores the role of PANI concentration in stabilizing the polymer matrix and highlights the trade-offs between conductivity and durability. For the P1 film (1 wt. % PANI), the FTIR spectrum before overoxidation displays characteristic PANI peaks, including the C=C stretching of benzenoid rings at ~1500 cm^{-1} and the C=N stretching of quinoid rings at ~1600 cm^{-1}. These features confirm the presence of PANI in its conductive emeraldine salt form. Peaks associated with the PVDF-PEO matrix, such as C–F stretching (~1170 cm^{-1}) and C–O–C stretching (~1100 cm^{-1}), are also evident. After overoxidation (OP1), the spectrum undergoes significant alterations: the quinoid (~1300 cm^{-1}) peaks diminish sharply, indicating the breakdown of π-conjugation in PANI's backbone. Concurrently, a new peak emerges at ~1700 cm^{-1}, attributed to C=O stretching from carbonyl groups. This formation of quinone or carbonyl defects signifies irreversible oxidative damage, which aligns with the drastic post-overoxidation conductivity loss observed in P1.

In contrast, the P3 film (3 wt. % PANI) exhibits stronger PANI-related peaks in its pristine state, reflecting a more robust conductive network due to higher PANI content. After overoxidation (OP3), the degradation is less severe. While the quinoid weakens moderately, the carbonyl peak at ~1700 cm^{-1} is weaker compared to OP1. This suggests that the intermediate PANI concentration partially shields the polymer matrix from oxidative attack, preserving some conductive pathways. The P5 film (5 wt. % PANI) demonstrates the most stable chemical structure. Its pristine spectrum features intense, well-defined quinoid and benzenoid peaks, indicative of a dense, well-organized PANI network. After overoxidation (OP5), these peaks show only a slight weakening, and no significant carbonyl formation is observed. The minimal structural changes confirm that high PANI content effectively mitigates oxidative damage. The dense PANI network likely restricts electrolyte infiltration, thereby protecting the polymer backbone from chain scission and preserving its conductive properties. Based

on Figure 4.9 (a-c), after overoxidation, a new broad peak emerges at around 3,300 cm^{-1}. This new broad peak suggested the formation of the O-H stretching (Lingegowda et al., 2012). O-H stretching indicates the formation of hydroquinone, which appeared possibly due to the overoxidation process (Izdebska, 2015). Meanwhile, the peak around 1,700 cm^{-1} becomes increasingly prominent after the excessive oxidation, suggesting the formation of the C=O group of benzoquinones (Gao et al., 2011). Among the overoxidized samples, upon overoxidation, the intensity of the O-H spectrum at ~3,300 cm^{-1} and C=O spectrum at ~1,700 cm^{-1} decreases as the concentration of PANI increases. Following overoxidation, this suggests that the formation of quinone compounds decreases with increasing PANI concentration.

4.4.3 Phase Characterization of Overoxidized PANI-SPE Using XRD

XRD is a powerful technique for probing the crystallinity, phase composition, and structural degradation of materials. It provides critical insights into how overoxidation alters the long-range order and molecular packing of polymer matrices, particularly in systems such as PANI-based SPEs. The oxidative degradation of PANI leads to the breakdown of its semi-crystalline structure, thereby reducing its ability to sustain efficient charge transport. In this study, XRD analysis was employed to investigate phase transitions and crystallinity changes in PANI-SPE films (OP1, OP3, OP5) after overoxidation, with the results presented in Figure 4.10. By comparing diffraction patterns of pristine and overoxidized samples, the structural consequences of oxidative stress, such as peak broadening, intensity reduction, or emergence of new reflections, are systematically evaluated to elucidate degradation pathways.

a)

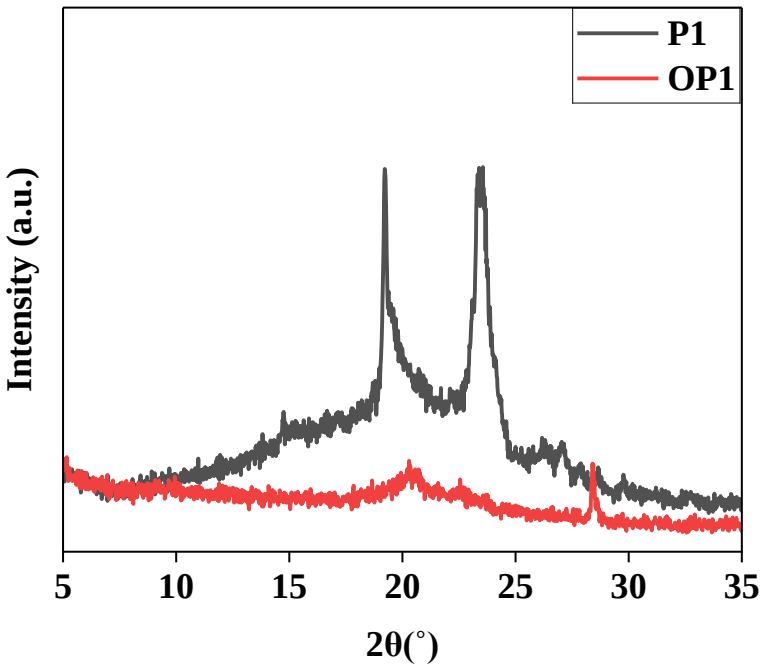
P1
OP1
Intensity (a.u.)
5
10
15
20
25
30
35
2θ(˚)

b)

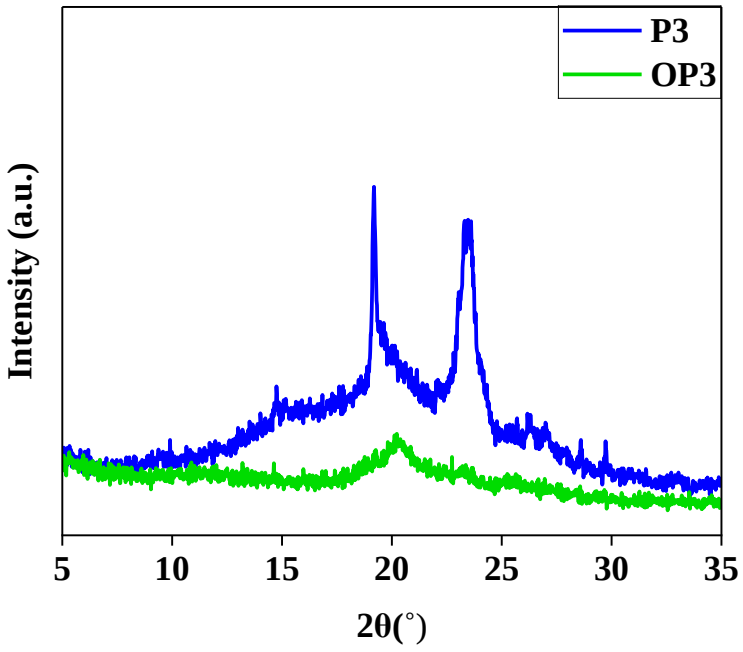
P3
OP3
Intensity (a.u.)
5
10
15
20
25
30
35
2θ(˚)

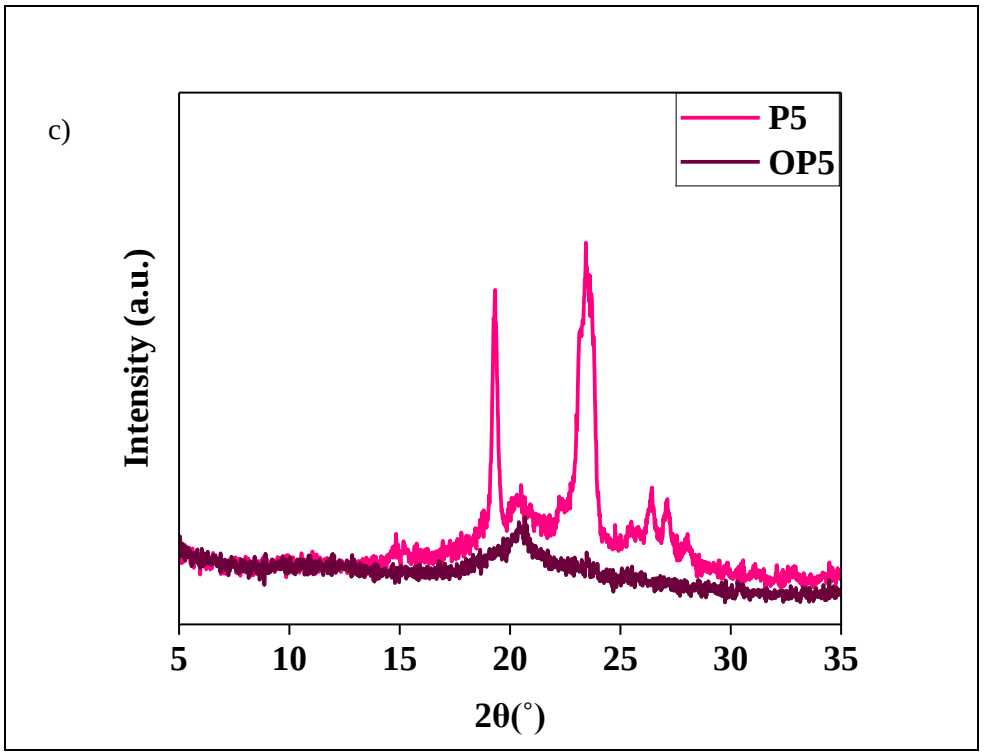

Figure 4.9 XRD patterns for (a) P1 and OP1 films, (b) P3 and OP3 films, and (c) P5 and OP5 films. Phase analysis was conducted using a Malvern Panalytical X'Pert3 diffractometer. Measurements were performed at room temperature with Cu Kα radiation (λ = 1.542 Å). The data were collected over a 2θ range of 5°-35° at a scanning rate of 0.5°/min with a step size of 0.001°

Overoxidation of PANI leads to hydrolysis of its quinoid segments, disrupting the conjugated polymer backbone and significantly altering the blend's morphology. These changes are evident in the overoxidized (OP) series, which shows marked deviations from their non-oxidized counterparts. For instance, in OP1 (overoxidized P1), the characteristic PANI peak at 25.2° nearly disappears, while partial crystallinity of PEO re-emerges. This indicates that as PANI degrades, its interference with polymer ordering diminishes, allowing PEO chains to reorganize. However, a slight increase in the amorphous background suggests the presence of fragmented PANI residues. In OP3 (from P3), crystallinity collapses further. PEO peaks weaken substantially, and PANI's structural signature is completely lost. A broad amorphous peak between 20° - 30° dominates the pattern, reflecting increased chain scission and plasticization of the blend.

This trend reaches its extreme in OP5 (from P5), where all crystalline features vanish into a broad peak around 22°, signifying a fully amorphous structure. Here, the degraded PANI fragments blend uniformly with the matrix, forming a disordered composite.

4.4.4 Conductivity Measurement of Overoxidized PANI-SPE Using EIS

The conductivity of overoxidized PANI-based SPE films prepared using the solvent casting method was analysed through EIS. Conductivity measurements were taken for PANI-SPE films both before and after overoxidation, allowing for a comparative analysis of the changes induced by the process. Figure 4.11 illustrates the conductivity of SPE films in two different conditions. Part (a) presents the conductivity profiles of PANI-blended films labelled P1, P3, and P5, while part (b) shows the conductivity of the corresponding overoxidized samples, designated as OP1, OP3, and OP5. The figure enables a comparative analysis between the original and overoxidized films, highlighting the changes in conductivity behaviour due to the overoxidation process. The decline in conductivity observed after overoxidation is directly relevant to the electrochemical performance of the SPE, as reduced electron transport within the polymer matrix limits the ability of the membrane to efficiently support charge storage and transfer during device operation, thereby contributing to the observed capacity reduction in subsequent electrochemical measurements.

a)

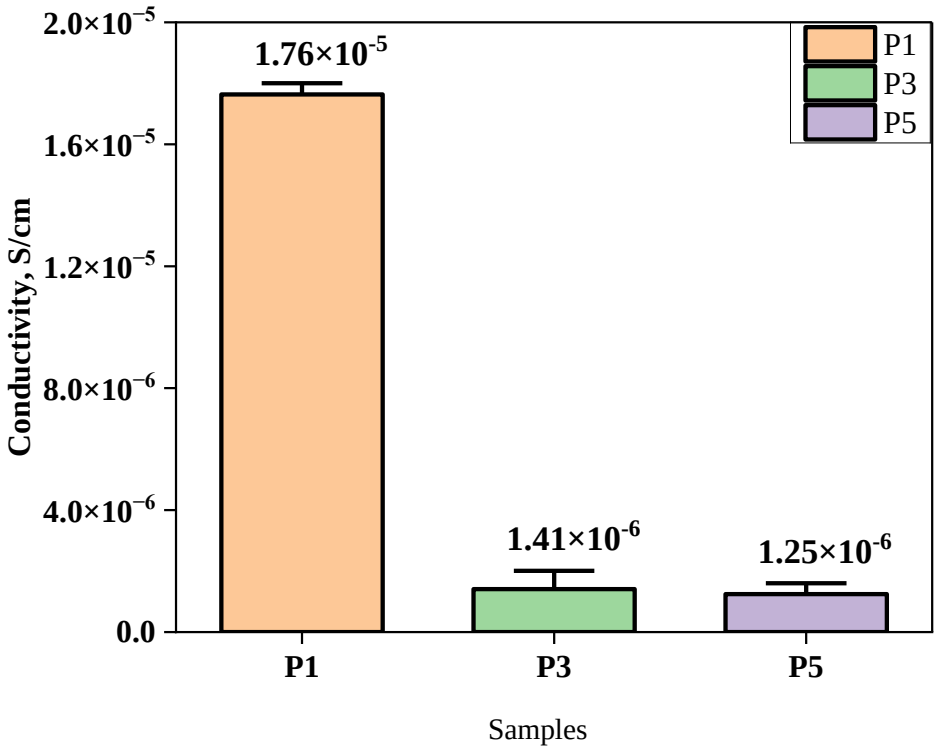
2.0×10⁻⁵
1.6×10⁻⁵
1.2×10⁻⁵
8.0×10⁻⁶
4.0×10⁻⁶
0.0
Conductivity, S/cm
1.76×10-5
1.41×10-6
1.25×10-6
P1
P3
P5
P1
P3
P5
Samples

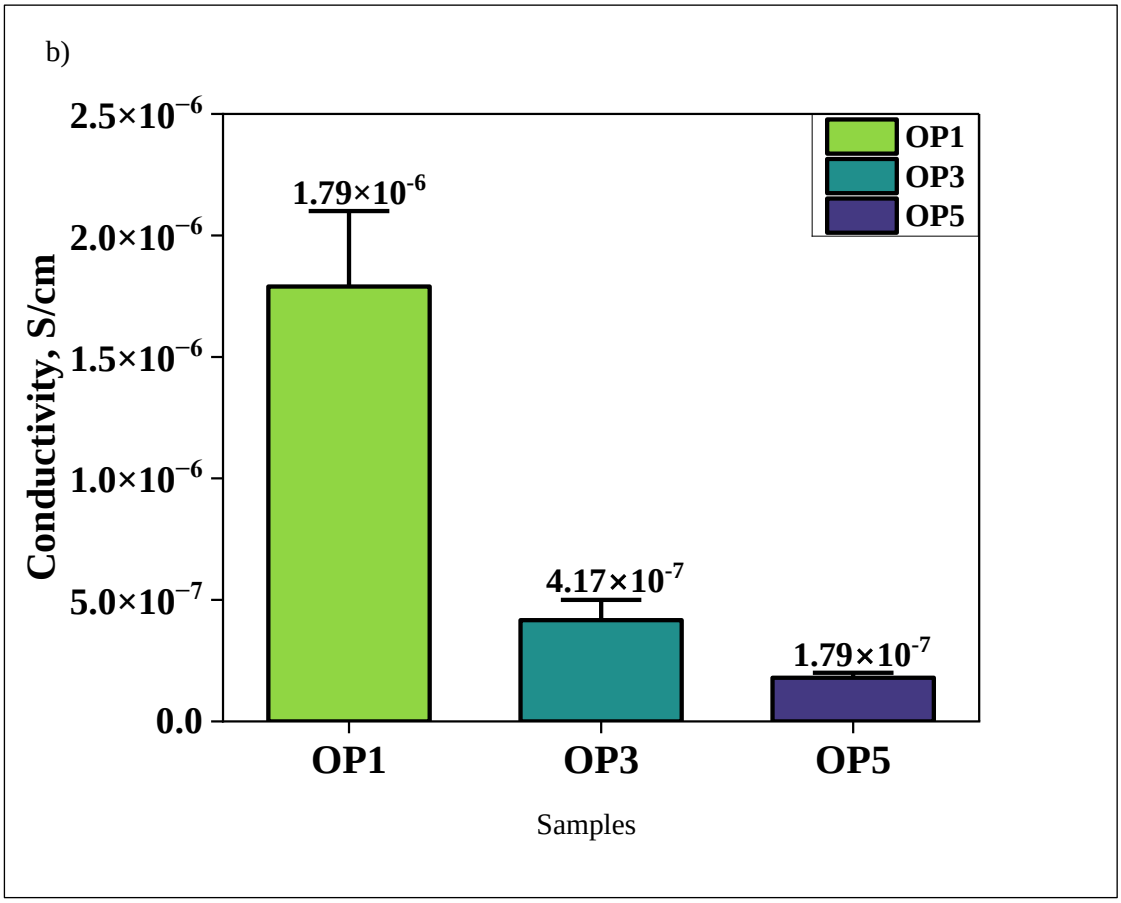

Figure 4.10 Conductivity of (a) PANI-blended films: P1, P3, and P5, and (b) overoxidized films: OP1, OP3, and OP5

The conductivity in PANI-doped PVDF: PEO: LiTFSI blends takes a decisive turn under the influence of overoxidation, a chemical transformation that hydrolyses PANI's quinoid structures, disrupts its conjugated system, and converts conductive imine sites into insulating carbonyl groups. Specifically, the transformation of conductive imine sites into non-conductive carbonyl and hydroxyl groups not only interrupts the electronic pathways but also limits the extent of redox-active sites available for charge storage. This structural degradation explains the pronounced capacity reduction observed in overoxidized films, as the diminished electron mobility and fewer active sites reduce the overall efficiency of the SPE in facilitating ion-electron interactions during electrochemical cycling. The conductivity behaviour of the films can be directly correlated with the morphological features observed in the FESEM images, as changes in surface structure, such as porosity, roughness, and particle distribution, strongly influence charge transport pathways within the films. The FESEM

images of the overoxidized samples (OP1, OP3, and OP5) reveal distinct morphological differences compared to their pristine counterparts (P1, P3, and P5). Before overoxidation, the PANI-blended films displayed relatively compact and uniform surfaces, with PANI domains dispersed throughout the polymer matrix. However, following overoxidation, the surfaces of OP1, OP3, and OP5 became noticeably rougher and more porous, with irregular features and disrupted continuity of the polymer network. This morphological degradation is attributed to the chemical modification of oxidizable sites in PANI during overoxidation, where amine and imine nitrogen, along with aromatic carbons, are converted into oxygenated or nitro-substituted groups. Such irreversible changes break the conjugated structure of PANI, leading to loss of structural integrity in the films.

These morphological observations are consistent with the conductivity results presented in Figure 4.11. The pristine P1, P3, and P5 films exhibited higher conductivity due to the intact conjugated network of PANI, which facilitated efficient electron transport. In contrast, OP1, OP3, and OP5 showed significantly reduced conductivity. The formation of oxygenated defects and the destruction of extended conjugation during overoxidation hinder electron delocalization, thereby suppressing electrical conductivity. The increased porosity and surface irregularities observed in overoxidized samples further hinder the continuous pathways for electron movement, leading to inefficient charge transport. Consequently, the SPE's ability to support reversible redox reactions is compromised, which directly translates into a measurable reduction in the electrochemical capacity of the device. Although the increased porosity observed in FESEM might benefit ionic transport pathways, the overall conductivity is dominated by the loss of electronic conduction in PANI. In summary, the FESEM analysis demonstrates that overoxidation not only alters the surface morphology of PANI-blended films, making them more porous and irregular, but also directly correlates with the substantial decline in conductivity. This highlights the detrimental effect of overoxidation on both the structural and electrical properties of the membranes.

Collectively, the FESEM, FTIR, XRD, and EIS results provide a coherent picture of overoxidation-induced degradation in PANI-SPE films. FESEM reveals morphological disruption and increased porosity, FTIR confirms chemical breakdown of the PANI backbone through carbonyl and hydroxyl formation, XRD demonstrates

loss of structural order, and EIS quantifies the resulting decline in conductivity. The consistency across these techniques confirms that overoxidation primarily destroys the conjugated structure of PANI, rather than merely altering surface morphology, underscoring the critical role of chemical stability in long-term SPE performance. Overall, the combined chemical, structural, and morphological changes induced by overoxidation not only diminish electronic conductivity but also limit the availability of redox-active sites, providing a mechanistic explanation for the substantial capacity reduction observed in the overoxidized PANI-SPE films. To facilitate a direct comparison of the electrical, structural, and chemical changes in the PANI-based composites, Table 4.1 summarizes the key parameters measured before and after overoxidation. The table highlights how varying PANI concentrations influence the initial conductivity, the significant conductivity loss following overoxidation, and the corresponding changes observed in FTIR spectra and FESEM images.

Table 4.1

Summary of conductivity, FTIR, and FESEM observations of PANI-based SPE composites before and after overoxidation

Samples	**PANI wt.%**	**Initial Conductivity (S/cm)**	**Final Conductivity (S/cm)**	**% Decrease**	**Changes in chemical structure**	**Changes in morphology**
P1	1	1.80×10^{-5}	1.79×10^{-6}	90.1%	O-H, C=O formed	Porous → cracks/pores
P3	3	1.41×10^{-6}	4.17×10^{-7}	70.4%	O-H, C=O formed	Dense → cracks
P5	5	1.25×10^{-6}	$1.79X10^{-7}$	85.7%	O-H, C=O formed	Dense → cracks/rupture

Table 4.1 shows that overoxidation caused a significant decline in conductivity for all PANI-SPE films, with reductions ranging from 70.4% (P3) to 89.8% (P1). This decrease is attributed to the chemical transformation of PANI, where conductive imine sites are converted into oxygenated groups (O-H, C=O), disrupting the conjugated backbone and limiting electron transport. Morphologically, the films became more

porous, with cracks and ruptures, further hindering continuous charge pathways. Although initial conductivity varied slightly with PANI content, overoxidation dominated the electrical behaviour, leading to severe conductivity loss across all samples. These findings indicate that both chemical degradation and morphological disruption synergistically impair the films' ability to support efficient charge transfer, providing a mechanistic explanation for the reduced electrochemical capacity observed in the overoxidized PANI-SPE films.

CHAPTER 5
CONCLUSIONS AND RECOMMENDATIONS

5.1 Conclusions

This study set out to investigate the effects of overoxidation on the morphological, structural, and electrical properties of novel PANI:PEO:PVDF:LiTFSI SPEs. The results showed that PANI loading played a decisive role in determining conductivity and microstructure. The 1 wt.% PANI composite demonstrated the most favourable balance, achieving the highest initial conductivity (1.76×10^{-5} S/cm), attributed to a well-formed IPN that facilitated ionic transport. Increasing the PANI content to 3 wt. % and 5 wt. % resulted in poorer conductivity, likely due to agglomeration and structural heterogeneity that disrupted efficient ion transport pathways. These findings confirm Objective (i), showing that composition strongly governs performance.

When subjected to cyclic voltammetry to induce overoxidation, all samples exhibited significant degradation in electrochemical behaviour, confirming Objective (ii). Conductivity values decreased across all films, with the 1 wt. % PANI sample showing nearly an order-of-magnitude reduction. The loss of redox reversibility indicates that overoxidation disrupts the conductive pathways within PANI and destabilizes the polymer matrix. Objective (iii) was addressed through FTIR, FESEM, and XRD analyses. FTIR confirmed the formation of hydroxyl and carbonyl groups, while FESEM revealed morphological disruption of interpenetrating polymer networks, and XRD showed reduced crystallinity. Collectively, these results provide a clear picture of how overoxidation induces irreversible chemical and structural modifications that directly correlate with conductivity loss. Beyond fulfilling its objectives, this study contributes two key novelties: it is the first to report on the PANI:PEO:PVDF:LiTFSI composite system, and it provides the first systematic analysis of overoxidation effects in such electrolytes. The insights are significant for the development of safer and more durable solid polymer electrolytes. In real-world contexts, the observed degradation mechanisms highlight the challenges of deploying PANI-based SPEs in lithium-ion batteries for electric vehicles, renewable energy storage, and portable electronics. The

findings emphasize that while PANI incorporation enhances conductivity at optimal levels, its susceptibility to oxidative degradation poses limitations that must be addressed through design strategies such as stabilizers, protective coatings, or alternative doping agents.

5.2 Recommendations

Future research should focus on strategies to improve both the conductivity and oxidative stability of PANI-based SPEs. One promising avenue is the use of doping modifications, such as sulfonic acid doping or incorporation of heteroatom-based dopants, which can stabilize PANI against overoxidation while maintaining its intrinsic conductive properties. Such chemical modifications could help prevent rapid degradation of the polymer backbone during electrochemical operation, extending the material's functional lifespan.

Another approach involves the integration of functional nanofillers into low-PANI systems, like the P1 formulation. Nanomaterials such as TiO_2, SiO_2, or graphene oxide could reinforce the polymer matrix, improve mechanical robustness, and act as radical scavengers. This strategy has the potential to decouple conductivity enhancement from oxidative vulnerability, allowing the SPEs to retain high ion transport performance without sacrificing stability.

Finally, it is essential to evaluate long-term electrochemical stability and explore alternative conducting polymers. Extended charge-discharge cycling experiments under real battery conditions can reveal degradation pathways and provide insight into the true lifespan of the composites. Advanced in situ or operando characterization techniques, such as synchronized Raman-EIS analysis or synchrotron-based X-ray tomography, can monitor degradation in real time. Additionally, comparative studies with other conducting polymers, such as PEDOT or PPy, could determine whether overoxidation is a general limitation of conducting-polymer-based SPEs or a challenge specific to PANI.

REFERENCES

Abd Mutalib, M., Rahman, M. A., Othman, M. H. D., Ismail, A. F., & Jaafar, J. (2017). Scanning Electron Microscopy (SEM) and Energy-Dispersive X-Ray (EDX) Spectroscopy. Membrane Characterization, 161–179. Elsevier Inc. https://doi.org/10.1016/B978-0-444-63776-5.00009-7

Agrawal, R. C., & Pandey, G. P. (2008). Solid polymer electrolytes: Materials designing and all-solid-state battery applications: An overview. Journal of Physics D: Applied Physics, 41(22). https://doi.org/10.1088/0022-3727/41/22/223001

Al-Akhras, M. A., Telfah, M., Shakhatreh, M. N., Telfah, A., Mousa, M. S., Narayanaswamy, V., & Obaidat, I. M. (2023). Optical and Chemical Investigations of PEO Thin Films Incorporated with Curcumin Nanoparticle: Effect of Film Thickness. Biointerface Research in Applied Chemistry, 13(2). https://doi.org/10.33263/BRIAC132.143

Alsabagh, A. M., Hassan, M. E., Dosouky, S. D. M., Nasser, N. M., Elsharaky, E. A., & Abdelhamid, M. M. (2016). Preparation of some thermal stable polymers based on diesters of polyethylene and polypropylene oxides macro monomers to use as surfactants at high temperature and pressure. Egyptian Journal of Petroleum, 25(3), 355–366. https://doi.org/10.1016/j.ejpe.2015.08.001

Ambalagi, S. M., Devendrappa, M., Nagaraja, S., & Sannakki, B. (2018). Dielectric Properties of PANI/CuO Nanocomposites. IOP Conference Series: Materials Science and Engineering, 310(1). https://doi.org/10.1088/1757-899X/310/1/012081

Armes, S. P., & Miller, J. F. (1988). Optimum Reaction Conditions for The Polymerization of Aniline in Aqueous Solution by Ammonium Persulfate. In Synthetic Metals, 22.

Arya, A., & Sharma, A. L. (2019). Tailoring of the structural, morphological, electrochemical, and dielectric properties of solid polymer electrolyte. Ionics, 25(4), 1617–1632. https://doi.org/10.1007/s11581-019-02916-7

Bae, H., Hwang, S. M., Seo, I., & Kim, Y. (2016). Electrochemical Lithium Recycling System toward Renewable and Sustainable Energy Technologies. Journal of The Electrochemical Society, 163(7), 199–205. https://doi.org/10.1149/2.0691607jes

Bae, H., & Kim, Y. (2021). Technologies of lithium recycling from waste lithium-ion batteries: A review. In Materials Advances, 2(10), 3234–3250. Royal Society of Chemistry. https://doi.org/10.1039/d1ma00216c

Beck, F., Barsch, U., & Michaelis, R. (1993). Corrosion of conducting polymers in aqueous media. In J. Electroanal. Chem, 351. Elsevier Sequoia S.A.

Bekaert, E., Buannic, L., Lassi, U., Llordés, A., & Salminen, J. (2017). Chapter One - Electrolytes for Li- and Na-Ion Batteries: Concepts, Candidates, and the Role of Nanotechnology. In Emerging Nanotechnologies in Rechargeable Energy Storage Systems. https://doi.org/10.1016/B978-0-323-42977-1/00001-7

Beuse, T., Fingerle, M., Wagner, C., Winter, M., & Börner, M. (2021). Comprehensive insights into the porosity of lithium-ion battery electrodes: A comparative study on positive electrodes based on lini0.6mn0.2co0.2o2 (NMC622). Batteries, 7(4). https://doi.org/10.3390/batteries7040070

Beygisangchin, M., Rashid, S. A., Shafie, S., Sadrolhosseini, A. R., & Lim, H. N. (2021). Preparations, properties, and applications of polyaniline and polyaniline thin films—a review. Polymers, 13(12). https://doi.org/10.3390/polym13122003

Bhadra, S., Khastgir, D., Singha, N. K., & Lee, J. H. (2009). Progress in preparation, processing, and applications of polyaniline. In Progress in Polymer Science (Oxford), 34(8), 783–810. https://doi.org/10.1016/j.progpolymsci.2009.04.003

Bhandari, S. (2017). Polyaniline: Structure and Properties Relationship. In Polyaniline Blends, Composites, and Nanocomposites, 23–60. Elsevier. https://doi.org/10.1016/B978-0-12-809551-5.00002-3

Bilal, S., Arif, M., Khan, M. S., & Shah, A. U. H. A. (2019). Characterization of sodium and potassium nitrate contaminated polyaniline-poly (ethylene oxide) composites synthesized via facile solution casting technique. Materials, 12(13). https://doi.org/10.3390/ma12132168

Chae, W., Kim, B., Ryoo, W. S., & Earmme, T. (2023). A Brief Review of Gel Polymer Electrolytes Using in Situ Polymerization for Lithium-ion Polymer Batteries. In Polymers, 15(4). MDPI. https://doi.org/10.3390/polym15040803

Chen, H., Zheng, M., Qian, S., Ling, H. Y., Wu, Z., Liu, X., Yan, C., & Zhang, S. (2021). Functional additives for solid polymer electrolytes in flexible and high-energy-density solid-state lithium-ion batteries. Carbon Energy, 3(6) 929–956. John Wiley and Sons Inc. https://doi.org/10.1002/cey2.146

Dallaev, R., Pisarenko, T., Sobola, D., Orudzhev, F., Ramazanov, S., & Trčka, T. (2022). Brief Review of PVDF Properties and Applications Potential. Polymers, 14(22). MDPI. https://doi.org/10.3390/polym14224793

Damdinov, B. B., Danilova, V. A., Minakov, A. V., & Pryazhnikov, M. I. (2021). ©Rheological Properties of PVDF Solutions. Journal of Siberian Federal University - Mathematics and Physics, 14(3), 265–272. https://doi.org/10.17516/1997-1397-2021-14-3-265-272

Dissanayake, M. A. K. L., Kumari, J. M. K. W., Senadeera, G. K. R., Jaseetharan, T., Mellander, B. E., Albinsson, I., & Furlani, M. (2020). Polyaniline (PANI) mediated cation trapping effect on ionic conductivity enhancement in poly(ethylene oxide) based solid polymer electrolytes with application in solid state dye sensitized solar cells. Reactive and Functional Polymers, 155. https://doi.org/10.1016/j.reactfunctpolym.2020.104683

Dowben, P. A., Rosa, L. G., Ilie, C. C., & Xiao, J. (2009). Adsorbate/absorbate interactions with organic ferroelectric polymers. Journal of Electron Spectroscopy and Related Phenomena, 174(1–3), 10–21. https://doi.org/10.1016/j.elspec.2009.03.005

Duan, H., Yin, Y. X., Zeng, X. X., Li, J. Y., Shi, J. L., Shi, Y., Wen, R., Guo, Y. G., & Wan, L. J. (2018). In-situ plasticized polymer electrolyte with double-network for flexible solid-state lithium-metal batteries. Energy Storage Materials, 10, 85–91. https://doi.org/10.1016/j.ensm.2017.06.017

Dunn, J. B., Gaines, L., Kelly, J. C., James, C., & Gallagher, K. G. (2015). The significance of Li-ion batteries in electric vehicle life-cycle energy and emissions

and recycling's role in its reduction. Energy and Environmental Science, 8(1), 158–168. https://doi.org/10.1039/c4ee03029j

Elgrishi, N., Rountree, K. J., McCarthy, B. D., Rountree, E. S., Eisenhart, T. T., & Dempsey, J. L. (2018). A Practical Beginner's Guide to Cyclic Voltammetry. Journal of Chemical Education, 95(2), 197–206. https://doi.org/10.1021/acs.jchemed.7b00361

Em, A., Am, A., Si, B., & Ma, M. (n.d.). Sciences Evaluation of optical parameters and structural variations of UV irradiated (PEO/PVP)/Au polymer nanocomposites. Research Journal of Pharmaceutical, Biological and Chemical, 7(2), 1877.

Epp, J. (2016). X-Ray Diffraction (XRD) Techniques for Materials Characterization. In Materials Characterization Using Nondestructive Evaluation (NDE) Methods, 81–124. Elsevier Inc. https://doi.org/10.1016/B978-0-08-100040-3.00004-3

Fan, L., Dang, Z., Nan, C.W., & Li, M. (2002). Thermal, electrical, and mechanical properties of plasticized polymer electrolytes based on PEO/P(VDF-HFP) blends. www.elsevier.com/locate/electacta

Fenniche, F., Khane, Y., Henni, A., Aouf, D., & Elhak Djafri, D. (2022). Synthesis and characterization of PANI nanofibers high-performance thin films via electrochemical methods. Results in Chemistry, 4. https://doi.org/10.1016/j.rechem.2022.100596

Fenoy, G. E., Azzaroni, O., Knoll, W., & Marmisollé, W. A. (2021). Functionalization strategies of PEDOT and PEDOT: PSS films for organic bioelectronics applications. Chemosensors, 9(8). Multidisciplinary Digital Publishing Institute (MDPI). https://doi.org/10.3390/chemosensors9080212

Fenton, D. E., Parker, M., & Wright, P. V. (1964). A-l) 1966, 4, 1563. In C. J. J. Am. Chem. Soc, 6.

Fong, K. D., Wang, T., Kim, H. K., Kumar, R. V., & Smoukov, S. K. (2017). Semi-Interpenetrating Polymer Networks for Enhanced Supercapacitor Electrodes. ACS Energy Letters, 2(9), 2014–2020. https://doi.org/10.1021/acsenergylett.7b00466

Gao, M., Zhang, G., Zhang, G., Wang, X., Wang, S., & Yang, Y. (2011). The resistance to over-oxidation for polyaniline is initiated by the resulting quinone-like molecules. Polymer Degradation and Stability, 96(10), 1799–1804. https://doi.org/10.1016/j.polymdegradstab.2011.07.017

Gelardi, G., Mantellato, S., Marchon, D., Palacios, M., Eberhardt, A. B., & Flatt, R. J. (2016). Chemistry of chemical admixtures. Science and Technology of Concrete Admixtures, 149–218. Elsevier Inc. https://doi.org/10.1016/B978-0-08-100693-1.00009-6

Gucci, F., Grasso, M., Russo, S., Leighton, G. J. T., Shaw, C., & Brighton, J. (2023). Electrical and Mechanical Characterisation of Poly(ethylene)oxide-Polysulfone Blend for Composite Structural Lithium Batteries. Polymers, 15(11). https://doi.org/10.3390/polym15112581

Hallinan, D. T., & Balsara, N. P. (2013). Polymer electrolytes. Annual Review of Materials Research, 43, 503–525. https://doi.org/10.1146/annurev-matsci-071312-121705

Holze, R. (2022). Overoxidation of Intrinsically Conducting Polymers. Polymers, 14(8). MDPI. https://doi.org/10.3390/polym14081584

Hsu, S. T., Tran, B. T., Subramani, R., Nguyen, H. T. T., Rajamani, A., Lee, M. Y., Hou, S. S., Lee, Y. L., & Teng, H. (2020). Free-standing polymer electrolyte for all-solid-state lithium batteries operated at room temperature. Journal of Power Sources, 449. https://doi.org/10.1016/j.jpowsour.2019.227518

Izdebska, J. (2015). Aging and Degradation of Printed Materials. Printing on Polymers: Fundamentals and Applications, 353–370. Elsevier Inc. https://doi.org/10.1016/B978-0-323-37468-2.00022-1

James, R. (2014). Parkland College X-Ray Diffraction. http://ljs.academicdirect.org/A16/001_012.htm

Jaya, R. P. (2020). Porous concrete pavement containing nanosilica from black rice husk ash. New Materials in Civil Engineering, 493–527. Elsevier. https://doi.org/10.1016/B978-0-12-818961-0.00014-4

K, B., Gueye, A. B., Rouxel, D., Kalarikkal, N., & Thomas, S. (2022). Lithium-ion battery separators based on electrospun PVDF: A review. Surfaces and Interfaces (Vol. 31). Elsevier B.V. https://doi.org/10.1016/j.surfin.2022.101977

Kam, W., Liew, C. W., Lim, J. Y., & Ramesh, S. (2014). Electrical, structural, and thermal studies of antimony trioxide-doped poly(acrylic acid)-based composite polymer electrolytes. Ionics, 20(5), 665–674. https://doi.org/10.1007/s11581-013-1012-0

Krische, B., & Zagorska, M. (1989). C257 C262 C257 Overoxidation in Conducting Polymers. Synthetic Metals, 28.

Lá, G. G., Ujvá, M., Vesztergom, S., Szekeres, K., & Zalka, D. (2018). Structural Changes During the Overoxidation of Poly(3,4-Ethylenedioxythiophene) Films Electrodeposited from Surfactant-Free Aqueous Solutions.

Leš, K., & Jordan, C. S. (2020). Ionic conductivity enhancement in solid polymer electrolytes by electrochemical: In situ formation of an interpenetrating network. RSC Advances, 10(68), 41296–41304. https://doi.org/10.1039/d0ra07966a

Li, J., Zhu, K., Wang, J., Yan, K., Liu, J., Yao, Z., & Xu, Y. (2022). Optimisation of conductivity of PEO/PVDF-based solid polymer electrolytes in all-solid-state Li-ion batteries. Materials Technology, 37(4), 240–247. https://doi.org/10.1080/10667857.2020.1827873

Li, Y., & Qian, R. (2000). Electrochemical overoxidation of conducting polypyrrole nitrate film in aqueous solutions. Electrochimica Acta, 45. www.elsevier.nl/locate/electacta

Lingegowda, D. C., Komal Kumar, J., Devi Prasad, A. G., Zarei, M., & Gopal, S. (2012). FTIR Spectroscopic Studies on Cleome Gynandra-Comparative Analysis of Functional Group Before and After Extraction, 22.

Manjunatha, H., Damle, R., & Kumaraswamy, G. N. (2022). Modification of polymer electrolyte blend PEO/PVDF–HFP by low-energy O+ ion irradiation to improve electrolyte behavior. Polymer Bulletin, 79(6), 3929–3950. https://doi.org/10.1007/s00289-021-03693-y

Matlin, S. A., Mehta, G., Hopf, H., & Krief, A. (2019). The Periodic Table of the Chemical Elements and Sustainable Development. In European Journal of Inorganic Chemistry, 2019(39–40), 4170–4173. Wiley-VCH Verlag. https://doi.org/10.1002/ejic.201801409

Miao, R., Liu, B., Zhu, Z., Liu, Y., Li, J., Wang, X., & Li, Q. (2008). PVDF-HFP-based porous polymer electrolyte membranes for lithium-ion batteries. Journal of Power Sources, 184(2), 420–426. https://doi.org/10.1016/j.jpowsour.2008.03.045

Mo, Y., Meng, W., Xia, Y., & Du, X. (2019). Redox-active gel electrolyte combined with branched polyaniline nanofibers doped with ferrous ions for ultra-high-performance flexible supercapacitors. Polymers, 11(8). https://doi.org/10.3390/polym11081357

Mondal, S., & Sangaranarayanan, M. V. (2016). Permselectivity and thickness-dependent ion transport properties of overoxidized polyaniline: A mechanistic investigation. Physical Chemistry Chemical Physics, 18(44), 30705–30720. https://doi.org/10.1039/c6cp04975c

Mossali, E., Picone, N., Gentilini, L., Rodrìguez, O., Pérez, J. M., & Colledani, M. (2020). Lithium-ion batteries towards circular economy: A literature review of opportunities and issues of recycling treatments. Journal of Environmental Management, 264. https://doi.org/10.1016/j.jenvman.2020.110500

Murata, K., Izuchi, S., & Yoshihisa, Y. (2000). An overview of the research and development of solid polymer electrolyte batteries. Electrochimica Acta, 45. www.elsevier.nl/locate/electacta

Namsheer, K., & Rout, C. S. (2021). Conducting polymers: a comprehensive review on recent advances in synthesis, properties, and applications. In RSC Advances, 11(10), 5659–5697. Royal Society of Chemistry. https://doi.org/10.1039/d0ra07800j

Nezakati, T., Seifalian, A., Tan, A., & Seifalian, A. M. (2018). Conductive Polymers: Opportunities and Challenges in Biomedical Applications. Chemical Reviews, 118(14), 6766–6843. American Chemical Society. https://doi.org/10.1021/acs.chemrev.6b00275

Nourisabet, T., Jamshidi Aval, H., Shidpour, R., & Naji, L. (2022). Fabrication of a PEO-PVDF blend-based polymer composite electrolyte with extremely high ionic conductivity via the addition of LLTO nanowires. Solid State Ionics, 377. https://doi.org/10.1016/j.ssi.2022.115885

Pang, A. L., Arsad, A., & Ahmadipour, M. (2021). Synthesis and factors affecting the conductivity of polypyrrole: a short review. Polymers for Advanced Technologies, 32(4), 1428–1454. John Wiley and Sons Ltd. https://doi.org/10.1002/pat.5201

Patil, A. 0, Heeger, A. J., & Wudl, F. (1988). Optical Properties of Conducting Polymers. Chem. Rev, 8(8).

Patla, S. K., Ray, R., Asokan, K., & Karmakar, S. (2018). Investigation of ionic conduction in PEO-PVDF-based blend polymer electrolytes. Journal of Applied Physics, 123(12). https://doi.org/10.1063/1.5022050

Plieth, W., Bund, A., Rammelt, U., Neudeck, S., & Duc, L. M. (2006). The role of ion and solvent transport during the redox process of conducting polymers. Electrochimica Acta, 51(11), 2366–2372. https://doi.org/10.1016/j.electacta.2005.03.087

Portia Makwarimba, C., Tang, M., Peng, Y., Lu, S., Zheng, L., Zhao, Z., & Zhen, A. (2022). iScience Assessment of recycling methods and processes for lithium-ion batteries. https://doi.org/10.1016/j.isci

Purkait, M. K., Sinha, M. K., Mondal, P., & Singh, R. (2018). Temperature-Responsive Membranes. Interface Science and Technology, 25, 67–113. Elsevier B.V. https://doi.org/10.1016/B978-0-12-813961-5.00003-6

Quartarone, E., Mustarelli, P., & Magistris, A. (1998). PEO-based composite polymer electrolytes. In Solid State Ionics, 110.

Refaey, S. A. M., Schwitzgebel, G., & Schneider, O. (1999). Electrochemical impedance studies on oxidative degradation, overoxidative degradation, deactivation, and reactivation of conducting polymers. Synthetic Metals, 98.

Rodríguez, I., Scharifker, B. R., & Mostany, J. (2000). In situ FTIR study of redox and overoxidation processes in polypyrrole films. Journal of Electroanalytical Chemistry, 491. www.elsevier.nl/locate/jelechem

Salam, M. H. A. El, Elkomy, G. M., Osman, H., Nagy, M. R., & El-Sayed, F. (2012). Structure-electrical conductivity of polyvinylidene fluoride/graphite composites. Journal of Reinforced Plastics and Composites, 31(20), 1342–1352. https://doi.org/10.1177/0731684412459286

Sarkar, D., Das, N., Saikh, Md. M., Biswas, P., Roy, S., Paul, S., Hoque, N. A., Basu, R., & Das, S. (2022). Human movement-mediated energy harvesting and weight sensing using flexible N-carbon dot-loaded PVDF nanocomposite. https://doi.org/10.21203/rs.3.rs-1765550/v1

Sasaki, T., Ukyo, Y., & Novák, P. (2013). Memory effect in a lithium-ion battery. Nature Materials, 12(6), 569–575. https://doi.org/10.1038/nmat3623

Sedlak, P., Sobola, D., Gajdos, A., Dallaev, R., Nebojsa, A., & Kubersky, P. (2021). Surface analyses of PVDF/NMP/[EMIM][TFSI] solid polymer electrolyte. Polymers, 13(16). https://doi.org/10.3390/polym13162678

Sengwa, R. J., & Dhatarwal, P. (2020). Predominantly chain segmental relaxation dependent ionic conductivity of multiphase semicrystalline PVDF/PEO/LiClO4 solid polymer electrolytes. Electrochimica Acta, 338. https://doi.org/10.1016/j.electacta.2020.135890

Shen, X., Liu, H., Cheng, X. B., Yan, C., & Huang, J. Q. (2018). Beyond lithium-ion batteries: Higher energy density battery systems based on lithium metal anodes. Energy Storage Materials, 12, 161–175. Elsevier B.V. https://doi.org/10.1016/j.ensm.2017.12.002

Shin, E. J., Kim, S., Noh, J. K., Byun, D., Chung, K. Y., Kim, H. S., & Cho, B. W. (2015). A green recycling process designed for LiFePO4 cathode materials for Li-ion batteries. Journal of Materials Chemistry A, 3(21), 11493–11502. https://doi.org/10.1039/c5ta02540k

Siddhanta, S. K., & Gangopadhyay, R. (2005). Conducting polymer gel: Formation of a novel semi-IPN from polyaniline and crosslinked poly(2-acrylamido-2-methyl propanesulphonicacid). Polymer, 46(9), 2993–3000. https://doi.org/10.1016/j.polymer.2005.01.084

Snyder, J. F., Carter, R. H., & Wetzel, E. D. (2007). Electrochemical and mechanical behavior in mechanically robust solid polymer electrolytes for use in multifunctional structural batteries. Chemistry of Materials, 19(15), 3793–3801. https://doi.org/10.1021/cm070213o

Sousa, E. A., Deniz, W. D. S., Arlindo, E. P. S., Sakamoto, W. K., & Fuzari, G. C. (2017). PVDF-PAni blend: a free-standing film with variable electrical resistance. Polymer Bulletin, 74(5), 1483–1492. https://doi.org/10.1007/s00289-016-1785-1

Speight, J. G. (2020). Chemistry and chemical technology. Handbook of Industrial Hydrocarbon Processes, 1–44. Elsevier. https://doi.org/10.1016/b978-0-12-809923-0.00001-1

Srivastava, N., & Tiwari, T. (2009). New trends in polymer electrolytes: a review. 146. http://www.e-polymers.org

Stephan, A. M. (2006). Review of gel polymer electrolytes for lithium batteries. European Polymer Journal, 42(1), 21–42. https://doi.org/10.1016/j.eurpolymj.2005.09.017

Sun, Z., Li, Y., Zhang, S., Shi, L., Wu, H., Bu, H., & Ding, S. (2019). G-C3N4 nanosheets enhanced solid polymer electrolytes with excellent electrochemical performance, mechanical properties, and thermal stability. Journal of Materials Chemistry A, 7(18), 11069–11076. https://doi.org/10.1039/c9ta00634f

Sydulu Singu, B., Srinivasan, P., & Pabba, S. (2011). Benzoyl Peroxide Oxidation Route to Nano Form Polyaniline Salt Containing Dual Dopants for Pseudocapacitor. Journal of The Electrochemical Society, 159(1), A6–A13. https://doi.org/10.1149/2.036201jes

Tan, S. J., Zeng, X. X., Ma, Q., Wu, X. W., & Guo, Y. G. (2018). Recent Advancements in Polymer-Based Composite Electrolytes for Rechargeable Lithium Batteries.

Electrochemical Energy Reviews, 1(2), 113–138. Springer Science and Business Media B.V. https://doi.org/10.1007/s41918-018-0011-2

Tang, Q., Liu, J., Chan, H. S., & Miao, Q. (2009). Benzenoid and quinonoid nitrogen-containing heteropentacenes. Chemistry - A European Journal, 15(16), 3965–3969. https://doi.org/10.1002/chem.200900160

Tara-Lunga-Mihali, M., Plesu, N., Macarie, L., Iliescu, S., & Ilia, G. (2014). Polyaniline composite designed for a solid polymer electrolyte. Pure and Applied Chemistry, 86(11), 1853–1860. https://doi.org/10.1515/pac-2014-0605

Tiquia-Arashiro, S., Li, X., Pokhrel, K., Kassem, A., Abbas, L., Coutinho, O., Kasperek, D., Najaf, H., & Opara, S. (2023). Applications of Fourier Transform-Infrared spectroscopy in microbial cell biology and environmental microbiology: advances, challenges, and future perspectives. Frontiers in Microbiology, 14. Frontiers Media SA. https://doi.org/10.3389/fmicb.2023.1304081

Ue, M. (2009). Role-Assigned Electrolytes: Additives. https://doi.org/10.1007/987-0-387-34445-4_4

Ujvári, M., Takács, M., Vesztergom, S., Bazsó, F., Ujhelyi, F., & Láng, G. G. (2011). Monitoring of the electrochemical degradation of PEDOT films on gold using the bending beam method. Journal of Solid-State Electrochemistry, 15(11–12), 2341–2349. https://doi.org/10.1007/s10008-011-1472-y

Wang, H., & Friedrich, B. (2015). Development of a Highly Efficient Hydrometallurgical Recycling Process for Automotive Li–Ion Batteries. Journal of Sustainable Metallurgy, 1(2), 168–178. https://doi.org/10.1007/s40831-015-0016-6

Wang, N., Wei, Y., Yu, S., Zhang, W., Huang, X., Fan, B., Yuan, H., & Tan, Y. (2024). A flexible PEO-based polymer electrolyte with a cross-linked network for a high-voltage all-solid-state lithium-ion battery. Journal of Materials Science and Technology, 183, 206–214. https://doi.org/10.1016/j.jmst.2023.10.005

Wang, Q., Ping, P., Zhao, X., Chu, G., Sun, J., & Chen, C. (2012). Thermal runaway caused a fire and explosion of a lithium-ion battery. Journal of Power Sources, 208, pp. 210–224). Elsevier B.V. https://doi.org/10.1016/j.jpowsour.2012.02.038

Wanger, T. C. (2011). The Lithium future-resources, recycling, and the environment. Conservation Letters, 4(3), 202–206. https://doi.org/10.1111/j.1755-263X.2011.00166.x

Wu, L., Zhang, C., Kim, S., Hatton, T. A., Mo, H., & Waite, T. D. (2022). Lithium recovery using electrochemical technologies: Advances and challenges. Water Research, 221. Elsevier Ltd. https://doi.org/10.1016/j.watres.2022.118822

Wu, S., & Han, X. (2005). Study on the electrochemical degradation of poly-N-acetyl aniline by electro-hydrolysis and electro-chlorination. Polymer Degradation and Stability, 90(3), 535–539. https://doi.org/10.1016/j.polymdegradstab.2005.04.002

Wu, Y., Li, Y., Wang, Y., Liu, Q., Chen, Q., & Chen, M. (2022). Advances and prospects of PVDF-based polymer electrolytes. Journal of Energy Chemistry, 64, 62–84. Elsevier B.V. https://doi.org/10.1016/j.jechem.2021.04.007

Xu, J., Thomas, H. R., Francis, R. W., Lum, K. R., Wang, J., & Liang, B. (2008). A review of processes and technologies for the recycling of lithium-ion secondary batteries. Journal of Power Sources, 177(2), 512–527. https://doi.org/10.1016/j.jpowsour.2007.11.074

Yang, T., Lu, Y., Li, L., Ge, D., Yang, H., Leng, W., Zhou, H., Han, X., Schmidt, N., Ellis, M., & Li, Z. (2020). An Effective Relithiation Process for Recycling Lithium-Ion Battery Cathode Materials. Advanced Sustainable Systems, 4(1). https://doi.org/10.1002/adsu.201900088

Yoshio, M., Brodd, R. J., & Kozawa, A. (2009). Lithium-ion batteries: Science and technologies. In Lithium-Ion Batteries: Science and Technologies. Springer New York. https://doi.org/10.1007/978-0-387-34445-4

Yoshitake, H. (2009). Functional electrolytes specially designed for lithium-ion batteries. In Lithium-Ion Batteries: Science and Technologies, 343–366. Springer New York. https://doi.org/10.1007/978-0-387-34445-4_19

Zhou, Q., Ma, J., Dong, S., Li, X., & Cui, G. (2019). Intermolecular Chemistry in Solid Polymer Electrolytes for High-Energy-Density Lithium Batteries. Advanced Materials, 31(50). https://doi.org/10.1002/adma.201902029

APPENDICES

APPENDIX 1

Published Articles

1. Fabrication of an Interpenetrating Polymer Network (IPN) Using PANI, PVDF, PEO, and LiTFSI for Solid Polymer Electrolyte (SPE) Applications
   Nur Najiha Abd Maliaman, *Awatif Hassim, Mohamad Arif Kasri, Muhammad Zharfan Mohd Halizan, Saiful Arifin Shafiee, Mohd Muzamir Mahat*

2. Integration of solid polymer electrolyte into an efficient and environmentally friendly electrochemical approach in lithium-ion batteries recycling
   Muhammad Zharfan Mohd Halizan, Awatif Hassim, Mohamad Arif Kasri, Saiful Ariffin Shafiee, ***Nurul Najiha Maliaman****, Muhammad Faiz Aizamddin, Siti Nur Amira Shaffee, Mohd Muzamir Mahat*

3. A Technical Review on the Implementation of Lithium-Ion Batteries Waste Recycling Method
   Muhammad Zharfan Mohd Halizan, Irina Harun, Mohd Fadzli Irwan Bahruddin, Nuraini Daud, Mohamad Arif Kasri, Awatif Hassim, ***Nur Najiha Maliaman****, Norazah Abd Rahman, Muhammad Faiz Aizamddin, Siti Nur Amira Shaffee, Mohd Muzamir Mahat*

4. Study of Conductivity and Morphological Properties Using Different Composition of PEDOT:PSS/PEO Film as a Membrane for Lithium-Ion Batteries Recycling
   Awatif Hassim, ***Nur Najiha Abd Maliaman****, Mohamad Arif Kasri, Fatin Nur Azmina Mohd Fauzi, Suzana Ratim, Mohd Muzamir Mahat*

APPENDIX 2

Conferences Attended

1. **Participated** in the Electronic Packaging Interconnect Technology Symposium (EPITS 2024), organized by Universiti Malaysia Perlis (UniMAP).
2. **Participated** in the IIUM Postgraduate Colloquium 2023 organized by the International Islamic University Malaysia (IIUM).
3. **Participated** in the 35th International Conference of Analytical Sciences (SKAM35) organized by Universiti Teknologi MARA Malaysia (UiTM)

AUTHOR'S PROFILE

Najiha holds a Bachelor of Science (BSc) in Applied Chemistry from the International Islamic University Malaysia (IIUM), Kuantan. Her academic interests lie in material science and technology, polymer technology, and applied chemistry. Currently, she is pursuing a Master's degree (MSc) under a Petronas Research grant, focusing on the development and fabrication of thin film membranes to serve as solid polymer electrolytes (SPEs) and separators for lithium-ion batteries (LIBs). Her research involves the use of various analytical techniques, including Fourier Transform Infrared Spectroscopy (FTIR), X-ray Diffraction (XRD), Field Emission Scanning Electron Microscopy (FESEM), and Electrochemical Impedance Spectroscopy (EIS).

LIST OF PUBLICATION:

1. Abd Maliaman, N. N., Hassim, A., Kasri, M. A., Mohd Halizan, M. Z., Shafiee, S. A., & Mahat, M. M. (2025). Fabrication of an interpenetrating polymer network (IPN) using PANI, PVDF, PEO, and LiTFSI for solid polymer electrolyte (SPE) applications. In N. R. Abdul Razak, M. A. A. Mohd Salleh, D. S. Che Halin, K. Abdul Razak, F. Somidin, & M. F. H. Baser (Eds.), *Proceedings of the Green Materials and Electronic Packaging Interconnect Technology Symposium* (Vol. 418, Springer Proceedings in Physics). Springer. https://doi.org/10.1007/978-981-96-2871-1_20
2. Halizan, M. Z. M., Kasri, M. A., Maliaman, N. N., Hassim, A., Shafiee, S. A., Aizamddin, M. F., Shaffee, S. N. A., & Mahat, M. M. (2025). Integration of solid polymer electrolyte into an efficient and environmentally friendly

electrochemical approach in lithium-ion batteries recycling. *Journal of Energy Storage, 131*(Part A), 117491. Elsevier. https://doi.org/10.1016/j.est.2025.117491

3. Halizan, M. Z. M., Harun, I., Bahruddin, M. F. I., Daud, N., Kasri, M. A., Hassim, A., Maliaman, N. N., Rahman, N. A., Aizamddin, M. F., Shaffee, S. N. A., & Mahat, M. M. (2024). *A Technical Review on the Implementation of Lithium-Ion Batteries Waste Recycling Methods* (pp. 21–37). https://doi.org/10.1007/978-3-031-48902-0_2

4. Hassim, A., Abd Maliaman, N. N., Kasri, M. A., Mohd Fauzi, F. N. A., Ratim, S., & Mahat, M. M. (2025). Study of conductivity and morphological properties using different composition of PEDOT:PSS/PEO film as a membrane for lithium-ion batteries recycling. In N. R. Abdul Razak, M. A. A. Mohd Salleh, D. S. Che Halin, K. Abdul Razak, F. Somidin, & M. F. H. Baser (Eds.), *Proceedings of the Green Materials and Electronic Packaging Interconnect Technology Symposium. ECOOP 1996* (Vol. 418, Springer Proceedings in Physics). Springer. https://doi.org/10.1007/978-981-96-2871-1_24